This is to certify that the

thesis entitled

Spectroscopic Studies of Alkali Metal Complexes
in Non-Aqueous Media

presented by

Adamantia Rokofilou-Hourdakis

has been accepted towards fulfillment
of the requirements for

Ph.D. degree in Chemistry

Major professor

Date 7/27/78

SPECTROSCOPIC STUDIES OF ALKALI METAL COMPLEXES IN NON-AQUEOUS MEDIA

By

Adamantia Rokofilou-Hourdakis

A DISSERTATION

Submitted to
Michigan State University
in partial fulfillment of the requirements
for the degree of

DOCTOR OF PHILOSOPHY

Department of Chemistry

1978

ABSTRACT

SPECTROSCOPIC STUDIES OF ALKALI METAL COMPLEXES IN NON-AQUEOUS MEDIA

By

Adamantia Rokofilou-Hourdakis

The complexation reaction of the dilactam of cryptand C222 with lithium, sodium and cesium ions in water and in several nonaqueous solvents was studied by using ^{7}Li, ^{23}Na, ^{133}Cs and ^{13}C NMR technique and far infrared measurements.

Alkali metal ion chemical shifts were determined as a function of dilactam/metal ion mole ratios. There is no indication of a Li^{+}-C222D complex formed in water, dimethyl sulfoxide, dimethylformamide and methanol while in formamide and acetone there is indication of a rather weak complex. Formation constants of lithium-C222D complexes were determined in acetonitrile, tetrahydrofuran, pyridine and nitromethane. The values obtained were: $\log K_{ACN} = 3.23 \pm 0.07$, $\log K_{THF} = 3.12 \pm 0.09$, $\log K_{Py} = 2.64 \pm 0.10$, and $\log K_{NM} > 4$. Sodium ion forms stronger complexes with C222D since its size is closer to the dimension of the dilactam cavity than that of the lithium ion. In methanol, dimethylformamide, nitromethane, acetonitrile and pyridine solutions $\log K > 4$ has been found. The large cesium ion does not fit conveniently into the C222D cavity. The Cs^{+}-C222D complex is rather weak in nitromethane, acetonitrile and pyridine solutions while there is no indication of complex formation in dimethylformamide and in aqueous solutions. In order to

calculate the formation constants of the Cs^+-C222D complex in the above solvents, the ion pairing which is particularly extensive in the case of pyridine, was also taken into account. The values obtained were: $\log K_{NM} = 1.79 \pm 0.03$, $\log K_{ACN} = 1.70 \pm 0.08$ and $\log K_{Py} = 2.86 \pm 0.01$.

The limiting chemical shifts of the complexed lithium and sodium ion are solvent-dependent, indicating incomplete insulation of the cation from the solvent, while the large difference in the limiting chemical shifts of the complexed cesium ion is a good indication that the metal ion remains exposed to the solvent.

Carbon-13 NMR spectra of the Li^+-C222D, Na^+-C222D and K^+-C222D complexes in nitromethane show that the complexes are of the inclusive type with the metal ion inside the ligand cavity.

Formation constants for the Cs^+-C222D and Li^+-C222D complexes in pyridine, nitromethane and acetonitrile were calculated at various temperatures and used to obtain the thermodynamic quantities ΔH and ΔS for the complexation reaction. The results for the Cs^+ with C222D reaction were: $\Delta H = -2.18 \pm 0.09$ kcal/mole, $\Delta S = 5.69 \pm 0.33$ cal/mole·^oK in pyridine, $\Delta H = -0.67 \pm 0.10$ kcal/mole, $\Delta S = 5.81 \pm 0.33$ in nitromethane and $\Delta H = -1.85 \pm 0.26$, $\Delta S = 1.37 \pm 0.93$ in acetonitrile.

The complexation of Li^+ with C222D is endothermic because the small lithium ion is strongly solvated and the energy required for the desolvation is not replaced in the

complexation step. The values obtained are: $\Delta H = 6.10 \pm 0.16$ kcal/mole, $\Delta S = 38.4 \pm 0.6$ cal/mole·^{o}K in nitromethane and $\Delta H = 1.58 \pm 0.22$ kcal/mole, $\Delta S = 21.7 \pm 0.9$ cal/mole·^{o}K in acetonitrile.

The complexing ability of 2,2'-Bipyridine with lithium, sodium and cesium ions in various solvents was studied by using ^{7}Li, ^{23}Na, ^{133}Cs and ^{13}C NMR technique. The metal ion chemical shifts were determined as a function of ligand/metal mole ratios.

There is no Li^{+}-2,2'-bipyridine complex formed in tetrahydrofuran, methanol and formamide while in propylene carbonate there is a weak complex formed. In nitromethane a strong complex of a 1:2 stoichiometry is formed as both the ^{7}Li and the ^{13}C data indicate.

The Na^{+}-2,2'-bipyridine complex seems rather weak in tetrahydrofuran, propylene carbonate and acetonitrile, while there is no indication of complexation in dimethyl sulfoxide, dimethylformamide and methanol. In nitromethane there is a complex formed but we cannot unambiguously conclude its stoichiometry.

The complexation of 2,2'-bipyridine with Cs^{+} was studied in nitromethane, dimethylformamide, pyridine, propylene carbonate, acetonitrile and methanol. In none of the above solvents is there an indication of a complex formed.

ACKNOWLEDGMENTS

The author wishes to thank Professor Alexander I. Popov for his guidance, counseling, and friendship throughout this study.

Professor Andrew Timnick is acknowledged for his many helpful suggestions as second reader.

Gratitude is also extended to the Department of Chemistry, Michigan State University and the National Science Foundation for financial support.

I would like to thank all the members of the laboratory of Dr. A. I. Popov for their friendship and encouragement during our association, and Mr. Frank Bennis and Mr. Wayne Burkhardt for their efforts in keeping the NMR spectrometer in operating condition.

Special thanks to our friends in the U.S.A., who contributed to render our stay in this country a pleasant and unique experience.

TABLE OF CONTENTS

TABLE OF CONTENTS (Continued)

LIST OF TABLES

LIST OF TABLES (Continued)

LIST OF FIGURES

LIST OF FIGURES (Continued)

LIST OF FIGURES (Continued)

CHAPTER I

HISTORICAL REVIEW

A. Complexation of Alkali and Alkaline Earth Metal Ions By Cryptands

Although alkali and alkaline earth metal cations play a role of great importance both in chemistry and in biology, their coordination chemistry has mainly been developing in recent years with the advent of natural (1) or synthetic macrocyclic and macropolycyclic ligands, which are capable of forming strong complexes with the above metal ions.

Macrocyclic polyethers or "crown" ethers, synthesized in 1967 by Pedersen (2,3) were the first such complexing agents to appear. A typical crown is shown in Figure 1. These macrocyclic ligands contain a molecular, two-dimensional cavity, the diameter of which can be varied by changing the number of methylene groups and the number of oxygens in the ring. Certain cyclic polyethers not only strongly bind particular alkali and alkaline earth metal ions but selectively bind one or more of these ions in preference to the others in each series (4,5). The parameters which influence the selectivity and binding properties of macrocycles include the type(s) and number of binding sites in the ring, the relative sizes of the ion and the macrocyclic cavity, the physical placement of the binding sites, steric hindrance in the ring, the solvent and extent of solvation of the ion and binding sites, and the electrical charge of the ion.

Shortly thereafter, Lehn and coworkers (6-10) introduced a new class of complexing agents, diaza-polyoxamacrobicycles called "cryptands", which contain tri-dimensional molecular

A. Complexation of Alkali and Alkaline Earth Metal Ions By Cryptands

Although alkali and alkaline earth metal cations play a role of great importance both in chemistry and in biology, their coordination chemistry has mainly been developing in recent years with the advent of natural (1) or synthetic macrocyclic and macropolycyclic ligands, which are capable of forming strong complexes with the above metal ions.

Macrocyclic polyethers or "crown" ethers, synthesized in 1967 by Pedersen (2,3) were the first such complexing agents to appear. A typical crown is shown in Figure 1. These macrocyclic ligands contain a molecular, two-dimensional cavity, the diameter of which can be varied by changing the number of methylene groups and/or ether oxygens in the ring. Certain cyclic polyethers not only strongly bind particular alkali and alkaline earth metal ions but selectively bind one or more of these ions in preference to the others in each series (4,5). The parameters which influence the selectivity and binding properties of macrocycles include the type(s) and number of binding sites in the ring, the relative sizes of the ion and the macrocyclic cavity, the physical placement of the binding sites, steric hindrance in the ring, the solvent and extent of solvation of the ion and binding sites, and the electrical charge of the ion.

Shortly thereafter, Lehn and coworkers (6-10) introduced a new class of complexing agents, diaza-polyoxamacrobicycles called "cryptands", which contain tri-dimensional molecular

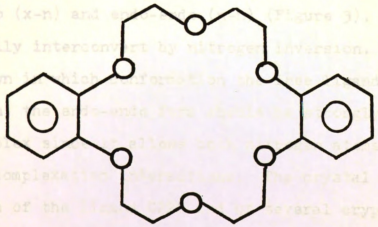

Figure 1. Dibenzo-18-crown-6. The number 6 refers to the total number of oxygens and 18 to the total number of atoms in the polyether ring.

cavities (Figure 2). The size of the cavity can be varied by changing the length of the ether bridges. In general, the selectivity of complexation and stability of complexes are several orders of magnitude greater than that of the crown ethers with the same number of oxygen atoms in the ring.

It has been suggested by Lehn that the term cryptand refer to the ligand and cryptate to the complex. In macrobicyclic complexes, the cryptand may exist in three forms differing by the configuration of the bridgehead nitrogens: exo-exo (x-x), exo-endo (x-n) and endo-endo (n-n) (Figure 3). These forms can easily interconvert by nitrogen inversion. Although it is not known in which conformation the free ligand exists in solution, the endo-endo form should be strongly favored in the complex since it allows both nitrogen atoms to participate in the complexation interactions. The crystal structure determination of the ligand C222 and of several cryptates (11-15) showed that the cation was indeed included in the center of the three-dimensional cavity of the macrocycle which was in the endo-endo form.

exo-exo endo-endo exo-endo

Figure 3. Exo-exo, endo-endo and exo-endo conformation of 222 cryptand.

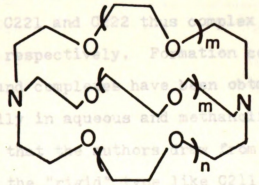

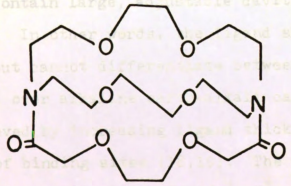

Figure 2. a) Cryptand, C.

C-211 m = 0, n = 1	C-322 m = 1, n = 2
C-221 m = 1, n = 0	C-332 m = 2, n = 1
C-222 m = n = 1	C-333 m = n = 2
	C-22C_8 m = 1 (third bridge = -$(CH_2)_8$-)

b) The dilactam of C-222.

Cryptates of alkali and alkaline earth cations, show cavity selectivity, the preferred cation being that whose size most closely fits the ligand cavity (Table 1). The cryptands C211, C221 and C222 thus complex preferentially Li^+, Na^+ and K^+ respectively. Formation constants of alkali-macrocyclic ligand complexes have been obtained (16-18) potentiometrically in aqueous and methanolic solutions. The conclusions that the authors draw from their study is that ligands of the "rigid" type like C211, C221 and C222 present a stability peak for the optimal cation. The ligands of the "flexible" type on the other hand as C322, C332 and C333 which contain large, adjustable cavities, show plateau selectivity. In other words, the ligand shows large selectivity for K^+/Na^+ but cannot differentiate between K^+, Rb^+ and Cs^+.

Control over alkaline earth-alkali cation selectivity may be achieved by increasing ligand thickness or change in the number of binding sites (18,19). The authors investigated the complexation selectivity for Na^+, K^+ and Ba^{2+} in methanol and water solutions. The effect of decreasing the number of binding sites is clearly shown by comparing cryptands C222 and $C22C_8$. While the first has a complexation selectivity $Ba^{2+}/K^+ \sim 10^4$, the latter compound with two oxygen binding sites less, gives $< 10^{-2}$ for the same ratio.

By replacing also the oxygen binding sites in cryptands C211, C221, C222 by nitrogen or sulfur, they found (20,21) that as the number of oxygen sites decreases the stability and selectivity of the alkali and alkaline earth cation

Table 1. Ionic Radii of Metal Cations. Approximate Cavity Radius and Number of Binding Sites of Ligands.

Cation	Ionic Radius r_i(A)[a]	Ligand	Cavity Radius (A)[b]	No. of Binding Sites
Li^+	0.78	C211	0.8	6
Na^+	0.98	C221	1.1	7
K^+	1.33	C222	1.4	8
Rb^+	1.49	C322	1.8	9
Cs^+	1.65	C332	2.1	10
Mg^{2+}	0.78	C333	2.4	11
Ca^{2+}	1.06			
Sr^{2+}	1.27			
Ba^{2+}	1.43			

[a] Pauling values.

[b] Measured on Corey-Pauling-Kaltun molecular models.

complexes decrease rapidly while they increase for transition metals and metals of group IB and IIB. An especially interesting feature is that the polyamine cryptands provide a means of trapping transition metal cations inside the molecular cavity imposing thus coordination geometries and may modify the spectral and redox properties of the cations.

The kinetics of the complexation by cryptands have been studied by a variety of techniques. Lehn et al. (22) studied the kinetics of the complexation by temperature variations in proton nmr measurements of K^+-C222, Na^+-C222 and Tl^+-C222 cryptates in D_2O solutions of cation exchange. They concluded that the mechanism is a dissociation-complexation process rather than a bimolecular process. The exchange becomes slower as the stability of the cryptate increases. The symmetrical splitting caused by Tl^+-H spin-spin coupling indicates that the ion is in the center of the molecular cavity. Dye and coworkers (23) studied the exchange rates of sodium-C222 cryptate in ethylenediamine by using the sodium-23 nmr technique. They found an activation energy of 12.2 ± 1.1 $kcal \cdot mol^{-1}$ for the dissociation of the complex. The rate of dissociation of the complex is also similar to that found by Lehn et al. (22) for aqueous solutions. Kintzinger and Lehn (24) used double probe ^{13}C and ^{23}Na nmr studies to obtain correlation times and ^{23}Na quadrupolar coupling constants for sodium cryptates. They found that the ^{23}Na nuclear quadrupole coupling constant decreased with an increasing

number of oxygen atoms in the ligand. The chemical shift (referred to a 0.25 M aqueous NaCl solution as external reference), has values of -11.15 ppm for Na^+-C211, +4.25 ppm for Na^+-C221, and +11.45 ppm for Na^+-C222. The line widths at half height were 132 ± 3, 46 ± 2 and 29 ± 1 Hz respectively.

Complexation studies were extended by Cahen et al. (25) to lithium ion complexes with cryptands C211, C221 and C222 in water and several nonaqueous solvents. They used ^7Li nmr technique and they found that the chemical shift of the lithium ion complexed by C211 is essentially solvent and anion independent, indicating that the lithium ion is completely shielded by the cryptand molecule, as was expected. On the other hand, the chemical shifts of Li^+-C221 and especially Li^+-C222 complexes are solvent dependent. They also determined the formation constants of Li^+-C222 in water and pyridine by using ^7Li nmr technique. The values obtained were log K = 0.99 ± 0.15 for water and log K = 2.94 ± 0.10 for pyridine.

By using temperature variations in ^7Li nmr measurements, they studied (26) the kinetics of complexation reactions of the lithium ion with cryptand C221 in pyridine, water, dimethyl sulfoxide, dimethylformamide, and formamide and with C221 in pyridine. Activation energies (E_a), rate constants (k_1), and values of $\Delta H_o^{\ddagger}$, $\Delta S_o^{\ddagger}$, and $G_o^{\ddagger}$ for the release of Li^+ from the cryptates in the above solvents, are reported.

Loyola et al. (27) used stopped-flow technique to measure the activation parameters for the formation of Ca^{2+}

complexes with C222, C221 and C211, Sr^{2+} with C222 and C221 and Ba^{2+} with C222 by using murexide and metal-phthalein indicators. They also determined the values for the dissociation of the Ca^{2+} complexes of the three cryptands by using appropriate alkali metal ions as scavengers for dissociated cryptands. They conclude that the reaction order that they found $Ca^{2+} < Sr^{2+} < Ba^{2+}$ toward C222 and $Ca^{2+} < Sr^{2+}$ toward C221 parallels the expected lability of the metal ion and indicates that desolvation of the metal ion is important before or at the rate-determining stage of cryptate formation. The pH dependence of formation of Ca^{2+}, Sr^{2+} and Ba^{2+} complexes of C222 has also been measured. Their results support the assumption of unreactivity of the protonated cryptands.

Alkali metals can be solubilized in nonpolar solvents by the addition of an appropriate cryptand to the solution (28). Dye and coworkers (29,30) first found spectrophotometric evidence for the existence of alkali metal anions (Na^-, K^-) in amine and ether solutions in which they used cryptand or crown to dissolve alkali metals. They were able to crystallize the Na^+-C222-Na^- compound (31) by dissolving pure sodium in ethylamine (EA) and in THF in the presence of C222. Due to the complexation of the cryptand with Na^+, the concentration of dissolved metal was greatly enhanced and the gold-colored Na^+-C222-Na^- compound precipitated at low temperature and its crystal structure was determined (32). They were able to monitor the ^{23}Na chemical shift of the sodium anion (33). At low temperatures they observed two nmr resonances, a broad

one for Na^+-C222 and a narrow one for Na^- which is about 63 ppm upfield from saturated aqueous NaCl solution. They extended the study and measured the ^{23}Na nmr spectrum of Na^+-C222-Na^- as a function of temperature as well as that of $^{87}Rb^-$ in EA and THF and of ^{133}Cs in THF.

In addition to the study of the complexation of metal ions with macrobicyclic ligands (denoted as [2]-cryptands), Lehn et al. also synthesized macrotricyclic ligands (denoted as [3]-cryptands) (35-38). They are formed by two macrocycles linked by two bridges (Figure 4). They define three cavities:

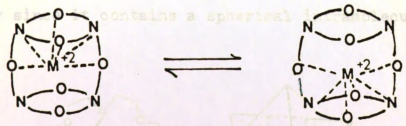

Figure 4. Intramolecular cation exchange in mononuclear complexes of a macrotricyclic cryptand.

two lateral circular cavities inside the macrocycles and a central cavity. The size of central and lateral cavities can be changed by modifying the size of the macrocycles and the length of bridges. They also form strong complexes with various metal cations. Their complexes are non-symmetric mononuclear and symmetric binuclear 3 -cryptates. Also

heteronuclear bimetallic [3]-cryptates can be obtained. The cation exchange rate between sites on two rings inside the cavity of a [3]-cryptate has been studied by ^{13}C nmr (39). The spectral changes observed agree with an internal cation exchange between "top" and "bottom" of the molecule as shown in Figure 4. Intermolecular exchange also occurs, but at much slower rate than the intramolecular one. Both intra- and intermolecular cation exchange is fast for the weak complexes of the ligand with alkali cations.

Another [3]-cryptand has been synthesized recently (40). As shown in Figure 5a, this molecule displays an attractive topology since it contains a spherical intramolecular cavity

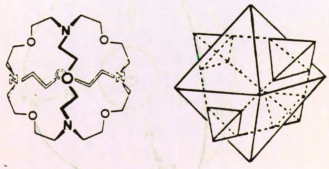

Figure 5. Newly synthesized macrotricyclic cryptand.

into which the substrate may be included. The spherical cavity has ten binding sites in an octahedrotetrahedral arrangement (Figure 5b). The four nitrogens are located at the corners of a tetrahedron and the six oxygens are at the corners of an octahedron, whose centers coincide and their

ten corners lie on the same sphere. The logarithms of the stability constants for the K^+, Rb^+ and Cs^+ complexes in water are 3.4, 4.2 and 3.4 respectively. The proton nmr kinetics study showed that the cation exchange rates are slow, and the activation energies for the dissociation of the complex are rather high, of the order of 16 kcal/mole. This ligand also forms very stable complexes with anions like Cl^- and Br^- (40). The anion cryptates have been studied by ^{13}C nmr. The structure proposed is shown below (Figure 6), and it has been confirmed by the determination of crystal structure (42).

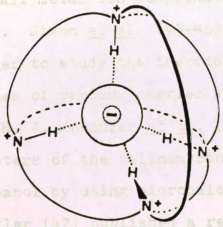

Figure 6. Anion cryptate.

The ligand is in the tetraprotonated form and the anion is held inside the cavity. The logarithms of the stability constants of the chloride and bromide inclusion complexes

of the tetraprotonated ligand have been determined to be > 4.0 and < 1.0 respectively in water. They display remarkable Cl^-/Br^- selectivity.

B. Study of the Thermodynamic Parameters of the Complexation of Crowns and Cryptands

As previously indicated, results of numerous studies of the stabilities of cation complexes of crowns and cryptands have been reported in the literature. From the formation constant, K, one can obtain the free energy of complexation ΔG_c. Analysis of the free energy of complexation into enthalpy, and entropy, gives a better understanding of the thermodynamics of the complexation reaction. However, the enthalpy and entropy of alkali metal ion complexation have not been studied in much detail. Simon et al. (43-45) used a computerized microcalorimeter to study the thermodynamic properties of alkali complexes of various carrier antibiotics in methanol and ethanol. H. J. Moschler et al. (46) studied the thermodynamic parameters of the valinomycin-potassium iodide complex in ethanol by using microcalorimetric technique as well. R. Winkler (47) published a review article on the kinetics and thermodynamics of alkali ion complexes in solution.

Frensdorff (48) in his original report of the thermodynamics of cyclic polyether complexation reactions, noted the remarkable increase in the stability of the complexes of cyclic polyethers over their linear counterparts. By comparing the complexes of Na^+ and K^+ with pentaglyme and

18-crown-6 in methanol, he noted a 10^3 to 10^4 enhancement of the stability constant in the cyclic ligand complexes. This phenomenon is described as the "macrocyclic effect" and the term was first postulated by Cabbiness and Margerum (49) who used this term in order to distinguish it from the chelate effect. Although it is well established that the chelate effect is of entropic origin, no agreement has been reached as to whether the macrocyclic effect is a result of a more favorable enthalpy or entropy terms in the cyclic ligand reactions. Cabbiness and Margerum (49) reported the macrocyclic effect for the cyclic tetraamines and proposed that ligand solvation and configuration were the important factors to be considered rather than the changes in translational entropy.

In a later publication, Hinz and Margerum (50) reported the detailed study of the thermodynamic properties of nickel(II)-tetramine complexes in water. They found that the enhanced stability of the cyclic as compared to the open-chain ligand (the macrocyclic effect), is almost entirely due to more favorable enthalpy changes. They attributed these changes to the decreased ligand solvation of the macrocycle which has less amine-hydrogen-bonded water to be displaced in complex formation. Dei and Gori (51) offer the same explanation as above after studying the enthalpies of reaction of these same ligands with Cu^{2+} in water. Paoletti et al. (52) conclude that the macrocyclic effect is due both to entropy and enthalpy terms, while Kodama and

Kimura (53) after studying the copper(II)-tetramine complexes by polarography state that the macrocyclic effect is due solely to the entropy term.

The enthalpy and entropy changes for the complexation reaction of crown ethers have been studied and a discussion of the results will help clarify the nature of the macrocyclic effect. There are distinct advantages in studying the macrocyclic effect using crown ethers as opposed to tetraamine ligands.

a) The ligands are uncharged at neutral pH and their complexing ability is not pH dependent,

b) the reaction kinetics are rapid so that equilibrium measurements are readily obtained,

c) among the metal ions which form complexes with these ligands are the alkali and alkaline earth cations which can be considered to be simple charged spheres, unlike transition metal ions which have specific stereochemical preferences.

Izatt et al. (54,58) used a precision thermometric titration calorimeter to study the thermodynamics of formation of complexes of crown ethers. They studied the interaction of 15-crown-5, 18-crown-6 and of two isomers of dicyclohexo-18-crown-6 with Na^+, K^+, Rb^+, Cs^+, Ag^+, Tl^+, NH_4^+, $CH_3NH_3^+$, Sr^{2+}, Ba^{2+}, Pb^{2+}, Hg^{2+} and Ca^{2+} ions in aqueous solutions at 25°C and μ = 0.1. With the exception of Na^+, Ag^+ and Hg^{2+} with the A isomer of dicyclohexo-18-crown-6, all the reactions studied are exothermic ($\Delta H < 0$). In many cases the entropy change of the complexation reaction is negative. Their data

contain no reproducible trends in ΔH or ΔS among the complexes of cations studied to explain the macrocyclic effect. They also performed (59) calorimetric titration studies of the interaction between Na^+, K^+, Rb^+, Cs^+, Ca^{2+}, Sr^{2+} and Pb^{2+} and the cyclic polyethers benzo-15-crown-5, 18-crown-6, dibenzo-24-crown-8 and dibenzo-27-crown-9 in CH_3OH-H_2O solvents. In all cases negative ΔH and ΔS values for the complexation reaction were found. They conclude that as the cyclic polyether ring size increases, the ΔS values for the 1:1 reaction of a given cation become more negative, suggesting that significant conformation changes may be important in the formation of these complexes.

Recently Izatt et al. (60) synthesized two compounds, 2,6-dioxo-18-crown-6 and 2,4-dioxo-18-crown-6 similar to 18-crown-6 having carbonyl groups as valinomycin does and studied their thermodynamic properties with various cations in methanol. They found decreased stabilities of the new complexes due to less exothermic ΔH values, but more favorable $T\Delta S$ values. By introducing a pyridine ring in 18-crown-6, they synthesized a new crown ether which forms unusually stable complexes with Na^+, K^+, Ag^+ and Ba^{2+} in methanol. They found that the entropy term is the one favoring complexation while the enthalpy term works in opposition.

Schori et al. (62) studied by conductance the thermodynamics of the complexation of various crown ethers with sodium salts in DMF and DME at different temperatures. They found that the complexation reaction in DME is both

entropy and enthalpy driven. E. Mei et al. (63,64) studied the kinetics and thermodynamics of the reaction of 18-crown-6 with Cs^+ in pyridine by using Cs-133 nmr technique. They found that the reaction occurs in two steps and that the enthalpy and entropy change for the second step are both negative.

An extension of the macrocyclic effect is the cryptate effect which is described as the enhancement of the stability of the macrobicyclic complexes as compared to the macromonocyclic ones. Kauffmann et al. (65) determined the enthalpies and entropies of formation of alkali and alkaline-earth cryptate complexes from calorimetric measurements. Their results with the alkali cations are listed in Table 2. They show large negative enthalpies and sometimes negative entropies of complexation. The Sr^{2+} and Ba^{2+} as well as $[Li^+C211]$, $[Na^+C221]$ cryptates are of the enthalpy dominant type with also a favorable entropy change. The Ca^{2+} and $[Li^+C221]$ cryptates are entirely entropy stabilized with about zero heat of reaction. They conclude that the cryptate effect is of enthalpic origin. The enthalpies of complexation show selectivity peaks as the stabilities do, whereas the entropy changes do not. E. Mei et al. (66) studied the thermodynamics of the complexation of Cs^+ with C222, cryptand in acetone, propylene carbonate and N,N'-dimethylformamide by using Cs-133 nmr technique. They found that two kinds of complexes exist in solutions, an inclusive and an exclusive one, and they calculated the enthalpy and entropy changes for both types.

Table 2. Thermodynamic Quantities of Alkali-Cryptate Complexation Reaction Measured by Calorimetry at 25°C in Water.

Ligand	Thermodynamic Parameter	Li^+(0.78 Å)	Na^+(0.98 Å)	K^+(1.33 Å)	Rb^+(1.49 Å)	Cs^+(1.65 Å)
211	ΔH_c	- 5.1	-5.4	---	---	---
(1.6 Å)	ΔS_c	8	-3	---	---	---
221	ΔH_c	0.0	-5.35	- 6.8	- 5.4	---
(2.2 Å)	ΔS_c	11.4	6.2	- 4.7	- 6.5	---
222	ΔH_c	---	-7.4	-11.4	-11.8	---
(2.8 Å)	ΔS_c	---	-7	-14.1	-19.8	---
322	ΔH_c	---	---	- 3	- 4.2	-5.4
(3.6 Å)	ΔS_c	---	---	0	- 4.7	-9.9

Note: ΔH_c, ΔS_c, enthalpies and entropies of cryptation

ΔH in kcal/mole

ΔS in entropy units e.u.

Conclusion

The transport of alkali ions by ionophors through artificial and biological membranes is a subject of considerable interest to chemists and to biologists. It has been shown that cyclic polyethers (crowns) as well as naturally occurring antibiotic ionophores, such as valinomycin (67), are alkali ion transporters. Cryptates, where the alkali ion is completely enclosed into a hydrophobic sheath, should be at least as good ion transporters as crowns. However, diazapolyoxa cryptands are quite basic. For example, the acidity constants of cryptand C222 are, $K_1 = 5.25 \times 10^{-8}$ and $K_2 = 2.51 \times 10^{-10}$ (18). Since the complexes can only be formed when the ligand is deprotonated, it is obvious that complexation reaction can only occur at high pH. As expected no ion transport was observed through black lipid membranes at neutral pH (68). Black lipid membranes are notoriously unstable at high pH's and attempts to measure ion transport in basic aqueous solutions were unsuccessful.

The penultimate step in the synthesis of cryptand C222 is the corresponding dilactam (Figure 2b). It is obvious that the compound is much less basic than the cryptand. Indeed, preliminary experiments seem to indicate that the C222-dilactam (C222D) does transport alkali ions through black lipid membranes (68).

It was of interest to us, therefore, to study the complexing ability and the thermodynamics of the complexation reaction of the C222D in water and in nonaqueous solvents

in order to see how this change in the structure of the ligands affects its interactions with alkali metal ions. There are no reports in the literature on complexation studies of this ligand.

CHAPTER II

EXPERIMENTAL PART

A. Salts

Lithium perchlorate (Fisher) was dried at 190°C for several days. Sodium tetraphenylborate (Baker) and sodium perchlorate (G. F. Smith) were used without further purification except for drying. They were dried under vacuum at 60°C for 72 hours. Cesium thiocyanate (Rocky Mountain Research, Inc.) was recrystallized from absolute ethanol and vacuum dried. Cesium tetraphenylborate was prepared by a metathetical reaction between equimolar amounts of sodium tetraphenylborate and cesium chloride in a tetrahydrofuran-water mixture. The cesium tetraphenylborate precipitate was filtered and washed with conductance water until flame photometry registered sodium content of the order of conductance water. Drying was done under vacuum [illegible] hours. Anhydrous silver perchlorate (G. Frederick Smith Chemical Co.) was dried over P_2O_5 under vacuum and kept in the dark to prevent decomposition. Potassium hexafluorophosphate (Alfa Products) was recrystallized from water and dried under vacuum over P_2O_5 for at least 24 hours before use. The preparation of ^6Li perchlorate is described in reference (69).

B. Ligands

The dilactam of cryptand 222 (C222D) was synthesized by a modification (70) of the method of Dietrich *et al.* (9) which has been described in detail (71). The ligands 2,2'-bipyridine, 4,4'-dimethyl,2,2'-bipyridine, and 2,2'-biquinoline were obtained from G. Frederick Smith and were dried under vacuum.

A. Salts

Lithium perchlorate (Fisher) was dried at 190°C for several days. Sodium tetraphenylborate (Baker) and sodium perchlorate (G. F. Smith) were used without further purification except for drying. They were dried under vacuum at 60°C for 72 hours. Cesium thiocyanate (Rocky Mountain Research, Inc.) was recrystallized from absolute ethanol and vacuum dried. Cesium tetraphenylborate was prepared by a metathetical reaction between equimolar amounts of sodium tetraphenylborate and cesium chloride in a tetrahydrofuran-water mixture. The cesium tetraphenylborate precipitate was filtered and washed with conductance water until flame photometry registered sodium content of the order of conductance water. Drying was done under vacuum at 80°C for 48 hours. Anhydrous silver perchlorate (G. Frederick Smith Chemical Co.) was dried over P_2O_5 under vacuum and kept in the dark to prevent decomposition. Potassium hexafluorophosphate (Alfa Products) was recrystallized from water and dried under vacuum over P_2O_5 for at least 24 hours before use. The preparation of ^6Li perchlorate is described in reference (69).

B. Ligands

The dilactam of cryptand 222 (C222D) was synthesized by a modification (70) of the method of Dietrich et al. (9) which has been described in detail (71). The ligands 2,2' bipyridine, 4,4'-dimethyl,2,2'-bipyridine, and 2,2'-biquinoline were obtained from G. Frederick Smith and were dried under vacuum.

C. Solvents

Nitromethane (spectroscopic grade, Aldrich) was fractionally distilled over phosphorus pentoxide under reduced pressure and dried for 24 hours over freshly activated 5A Linde molecular sieves. Dimethyl sulfoxide (Fisher), was dried over Linde 4A molecular sieves for 2 days. Methanol (Fisher) was first fractionally distilled from calcium hydride and then from magnesium turnings in a nitrogen atmosphere. Dimethylformamide (Fisher) was vacuum distilled over P_2O_5. Propylene carbonate (Aldrich) was dried for 2 days over Linde 4A molecular sieves followed by vacuum distillation. Acetonitrile (Matheson Coleman and Bell) was refluxed over calcium hydride and then fractionally distilled over granulated barium oxide. Pyridine (Fisher) was refluxed over granulated barium oxide and then fractionally distilled in nitrogen atmosphere. Tetrahydrofuran (Baker) was dried over metallic sodium and benzophenone by refluxing.

The molecular sieves used were activated by heating them at 500°C under dry argon for 12 hours. Analyses for water in salts and solvents, where possible, were carried out with an automatic Karl Fischer Aquatest II (Photovolt Corp.) titrator. In all solvents the water content was < 100 ppm. Important solvent properties and solvent abbreviations used in this thesis are listed in Table 3.

Table 3. Key Solvent Properties and Correction for Magnetic Susceptibility on DA-60.

Solvents	Volumetric Susceptibility X 10^6	Dielectric Constant	Gutmann's Donor Number	Correction on DA-60 (ppm)
Acetonitrile	-0.534	37.5	14.1	-0.39
Dimethylformamide (DMF)	-0.573	36.71	26.6	-0.31
Dimethylsulfoxide (DMSO)	-0.605	46.68	29.8	-0.24
Methanol	-0.515	32.7	25.7*	-0.43
Nitromethane	-0.391	35.9	2.7	-0.69
Propylene Carbonate (PC)	-0.634	65.0	15.1	-0.18
Pyridine	-0.612	12.40	33.1	-0.23
Tetrahydrofuran (THF)	-0.613	7.58	20.0	-0.22
Water	-0.720	78.54	33.0*	0.00

*Predicted (72)

D. Sample Preparation

Since lithium salts are very hygroscopic, the water content of each solution was carefully maintained at the lowest possible level so that its total concentration remained less than 1% of the salt concentrations. All lithium, sodium and cesium salt solutions were prepared in a dry-box under nitrogen atmosphere. Dilute solutions of the salts were prepared by an appropriate dilution of a stock solution. Ligands were weighed out in the desired amount into 1 ml volumetric flask and then introduced into a dry-box for subsequent manipulation.

E. Instrumental Measurements

1. Lithium-7, Sodium-23 and Cesium-133 NMR

Sodium-23, lithium-7 and cesium-133 nmr measurements were made on a Fourier transform instrument using the magnet of a Varian DA-60 nmr spectrometer equipped with a wide-band probe capable of multinuclear operation (73), and computer controlled rf pulse generation and data collection which has been described previously (74). An external ^{1}H field lock was used to maintain field stability. A Nicolet Instrument Corporation 1082 computer was used. The computer program (74) was used to generate a single rf pulse and to collect the resultant free induction decay (FID) signal. Data treatment was performed by the Nicolet FT-NMR Program (NIC-80/S-7202D) (75). The instrument was operated at a field of 1.4092 T and at frequencies of 15.871 MHz, 23.318 MHz and 7.871 MHz for ^{23}Na, ^{7}Li and ^{133}Cs respectively.

The references used were 4.0 M $LiClO_4$ in water and 3.0 M $LiClO_4$ in methanol for the lithium-7 measurements, 3.0 M NaCl in water and 2.5 M $NaClO_4$ in methanol for the sodium-23 measurements and 0.5 M CsBr in water and 0.2 M CsBr in methanol for the cesium-133 measurements. 10 mm nmr tubes were used.

All the chemical shifts reported in this thesis are with respect to 4.0 M $LiClO_4$ in water and 3.0 M NaCl in water and infinite dilution chemical shift of the cesium ion in water. A positive value of δ indicates a shift to higher field.

The chemical shifts reported are corrected for differences in bulk diamagnetic susceptibility between sample and reference according to the relationship of Live and Chan for non-superconducting spectrometers (76).

$$\delta_{corr} = \delta_{obs} + \frac{2\pi}{3}(X_v^{ref} - X_v^{sample}) \qquad (1)$$

where X_v^{ref} and X_v^{sample} are the volume susceptibility of the reference and sample solutions respectively and δ_{obs} and δ_{corr} were calculated on the basis of published magnetic susceptibilities of various solvents (77). The magnitudes of corrections for various solvents are shown in Table 3.

2. Carbon-13 NMR

Carbon-13 nmr measurements were made on a Varian CFT20 Fourier transform nmr spectrometer equipped with computer controlled pulse generation and data collection. The

instrument was operated at a field strength of 1.8682 T and at a frequency of 20 MHz (78).

For all ^{13}C nmr studies, methanol was used as an external reference and D_2O was used for locking the system. The solvent peak was used as a secondary reference. All chemical shifts reported are referenced to TMS. The sample solution was in an 8 mm nmr tube which was coaxially centered in the 10 mm nmr tube containing the external methanol reference with D_2O for locking the system.

3. Far-Infrared Spectra

The far-infrared spectra were obtained with a Digilab FTS-16 spectrometer. The FTS-16 is essentially a rapid-scan Michelson interferometer operated under computer control. The theory and operation of this instrument have been previously described (79). All spectra were obtained by using the 3- or 6- μm mylar beam splitters which cover the ranges of 600-150 and 425-100 cm^{-1}, respectively. The spectra were obtained at a nominal resolution of 4 cm^{-1}, which gives a data point every 2 cm^{-1}. The instrument was operated in the single beam mode. The reference spectrum was stored in the computer memory and subtracted from the solution spectra. Standard demountable cells (Barnes Engineering Co.) were used with 2-mm polyethylene discs, and the path length was maintained at 0.1 or 0.2 mm. All spectra were smoothed by using the 9-point smoothing routine developed by P. R. Handy (79).

4. Data Handling

Extensive use of the CDC-6500 computer was made to evaluate data. Program KINFIT (80) was employed to determine complexation constants. A linear least squares program was used to obtain enthalpies and entropies.

CHAPTER III

SPECTROSCOPIC STUDIES OF COMPLEXATION OF ALKALI METAL IONS, WITH THE DILACTAM OF C222

A. Lithium-7, Sodium-23 and Cesium-133 NMR Study of C222D Complexes in Various Solvents

Nuclear magnetic resonance (nmr) of alkali nuclei such as ^{7}Li, ^{23}Na, ^{39}K and ^{133}Cs is one of the most powerful techniques for the elucidation of the nature of the various alkali species in solutions and the equilibria among these species. The chemical shifts and line widths of the nuclear resonances of alkali metal ions nuclei can give information about ion-ligand, ion-solvent and ion-ion interactions.

Lithium-7 and cesium-133 nuclei are highly suitable for nuclear magnetic resonance studies because the resonance lines of Li^{+} and Cs^{+} ions in solutions are exceptionally narrow and chemical shifts can be measured with considerable accuracy. Sodium-23 has a large quadrupole moment (0.1×10^{-24} cm^{2}), and its chemical shift range is rather large (about 40 ppm). These two factors make ^{23}Na nucleus a sensitive probe of the electronic environment around the nucleus as previous studies in this laboratory (81-84) and elsewhere (85-87) have shown. ^{7}Li, ^{23}Na and ^{133}Cs nmr have been found to be useful techniques for the determination of the formation constants of weak and medium strength complexes (25,88,89,90).

The purpose of the study of this chapter is the investigation of the complexation reaction of Li^{+} ion, Na^{+} ion and Cs^{+} ion with the dilactam of C222 in different solvents and the determination of the formation constants, where possible.

Alkali metal ion chemical shifts were determined as a function of dilactam/metal ion mole ratios and the results are shown in Tables 4-6. In all cases only one resonance of the metal ions was observed irrespective of the ligand/metal ion mole ratio. In general, if the rate of exchange of the metal ion between the two sites (free ion in the bulk solution and the complex), is larger than $\sqrt{2}/\pi\Delta\nu$, ($\Delta\nu$ = difference between the characteristic resonance frequency in Hz in each site) only one population-average resonance is observed.

The frequency of the lithium-7 resonance in water, dimethyl sulfoxide, dimethylformamide and methanol was found to be essentially independent of the ligand/Li^+ mole ratio (Figure 7). It is evident that in these solvents the immediate environment of the lithium ion is not changed upon addition of an excess of ligand and, therefore, that at best only a very weak Li^+-C222D complex is formed. It should be noted that the above solvents have a strong solvating ability as indicated by the respective Gutmann donor numbers of 33.0, 29.8, 26.6, 25.7 (91), and consequently in these media a relatively weak complexing agent is not capable of effectively desolvating lithium ion. The above results agree with previous observations that in dimethyl sulfoxide solutions (25) C222 cryptand does not form a stable complex with lithium ion.

On the other hand, as seen in Figure 8, in solvents of medium to weak donor ability such as acetone, tetrahydrofuran

Table 4. Lithium-7 Chemical Shifts at Various Mole Ratios, $[C222D]/[Li^+]$, in Nitromethane at 33 ± 2° C.

Salt	$[Li^+]$M	$[C222D]/[Li^+]$	δ(ppm)
$LiClO_4$	0.012	0.00	0.34
		0.25	0.19
		0.43	0.11
		0.58	0.00
		0.67	-0.12
		0.75	-0.23
		0.83	-0.34
		0.95	-0.44
		1.00	-0.52
		1.21	-0.52
		1.33	-0.52
		1.54	-0.54
		1.75	-0.54
		2.00	-0.59
		2.51	-0.60

Table 5. Sodium-23 Chemical Shifts at Various Mole Ratios, $[C222D]/[Na^+]$, in Various Solvents, at 25 ± 2°C.

Solvent	Salt	$[Na^+]$M	$[C222D]/[Na^+]$	δ(ppm)	$\Delta\nu_{\frac{1}{2}}$(Hz)
Pyridine	$NaClO_4$	0.015	0.00	1.0	44
			0.33	0.6	112
			0.66	0.5	154
			0.94	0.1	208
			1.27	-0.1	217
			1.60	0.1	270
			2.11	0.1	272
CH_3NO_2	$NaBPh_4$	0.05	0.00	14.5	16
			0.49	7.3	212
			1.00	4.7	607
			1.27	5.1	605
			1.99	4.8	646
CH_3CN	$NaClO_4$	0.015	0.00	7.6	8
			0.53	4.9	51
			0.84	3.3	93
			1.00	2.3	114
			1.19	2.0	119
			1.28	1.7	125
			1.40	1.7	205
			1.93	1.7	180

Table 5. Continued

Solvent	Salt	$[Na^+]$M	[C222D]/$[Na^+]$	δ(ppm)	$\Delta\nu_{\frac{1}{2}}$(Hz)
MeOH	$NaClO_4$	0.015	0.00	4.0	18
			0.46	3.6	24
			0.93	3.7	39
			1.40	3.5	68
			2.20	3.4	120
H_2O	$NaClO_4$	0.010	0.00	0.53	14
			0.50	0.46	15
			1.00	0.62	14

Table 6. Cesium-133 Chemical Shifts at Various Mole Ratios, [C222D]/[Cs^+], in Various Solvents, at 25 ± 2°C.

Solvent	Salt	[Cs^+]M	[C222D]/[Cs^+]	δ(ppm)
DMF	$CsBPh_4$	0.015	0.00	0.34
			0.40	- 0.28
			1.13	0.34
			2.00	- 0.28
	CsSCN	0.010	0.00	54.62
			0.27	50.59
			0.59	46.33
			0.99	42.69
			1.30	39.82
			1.60	36.87
			2.13	33.47
			2.70	30.12
			3.20	28.57
			5.20	22.21
H_2O	CsBr	0.010	0.00	-1.07
			0.96	-0.75
			2.02	-0.44
CH_3CN	CsSCN	0.010	0.00	-33.86
			0.44	-32.93
			0.77	-32.16
			1.29	-31.54
			1.80	-30.92

Table 6. Continued

Solvent	Salt	$[Cs^+]\underline{M}$	[C222D]/$[Cs^+]$	δ(ppm)
CH_3CN	CsSCN	0.010	2.20	-30.30
			2.60	-29.98
			2.99	-29.52
			3.54	-29.37
			4.25	-28.75
			5.00	-28.90
Pyridine	$CsBPh_4$	0.015	0.00	39.41
			0.53	22.91
			0.80	16.41
			1.20	8.21
			1.81	- 1.39
			2.07	- 3.89
			2.33	- 6.19
			2.80	- 9.54
			3.66	-12.69
			4.37	-14.89
			4.98	-16.49
			10.00	-21.59

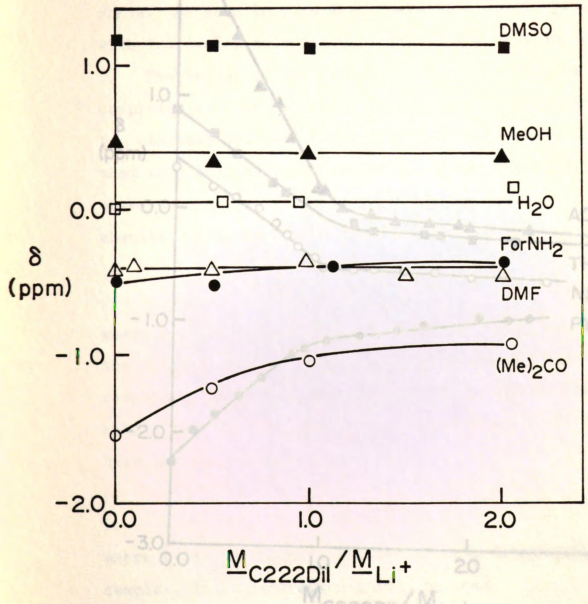

Figure 7. Lithium-7 chemical shift as a function of C222D/Li^+ mole ratio in dimethyl sulfoxide, methanol, aqueous, formamide, dimethylformamide, and acetone solutions. (From Ref. 71).

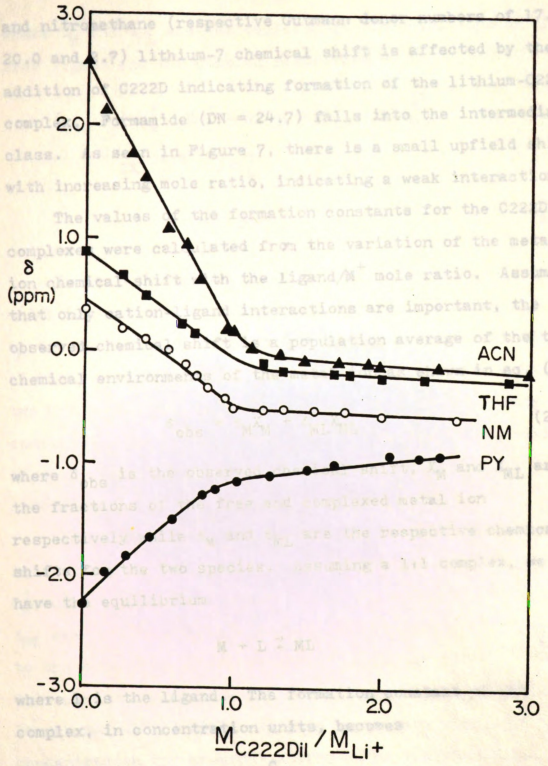

Figure 8. Lithium-7 chemical shifts as a function of C222D/Li^+ mole ratio in acetonitrile,* tetrahydrofuran,* nitromethane and pyridine* solutions. (*From Ref. 71).

and nitromethane (respective Gutmann donor numbers of 17.0, 20.0 and 2.7) lithium-7 chemical shift is affected by the addition of C222D indicating formation of the lithium-C222D complex. Formamide (DN = 24.7) falls into the intermediate class. As seen in Figure 7, there is a small upfield shift with increasing mole ratio, indicating a weak interaction.

The values of the formation constants for the C222D complexes were calculated from the variation of the metal ion chemical shift with the ligand/M^+ mole ratio. Assuming that only cation-ligand interactions are important, the observed chemical shift is a population average of the two chemical environments of the metal ion as shown in eq. (2),

$$\delta_{obs} = \delta_M X_M + \delta_{ML} X_{ML} \qquad (2)$$

where δ_{obs} is the observed chemical shift, X_M and X_{ML} are the fractions of the free and complexed metal ion respectively while δ_M and δ_{ML} are the respective chemical shifts for the two species. Assuming a 1:1 complex, we have the equilibrium

$$M + L \rightleftarrows ML \qquad (3)$$

where L is the ligand. The formation constant of the complex, in concentration units, becomes

$$K = \frac{C_{ML}}{C_M C_L} \qquad (4)$$

where C_M and C_{ML} are the equilibrium concentrations of the free ligand and the complex respectively.

$$\delta_{obs} = (KC_M^t - KC_L^t - 1) \pm (K^2C_L^{t^2} + K^2C_M^{t^2} - 2K^2C_M^tC_L^t + 2KC_L^t + 2KC_M^t + 1)^{\frac{1}{2}}$$

$$\frac{\delta_M - \delta_L}{2KC_M^t} + \delta_{ML} \qquad (5)$$

In eq. (5), C_M^t and C_L^t, the total concentration of the metal ion and of the ligand respectively, are known and δ_M can be easily determined from measurements on solutions of lithium salts without the ligand. Eq. (5) then contains two unknowns K and δ_{ML}. In the case of a rather strong complex δ_{ML} can be determined experimentally by the addition of such excess of L that essentially all of the metal is complexed.

In the case of weak complexes eq. (5) is solved by the following procedure. The experimental parameters δ_{obs}, C_M^t, C_L^t and δ_M are substituted into the equation, and K and δ_{ML} are varied until the calculated chemical shifts correspond to the experimental values within the error limits. The data were analyzed on a CDC-6500 computer using the FORTRAN IV program KINFIT (80). Weighed input data were used for concentration and chemical shifts. The results of the above calculations are shown in Table 7.

For more stable complexes with $K_f > 10^4$ the chemical shift-mole ratio plot consists of two straight lines

intersecting at 1:1 mole ratio. Such a plot cannot be analyzed by our equation, and in such cases we can only conclude that $K_f > 10^4$. This behavior was observed for Li^+-dilactam solutions in nitromethane which is not surprising since nitromethane is a very poorly solvating solvent with Gutmann donor number of 2.7.

A more unexpected behavior was observed in pyridine solutions where the lithium-dilactam complex formation constant was found to have a respectable value of log K_f = 2.64. Yet pyridine should be a good solvating solvent as indicated by the donicity of 33 and the magnitude of its sodium-23 chemical shift (92). It is possible however, that pyridine, being a nitrogen donor, or a "soft base", does not solvate strongly a "hard acid" such as Na^+ ion (92). A recent pmr study of Na^+ ion solvations in nonaqueous solvents by Ahmad and Day (93) strongly supports this conclusion.

The lithium-dilactam complex is only slightly more stable in acetonitrile and tetrahydrofuran solutions than in the solvents mentioned above. In the former case replacement of the perchlorate counterion by bromide did not influence the formation constant of the complex.

As seen from Figure 8, ^7Li chemical shifts seem to converge at high dilactam/Li^+ mole ratios. These results seem to indicate that the lithium ion must be inside the dilactam cavity but that it is not insulated completely from the solvents as was the case of Li^+ ion enclosed in the C211 cryptand (25).

The study of the sodium complex with C222D by ^{23}Na nmr was complicated by the limited solubility of the complex in most nonaqueous solvents and also by the quadrupolar broadening of the ^{23}Na resonance due to the unsymmetric structure of the dilactam. Some of the linewidth at half height are $\sim$ 700 Hz and, therefore, the measurements of the chemical shift are much less precise than in the case of ^{7}Li. It should be noted that the quadrupole moment of ^{23}Na is considerably higher than that of ^{7}Li (0.1×10^{-24} cm^2 compared to -4.2×10^{-26} cm^2). Solvents like propylene carbonate (PC), acetone, diglyme, benzene, chloroform, tetrahydrofuran and ethylenediamine were tried, but the solubility was very limited.

It is natural to expect that Na^+ ion will form stronger complexes with C222D than Li^+ since its size is closer to the dimension of the dilactam cavity. Indeed, as shown in Figure 9, sodium-23 chemical shifts--dilactam/Na^+ mole ratio plots show in methanol, dimethylformamide, nitromethane, acetonitrile, and pyridine solutions sharp breaks at 1:1 mole ratio indicating that $K_f > 10^4$. The limiting chemical shifts of the complexed sodium ion are solvent-dependent indicating incomplete insulation of the cation from the solvent.

In dimethyl sulfoxide solutions the ^{23}Na resonance line becomes extremely broad upon addition of C222D. Consequently, the chemical shifts cannot be measured accurately, and no definite conclusions can be made on the stability of the dilactam-Na^+ complex in this solvent.

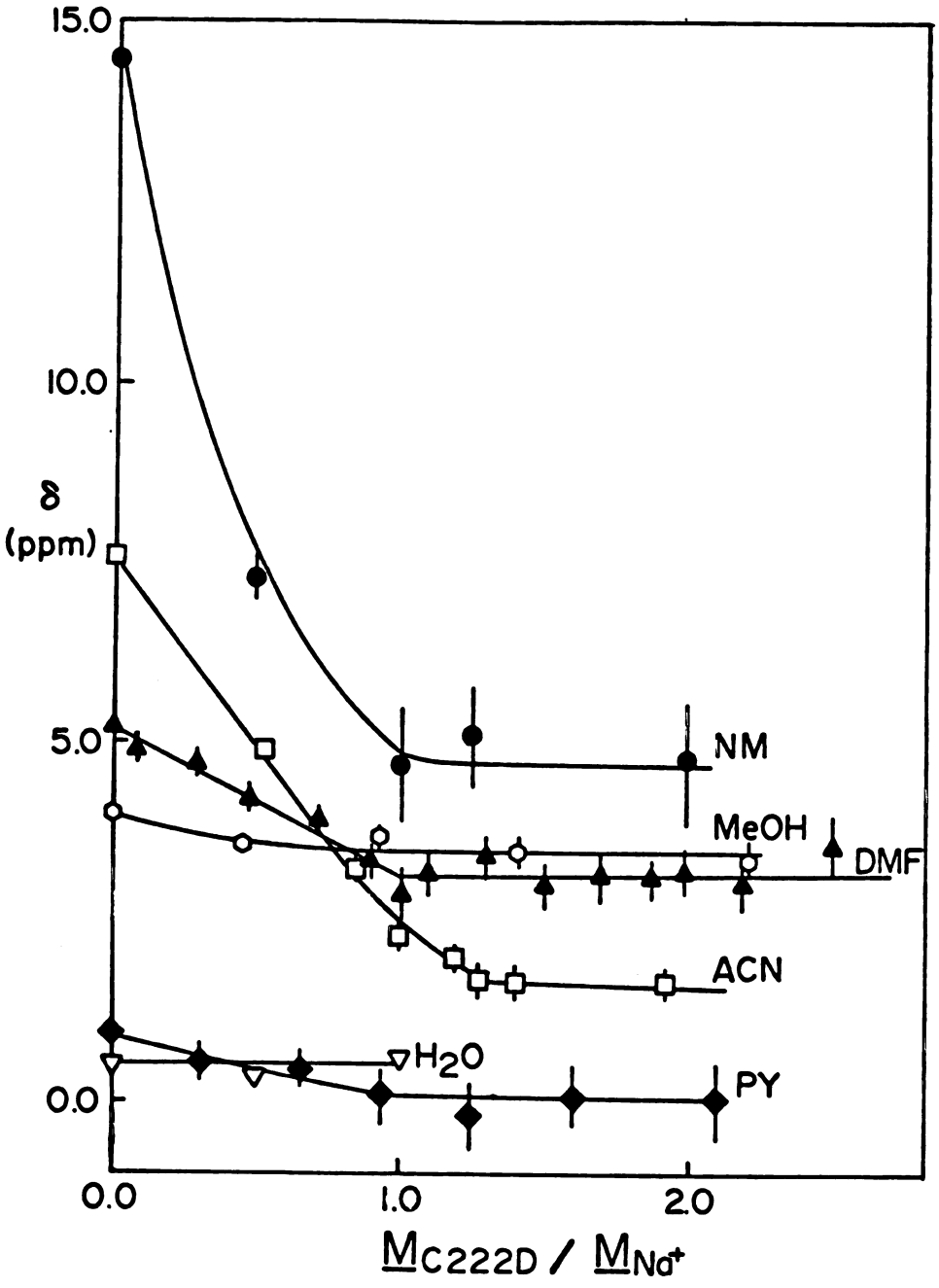

Figure 9. Sodium-23 chemical shifts as a function of C222D/Na^+ mole ratio in nitromethane, methanol, dimethylformamide, acetonitrile, aqueous and pyridine solutions.

The large cesium ion does not fit conveniently into the C222D cavity. As indicated in Figure 10, no ^{133}Cs chemical shift is observed upon addition of the dilactam to cesium salt in DMF solutions. In the case of nitromethane and pyridine solutions (Figure 10) and acetonitrile solutions (Figure 11), addition of the dilactam produced large but gradual downfield shifts indicating formation of weak complexes. The large difference in the limiting chemical shifts of the Cs^+-C222D complex in the above solvents is a good indication that the metal ion remains exposed to the solvent.

Computer analysis of the data for the cesium-dilactam system gave log K = 1.67 ± 0.02 in nitromethane, log K = 1.96 ± 0.01 in pyridine and log K = 1.68 ± 0.08 in CH_3CN. It should be noted, however, that in all three solvents cesium salts are ion paired. Therefore, the formation constants given above reflect competition between the anions and the dilactam for the cesium ion.

In pyridine solutions it was found that the ion pair formation constant for $Cs^+BPh_4^-$ is 370 ± 20 (94) while for CsSCN in nitromethane and acetonitrile it is 44.1 ± 1.2 and 13.2 ± 3.8 respectively (95). Comparison of the above values of the formation constants of the cesium-C222D complexes with the ion pair formation constants makes it quite apparent that the anion should be taken into consideration as both ligand and anion compete for the cesium ion in solution. The observed chemical shift

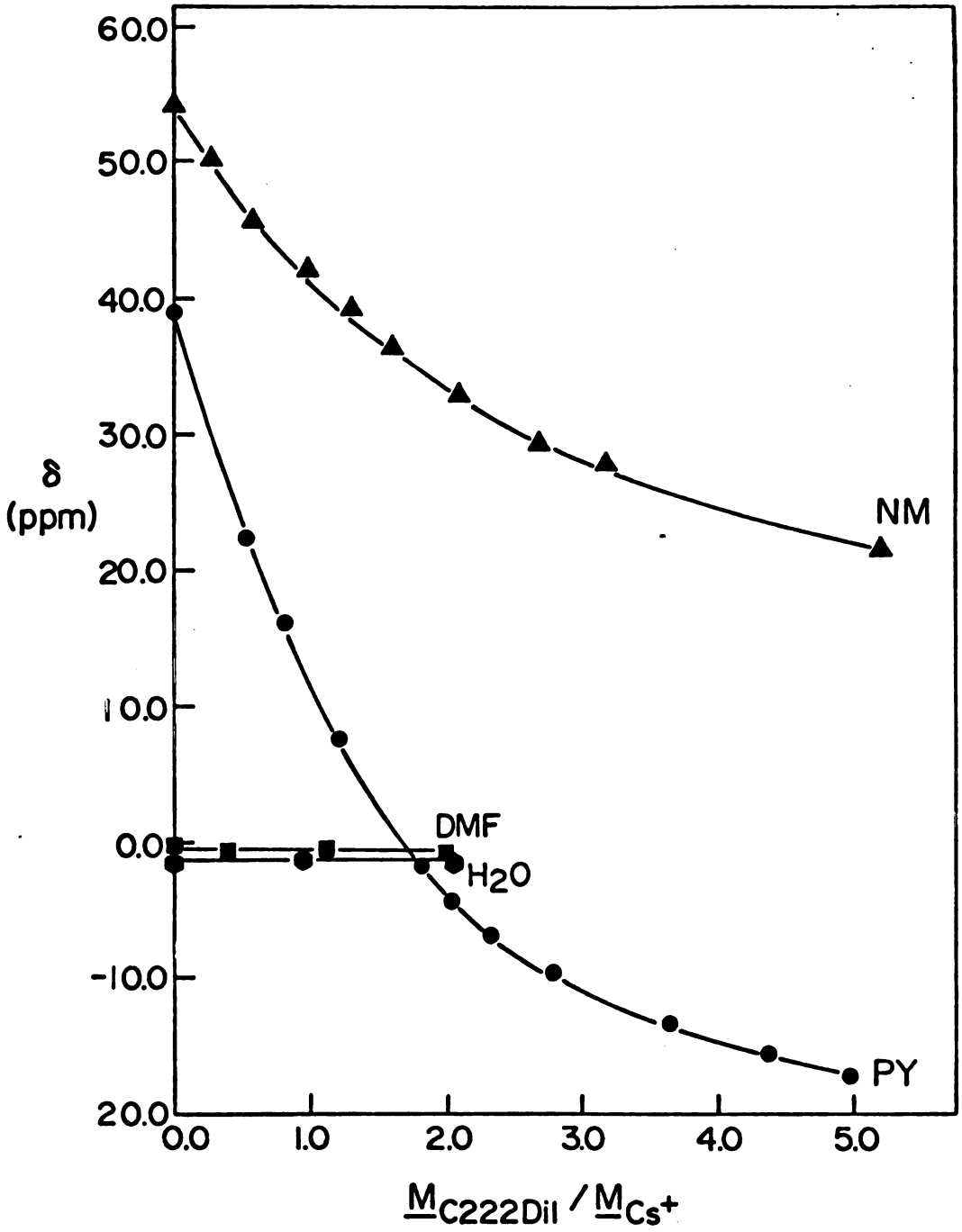

Figure 10. Cesium-133 chemical shifts as a function of C222D/Cs^+ mole ratio in nitromethane, dimethylformamide, aqueous and pyridine solutions.

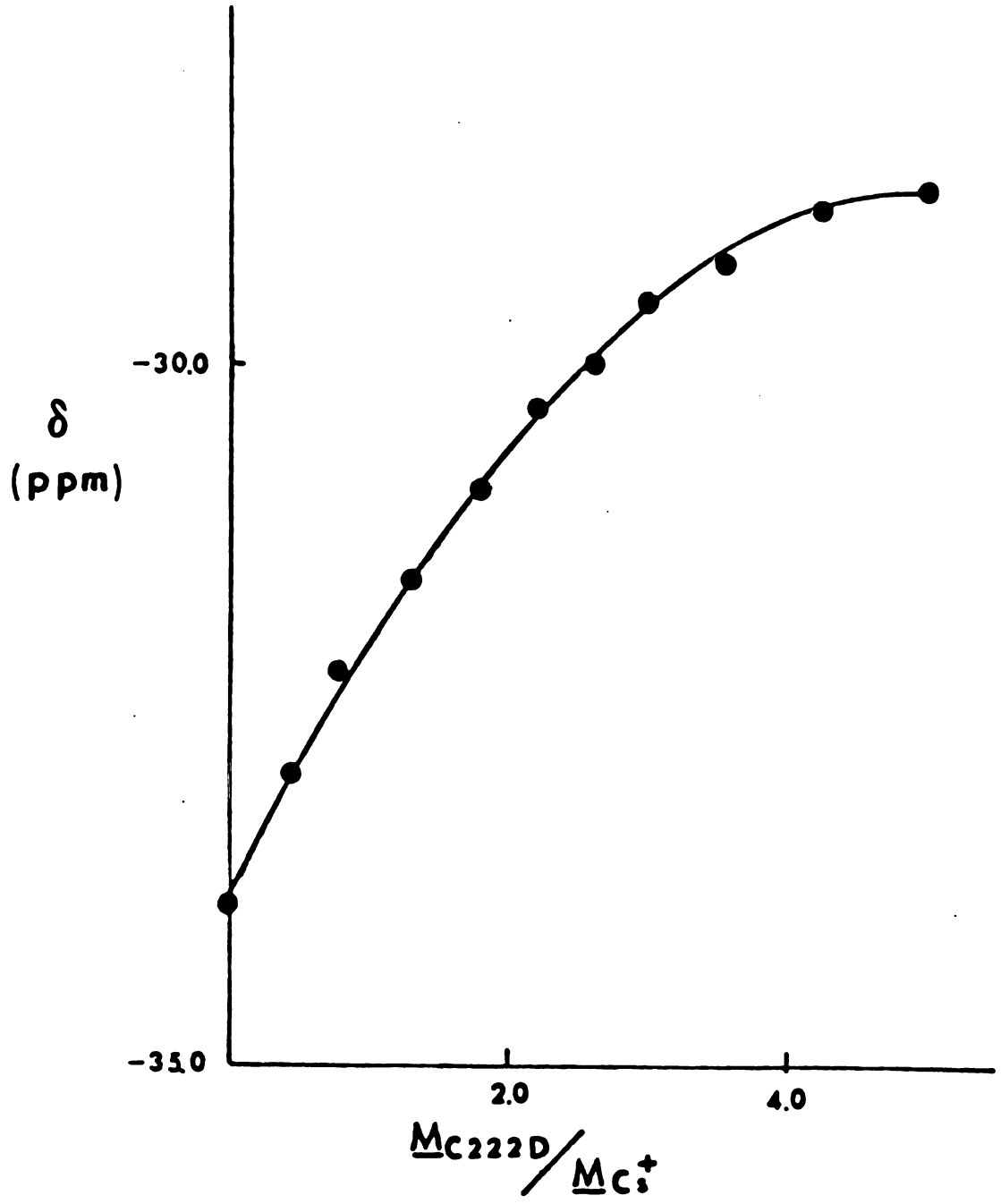

Figure 11. Cesium-133 chemical shifts as a function of C222D/Cs^+ mole ratio in acetonitrile.

therefore, is modified to include a third factor, the chemical shift characteristic of the ion pair:

$$\delta_{obs} = X_M\delta_M + X_{ML}\delta_{ML} + X_{MA}\delta_{MA} \qquad (6)$$

The derivation of the final expression for the observed chemical shift can be obtained by applying the following equations

$$K_{ip} = [MA]/[M][A] \qquad (7)$$

$$K_f = [ML]/[M][L] \qquad (8)$$

$$C_L = [ML] + [L] \qquad (9)$$

$$C_M = [ML] + [M] + [MA] \qquad (10)$$

$$[A] = [ML] + [M] \qquad (11)$$

where K_{ip} is the ion pair association constant, K_f is the formation constant of the complex, [MA], [M] and [A] are the concentrations of the ion pair, free metal ion and free anion respectively, and C_L and C_M are the analytical concentrations of the ligand and salt. With these five equations and simple algebraic manipulations, the following expression is readily derived.

$$K_fK_{ip}[M]^3 + (K_fK_{ip}C_L + K_{ip} + K_f)[M]^2 +$$

$$(K_fC_L + 1 - K_fC_M)[M] - C_M = 0 \qquad (12)$$

A detailed derivation of the above equation and the description of the subroutine EQN used in KINFIT are given in Appendix II. In order to use this model, the ion pair formation constant has to be known. Using the values reported above, new formation constants were obtained for the cesium-C222D complexes and the values are reported in Table 7. Comparing the new formation constants obtained considering the ion pairing with the previously obtained ones we see that they are larger especially in the case of pyridine where the difference is about an order of magnitude. It is quite evident that for the weak cesium-C222D complex, the anion and the solvent can have strong influence on the complexation interaction. The ^{133}Cs chemical shifts of the complex in the above solvents do not approach the same value, which seems to indicate that the cesium ion is exposed to the solvent. If we compare the cesium-C222D complexes to the cesium-C222 ones (90), we see that the former are much weaker. It seems that the two carbonyl groups in the C222D molecule make it more rigid than the C222 molecule and thus it is more difficult for the large cesium ion to approach the binding sites of the ligand.

It should be noted that in aqueous solutions all three cations studied above do not show evidence of complex formation. This apparent contradiction of the results obtained in the black lipid membrane transport experiments can perhaps be explained by the fact that very small amounts of the complex can significantly lower the resistance of the

Table 7. Formation Constants of C222-Dilactam Complexes in Nonaqueous Solvents at 25°C.

Salt	Solvent	log K_f
$LiClO_4$	Pyridine	2.64 ± 0.10[a]
$LiClO_4$	Tetrahydrofuran	3.12 ± 0.09[a]
$LiClO_4$	Acetonitrile	3.23 ± 0.07[a]
LiBr	Acetonitrile	3.13 ± 0.12[a]
$LiClO_4$	Nitromethane	> 4[a]
$NaPh_4B$	Dimethylformamide	> 4[a]
$NaClO_4$	Pyridine	> 4[b]
$NaClO_4$	Acetonitrile	> 4[b]
$NaPh_4B$	Nitromethane	> 4[b]
CsSCN	Nitromethane	1.67 ± 0.02[b]
CsSCN	Nitromethane	1.79 ± 0.03[c]
$CsPh_4B$	Pyridine	1.96 ± 0.01[b]
$CsPh_4B$	Pyridine	2.86 ± 0.01[c]
CsSCN	Acetonitrile	1.68 ± 0.08
CsSCN	Acetonitrile	1.70 ± 0.08[c]

[a] 33°C

[b] 25°C

[c] Corrected for ion pairing

black lipid membranes (BLM). For example, 10^{-6} M valinomycin found to change the BLM resistance from 10^9 ohms to $\sim 10^5$ ohms (68).

Our alkali metal nmr data do not permit the differentiation between inclusive and exclusive types of cryptate complexes. An inclusive cryptate complex refers to one in which the metal ion is totally within the cavity of the ligand. In all cases, however, there is some influence of the solvent on the limiting chemical shift of the complexed cation, the influence being in the order $Li^+ < Na^+ < Cs^+$. In view of the ^{133}Cs results and the size considerations, it seems plausible to assume that in the last case the complex may be of the exclusive type.

All the above values are the concentration constants. However, since the complexation reaction

$$M^+ + C222D \rightleftarrows M^+\text{-}C222D \qquad (13)$$

does not involve separation of charges, these values should represent reasonable approximations of the thermodynamic constants.

B. pH Dependence of the ^{23}Na Chemical Shift

It was mentioned above that in aqueous solutions C222D does not show evidence of complex formation with lithium, sodium or cesium metal ions. The metal ion chemical shift is independent of the ligand/M^+ mole ratio. It was interesting

to find out if changing the pH of the solution caused any change in the interaction of C222D with the metal ion. A 0.01 M NaCl and 0.01 M C222D aqueous solution was prepared and the measured pH of the solution was 7.85. The sodium-23 chemical shift of the solution is 0.15 ppm. By adding 0.096 N $(Bu)_4NOH$ into the solution of the pH of the solution was changed and the ^{23}Na chemical shift was monitored at different pH values with the results shown in Table 8. Altering the pH of the solution within the range of 11.50 and 1.25 the ^{23}Na chemical shift remains constant, which indicates that there is no change in the interaction between the ligand and the sodium ion. The pH of the solution was changed by the addition of 6 N HCl.

The same experiment was performed by using cryptand C222 as the ligand with the results listed in Table 8. At the mole ratio of $[C222]/[Na^+] = 1.0$ essentially all Na^+ is complexed and the ^{23}Na resonance line has a chemical shift of 8.0 ppm and a linewidth at half-height of approximately 70 Hz. At mole ratios less than one, the ^{23}Na resonance line is an unresolved doublet. To study the pH dependence of the ^{23}Na chemical shift, a solution of 0.05 M NaCl and 0.05 M C222 in water was prepared. The pH of this solution was measured to be 10.68. Adding HCl to the solution to lower the pH, the Na^+-C222 peak broadens and at a pH value of 7.70 starts to split. As the pH is lowered further, the peak characteristic for the free Na^+ grows larger and that of the complexed becomes smaller until it completely

Table 8. pH Dependence of ^{23}Na Chemical Shift for Aqueous Solutions of Sodium Chloride.

Ligand	$[Na^+]$	[Ligand]/$[Na^+]$	pH	$\Delta\delta$(ppm)	$\Delta\nu_{\frac{1}{2}}$(Hz)
C222D	0.01	1.0	7.85	0.15	15
			9.15	0.15	15
			9.55	0.15	15
			10.11	0.15	15
			10.50	0.31	15
			10.90	0.30	15
			11.50	0.31	15
			1.25	0.31	15
C222	0.05	1.0	10.68	8.0	70
			8.55	6.8	95
			8.22	6.8	108
			8.00	6.3	120
			7.70	3.5	
			7.55	1.23	
			7.00	0.3	27
			6.35	0.4	15
			1.65	0.4	15

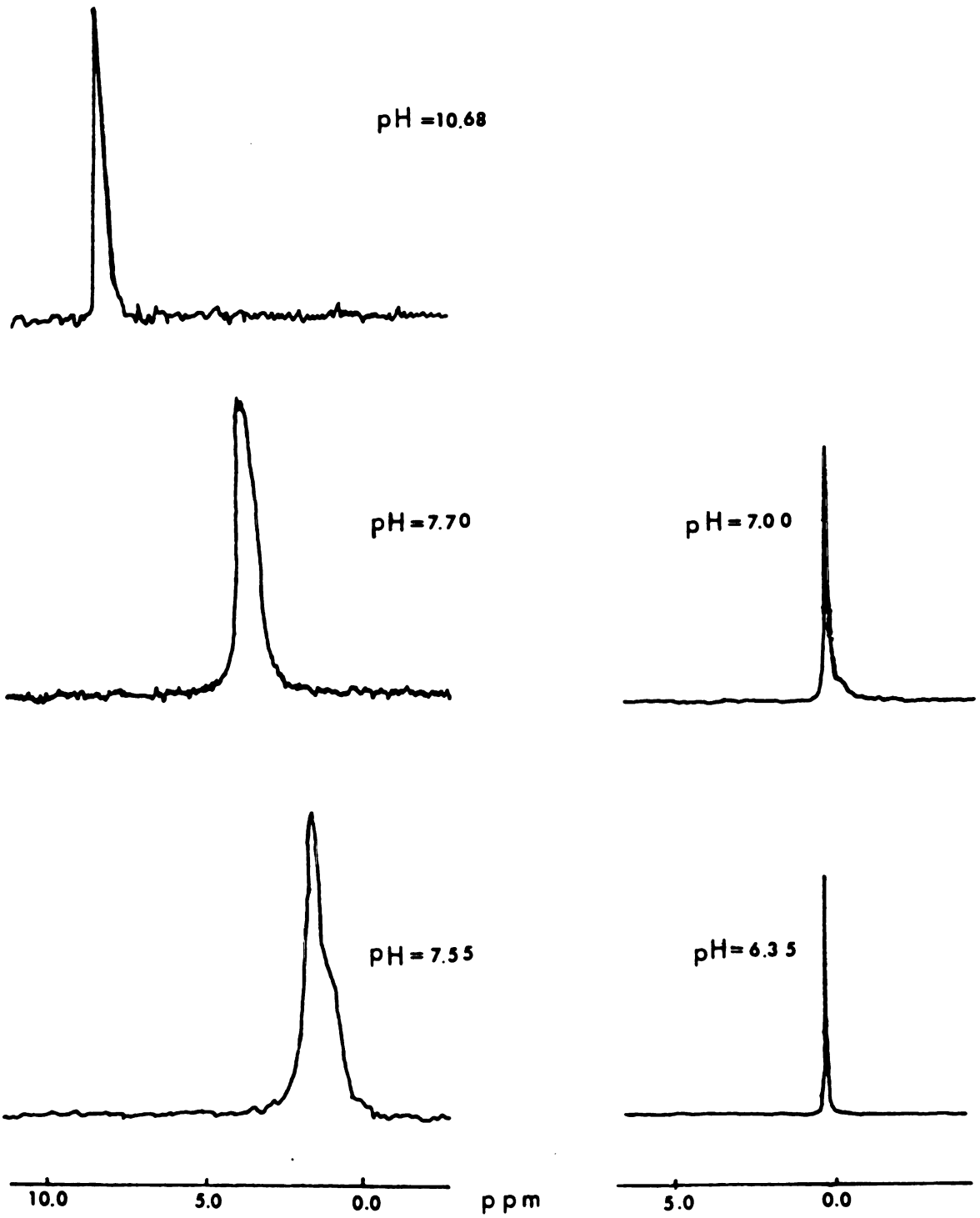

Figure 12. Changes in Na^+ resonance as the relative amounts of free and complexed Na^+ vary with changing pH for 0.05 M aqueous NaCl with C222 / Na^+ = 1.0.

disappears at a pH of 6.35. Figure 12 shows the changes in chemical shifts as more of the Na^+ is released from the Na^+-C222 complex on changing the pH of the solution. At this pH value according to the results of Mei-Tak Lok (96) all cryptand is in the diprotonated form. Lowering the pH further produces no observable change of the Na^+ peak. Apparently the diprotonated crypt does not complex sodium at all. For the monoprotonated crypt no conclusion can be drawn, because at the pH level at which it exists, all three species CNa^+, CH^+, CH_2^{++} exist in solution and exchange among them is rapid. From the above experiments it is evident that the acid-base properties of C222D and C222 are quite different.

C. pK_a Determination of C222D

To determine the pK_a of C222D, 25 ml of a 4×10^{-3} M solution of C222D in conductance water were titrated with 5×10^{-2} M HCl. Tetramethyl ammonium bromide was used to maintain constant ionic strength at 7×10^{-2} M. Nitrogen was bubbled through the solution to expel the carbon dioxide present. The results obtained are plotted in Figure 13. As is seen from the graph, there is a sudden drop of the pH of the solution from 7.28 to 4.16 after the first drop of HCl was added and after that the pH changed smoothly. It was expected that the titration curve would show two breaks, one after the addition of 2.0 ml HCl and another after the

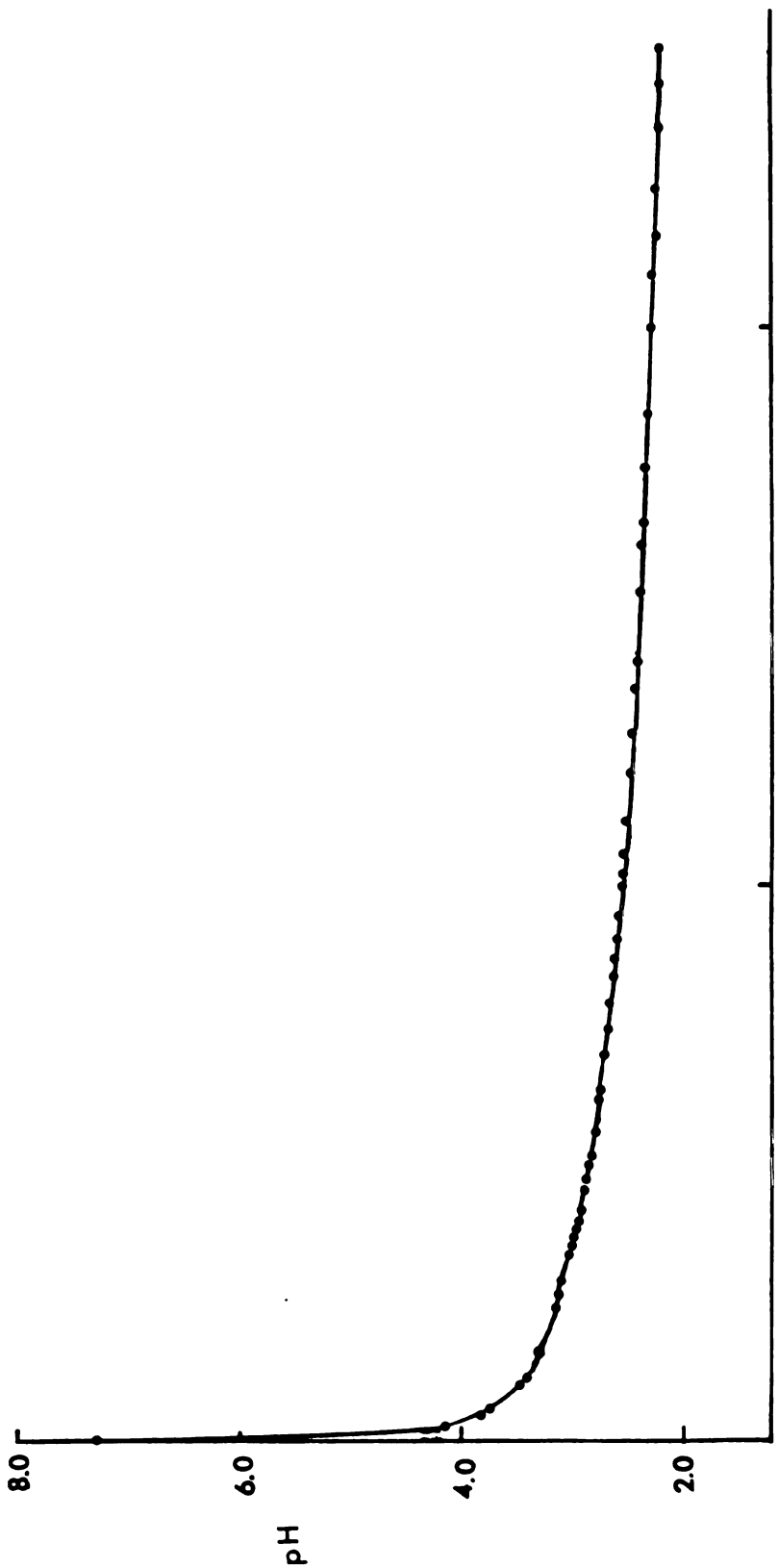

Figure 13. Titration curve for the titration of 25.0 ml of 4 X 10^{-3} M aqueous C222D with 0.05 M HCl.

addition of 4.0 ml HCl. There is no indication of the breaks in the titration curve of Figure 13 which means there is no indication of protonation either of the nitrogens or of the carbonyl oxygens of the amide.

25 ml of 7 X 10^{-2} M $(Me)_4NBr$ were also titrated with 5 X 10^{-2} M HCl solution. The shape of the titration curve is exactly the same as the one for the titration of the C222D. The only difference is that the initial pH value of the blank solution was 5.4.

The above results show that the acid-base properties of the C222D are quite different of those of C222. This was expected to a certain degree since C222 is an amine and, therefore, it is highly basic while C222D is a diamide which is almost neutral. The above behavior of the C222D, i.e. no indication of protonation, supports the results obtained by ^{23}Na nmr. Since the C222D does not protonate on lowering the pH of the solution a change in pH should not affect the interaction of the C222D and sodium ion.

D. Far Infrared Study of Lithium and Sodium Complexes with C222D in Nonaqueous Solvents

Far infrared spectroscopy has been used extensively (69,97-107) for the investigations of the motion of alkali metal cations relative to their immediate environment. In general, variations of the cation's motional frequencies in solution are expected to occur with variations in the immediate environment of the cation, and are indicative of interactions occurring in solutions.

When a macrocyclic polyether complexes an alkali metal ion, it insulates it from the medium and a cation-ligand vibration is observed. Tsatsas et al. (108) investigated the far infrared spectra of the sodium and potassium-dibenzo-18-crown-6 systems in several solvents and found a band whose frequency was solvent independent. The authors attributed this band to the vibration of the metal-ligand bonds. Cahen and Popov (109) studied the far infrared spectra of sodium-C222, sodium-C221, lithium-C211 and lithium-C221 cryptates and found bands at 234 $\pm$ 2 cm^{-1} for the Na^+-C222 vibration, at 218 $\pm$ 1 cm^{-1} for the Na^+-C221 vibration, at 348 $\pm$ 1 cm^{-1} for the Li^+-C211 vibration and at 243 $\pm$ 3 cm^{-1} for the Li^+-C221 vibration which could not be assigned to the free metal or ligand. All the above bands were found to be solvent and anion independent, and were assigned to the vibration of the metal ion in the cryptand cage.

In the present study far infrared measurements were carried out on the Li^+-C222D complex in acetonitrile and pyridine solutions and on Na^+-C222D in dimethylformamide and dimethyl sulfoxide. These are the only solvents in which the solubilities of the complexes were high enough to allow far infrared measurements. The spectra of $LiClO_4$ solutions in the two solvents show the band due to the vibration of the cation in the solvent cage at 405 cm^{-1} in acetonitrile and at 385 cm^{-1} in pyridine. Upon addition of one equivalent of dilactam to these solutions, the above bands disappear and a new band appears at

$\sim$ 460 cm^{-1} whose frequency is independent of the solvent. It is believed that the 460 cm^{-1} band is indicative of the vibration of the cation in the cavity of the ligand. Isotopic substitution of ^{7}Li by ^{6}Li shifted this band to higher frequency.

The spectra of $NaBPh_4$ in DMF and DMSO show the band due to the vibration of Na^+ in the solvent cage at 190 cm^{-1} and at 205 cm^{-1} respectively. Upon addition of the dilactam to the $NaBPh_4$ in DMF solution, the 190 cm^{-1} Na^+ solvation band disappeared while a new band appeared at 125 cm^{-1}. This latter band represents the vibration of the Na^+ in the C222D cavity although it is difficult to understand why the band shifts to lower frequency. In the case of Na^+-C222 cryptate the vibration of the Na^+ cation in the cryptand cavity was observed at 234 cm^{-1} (109). In the case of DMSO the spectrum does not show any change upon addition of the dilactam. The 205 cm^{-1} solvated Na^+ band remains unchanged which indicates that there is no change in the immediate environment of the sodium ion. This result agrees with the ^{23}Na nmr data (71) that the ^{23}Na chemical shift in DMSO was independent of the ligand/M^+ mole ratio.

Unfortunately the far infrared study cannot be extended to other solvents because of solubility problems. From the above data it cannot be concluded if the Li^+-C222D and the Na^+-C222D complexes are definitely of the inclusion type and if the solvent influences the frequency of the vibration of the M^+-C222D. There is only an indication that the metal ion is inside the ligand cavity.

E. Carbon-13 NMR Study of Lithium, Sodium and Potassium Complexes with C222D in Nitromethane

The carbon-13 spectra of the free ligand C222D and of the complexes Li^+-C222D, Na^+-C222D and K^+-C222D in nitromethane were obtained.

The free ligand has nine different types of carbon atoms, which are indicated in Figure 14. Therefore, nine resonance lines are expected, one for the carbonyl carbon atoms, six for the O-C and two for the N-C carbon atoms. Since C222D is an amide the nitrogen atom and the carbonyl group are coplanar and one of the two strands attached to the nitrogen atom is cis and one is trans to this plane. The exchange between them is slow and this makes the carbon atoms of the two strands nonequivalent.

The carbon-13 spectrum obtained by using the CFT-20 nmr spectrometer shows seven resonance lines for the free ligand (Figure 14a). The carbonyl peak is not shown in the figure. The peak at 63.31 ppm is the nitromethane peak and the 50.97 ppm peak is the methanol peak used as the external reference. The four peaks downfield from nitromethane are assigned to the C-O and the two peaks upfield from nitromethane to the N-C carbon atoms. Since six resonance lines for the C-O carbon atoms were expected but only four were obtained, the carbon-13 spectrum of the C222D in nitromethane was taken by using the Bruker-180 nmr spectrometer which has higher resolution than the CFT-20. The new spectrum indeed shows nine resonance lines (Figure 15). The 72.03 ppm and

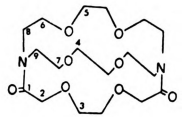

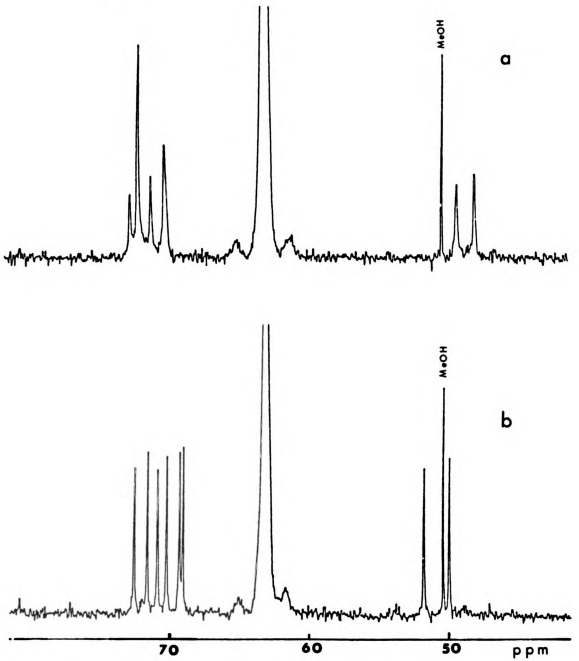

Figure 14. Carbon-13 spectra of: a) 0.10 M C222D in CH_3NO_2; b) 0.10 M C222D with 0.2 M $LiClO_4$ in CH_3NO_2.

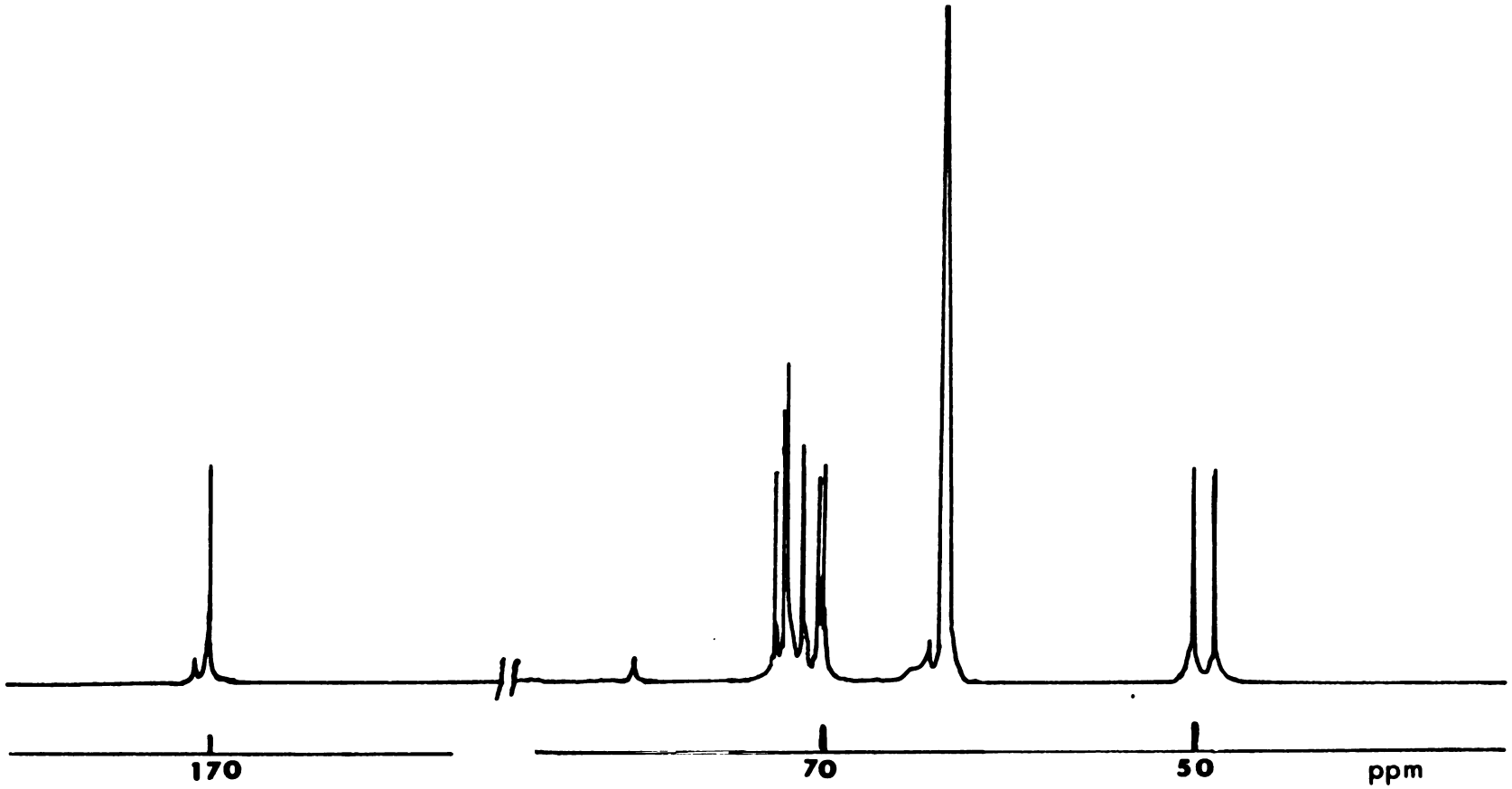

Figure 15. Carbon-13 spectrum of 0.25 M C222D in CH_3NO_2 (Bruker 180 NMR spectrometer).

the 70.20 ppm peaks are both doublets but the chemical shift difference is only 0.17 ppm in the former and 0.24 ppm in the latter case and the resolution of our instrument is not high enough to separate them.

The carbon-13 nmr spectrum of the 2:1 $[Li^+]/[C222D]$ complex was obtained (Figure 14b) by using the CFT20 NMR spectrometer. At this mole ratio all ligand is complexed. The Li^+-C222D spectrum also shows six C-O peaks all of them upfield from the ones of the free ligand, and two N-C peaks downfield from the ones of the free ligand. The lithium ion should be inside the ligand cavity but it is small enough not to change the conformation and the symmetry of the ligand.

The Na^+-C222D spectrum (Figure 16a) and the K^+-C222D spectrum (Figure 16b) show only two peaks in the O-C region and one at the N-C region. Sodium and potassium ions are much larger than the lithium ion and as they enter the ligand cavity they make the molecule more rigid. As a result of this the two strands attached to the nitrogen atoms cannot be <u>cis</u> and <u>trans</u> to the nitrogen-carbonyl plane anymore but have an intermediate position. At this position they can exchange rapidly between the two positions making many carbon atoms equivalent. Another assumption is that since the molecule is more rigid after complexation with sodium or potassium ion the conjugation between nitrogen and carbonyl is destroyed and the double bond is on the carbonyl group only. In such a case, the infrared absorption band

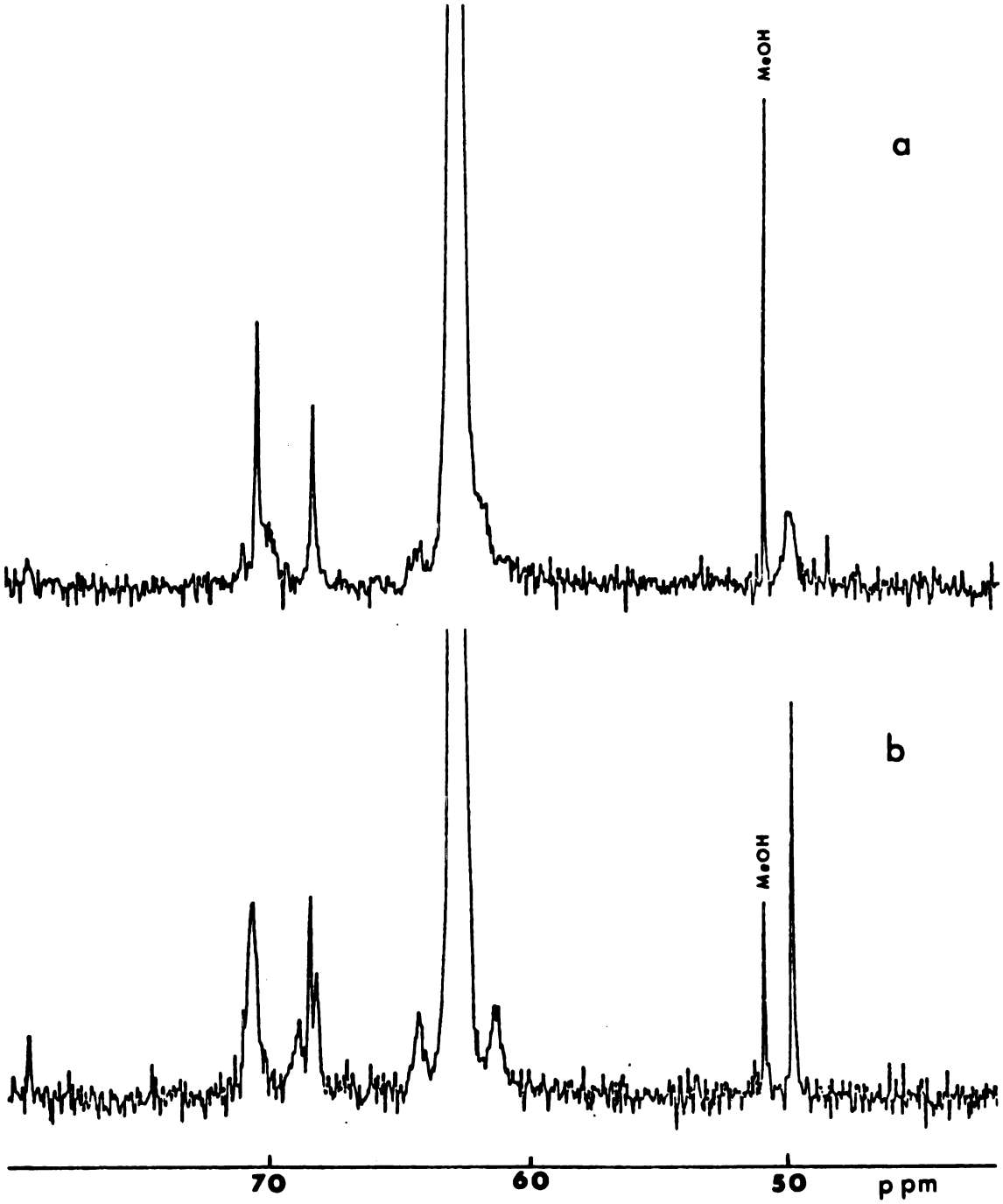

Figure 16. Carbon-13 spectra of: a) 0.05 M C222D with 0.06 M $NaB\phi_4$ in CH_3NO_2; b) 0.05 M C222D with 0.1 M KPF_6 in CH_3NO_2.

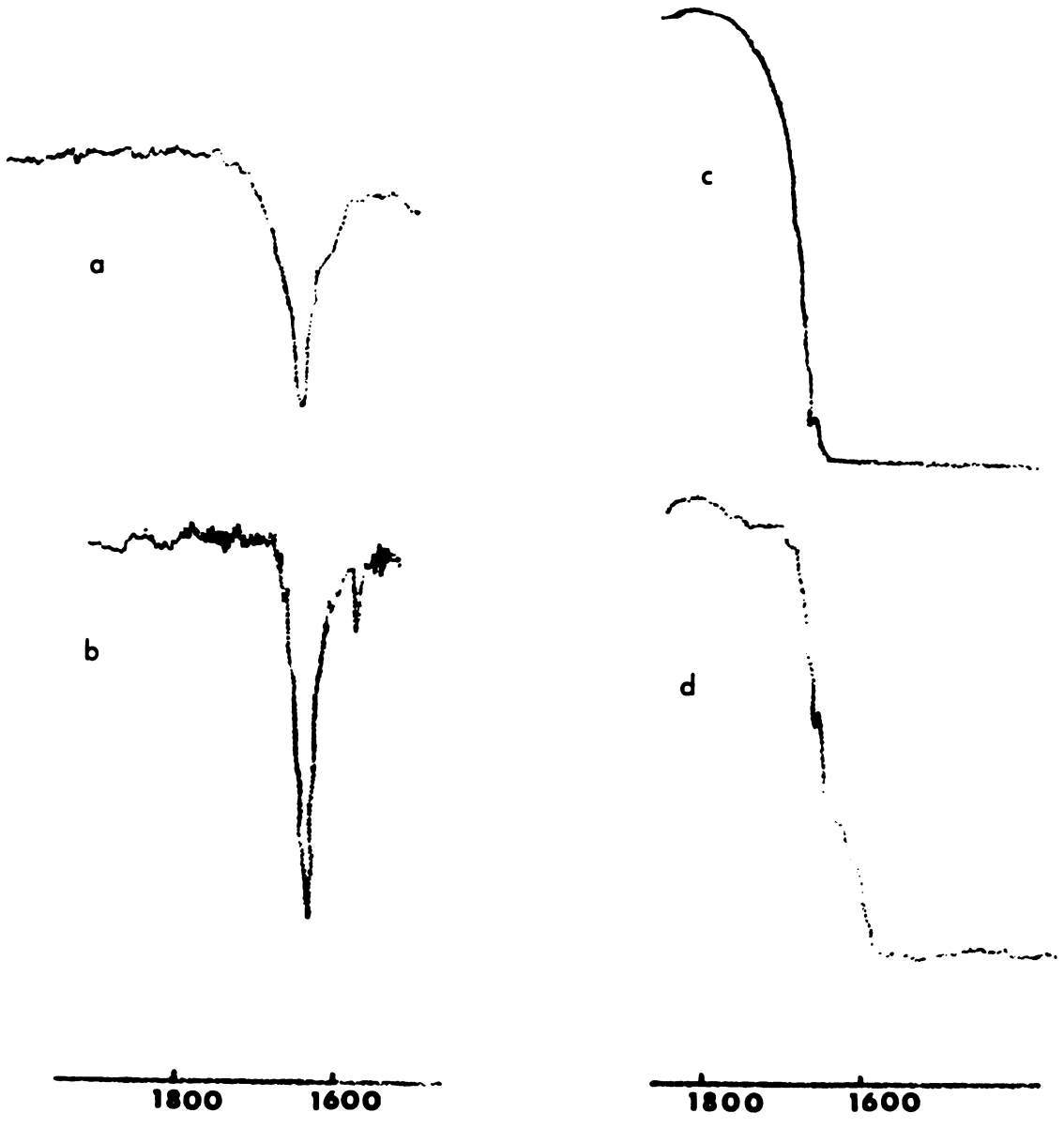

Figure 16A. IR Spectra of the Carbonyl Absorption of:
a) C222D in nujol; b) Na^+-C222D in nujol;
c) $[Li^+]/[C222D] = 2.0$ in CH_3NO_2; and
d) $[K^+]/[C222D] = 1.6$ in CH_3NO_2.

for the carbonyl group which appears at 1640 cm^{-1} for the free ligand, should move to higher frequency. The infrared spectra of Li^{+}-C222D, Na^{+}-C222D and K^{+}-C222D in nitromethane do not show any new peak at frequencies higher than than 1640 cm^{-1} (Figure 16A). This proves that our first assumption was correct.

From the carbon-13 study it seems reasonable to conclude that all three cations studied above form inclusion type complexes with the C222D in nitromethane.

CHAPTER IV

STUDY OF THE THERMODYNAMICS OF THE COMPLEXATION REACTION OF C222D WITH LITHIUM AND CESIUM IONS IN VARIOUS SOLVENTS

INTRODUCTION

A deeper understanding of the thermodynamics of the complexation reaction may be provided by dividing the free energy of complexation, ΔG, into enthalpy, ΔH, and entropy, ΔS, of complexation. There are altogether four possible combinations of the thermodynamic quantities leading to stable complexes ($\Delta G < 0$): a) $\Delta H < 0$ and dominant, $T\Delta S > 0$; b) $\Delta H < 0$ and dominant, $T\Delta S < 0$; c) $T\Delta S > 0$ and dominant, $\Delta H < 0$; d) $T\Delta S > 0$ and dominant, $\Delta H > 0$ (65).

For electrostatic complexes between charged ligands and "hard" cations, $T\Delta S$ is generally positive and dominant. These are entropy stabilized (110,111). For complexes with more covalent character like the ones of the "soft" cations, ΔH is generally negative and dominant (110,111). In the case of the alkali metal cryptates enthalpic type behavior is expected because the ligands are uncharged. However, entropy dominant behavior is also possible since alkali metal cations are "hard" cations.

The strength of the complexes of cryptand C222D with alkali metal cations was discussed in Chapter III, as well as the solvent and the size of the metal ion effect on the complexation reaction. In this thesis an evaluation of thermodynamic quantities of the complexation reaction is attempted. To obtain the needed information, the effects of the variations of mole ratios and temperature on the ^{133}Cs and ^{7}Li chemical shifts of the Cs^{+}-C222D and

Li^+-C222D complexation reactions in pyridine, nitromethane and acetonitrile were determined.

RESULTS AND DISCUSSION

The complexation of cesium and lithium ion with C222D cryptand can be described by the following equilibrium, assuming that a 1:1 complex is formed,

$$M^+S_x + LS_y \rightleftarrows M^+L\,S_z + (x + y - z)S$$

where S is the solvent molecule, L is the ligand and x, y and z are the solvation numbers of the cation, ligand and the complex respectively. The variation of chemical shift with changing temperature was studied for the above complexation reaction. The systems studied were $LiClO_4$ and C222D in acetonitrile, nitromethane and pyridine, $CsBPh_4$ with C222D in pyridine, CsSCN with C222D in nitromethane and CsSCN with C222D in acetonitrile. At each temperature the chemical shift of the metal ion was monitored as a function of dilactam/metal ion mole ratios. In all cases studied, only one population average signal was observed which indicated that the exchange of the metal ion between the two sites, that of the free ion in the bulk solution and that of the complexed ion, was faster than 10^7 per second. All chemical shifts reported in this study have been corrected for bulk magnetic susceptibility of the solvent and temperature effects on the reference solution. The ^7Li chemical shifts have been adjusted to the final reference

point of the 4.0 M aqueous $LiClO_4$ at 25°C, while the ^{133}Cs chemical shifts have been adjusted to the final reference point of the infinitely dilute concentration of the cesium ion in water at 25°C. The linewidths observed for the uncomplexed cesium and lithium ion are narrow (about 3-5 Hz) and are limited by the inhomogeneity of the magnetic field. No line broadening due to complexation is observed, the only exception being Cs^+-C222D in pyridine where at low temperatures some broadening is observed, the maximum line width being on the order of 50 Hz. All the lithium-7 chemical shifts measured at various temperatures are listed in Tables 9-11 and shown in Figures 17-19. The formation constants were computed by the KINFIT program and the results are listed in Table 12.

In all three solvents studied, i.e. acetonitrile, nitromethane and pyridine, the curvature in the mole ratio plots increases with increasing temperature, indicating an endothermic behavior. The calculated formation constants show the same trend (Table 12). In acetonitrile log K = 3.19 ± 0.07 at -45°C and at 28°C it is 3.54 ± 0.25 while at 86°C the complex is even stronger and from data simulation we get only an estimate of its value about 3.90. In nitromethane the calculated formation constant is log K = 2.93 ± 0.06 at -29°C. At temperatures ≥ 27°C the mole ratio plots consist of two straight lines which intersect at the 1:1 mole ratio. In this case the formation constants cannot be calculated by the equation normally used and

Table 9. Li-7 Chemical Shifts of $LiClO_4$ (0.010 M) in the Presence of C222D in CH_3CN at Various Temperatures.

Mole Ratio	Temperature, °C		Mole					
	-32°	-7°		-45°	-21°	5°	28°	86°
0.00	3.41	3.25	0.00	3.46	3.36	3.22	2.99	2.75
0.27	2.68	2.49	0.30	2.64	2.73	2.38	2.31	1.91
0.52	2.00	1.73	0.49	2.10	2.16	1.86	1.74	1.34
0.62	1.87	1.60	0.64	1.67	1.74	1.39	1.27	0.87
0.77	1.40	1.04	0.77	1.36	1.47	1.21	1.06	0.60
0.89	1.03	0.69	0.89	1.21	1.26	0.98	0.88	0.24
0.99	0.87	0.55	0.99	1.10	1.12	0.82	0.72	0.07
1.21	0.79	0.47	1.19	0.89	0.93	0.52	0.54	-0.03
1.41	0.68	0.39	1.41	0.79	0.85	0.45	0.45	-0.03
1.63	0.62	0.34	1.61	0.67	0.79	0.44	0.43	-0.08

Table 9. Continued

Mole Ratio	Temperature, °C		Mole Ratio	Temperature, °C				
	-32°	-7°		-45°	-21°	5°	28°	86°
1.80	0.60	0.34	1.78	0.62	0.74	0.43	0.38	-0.08
2.20	0.55	0.30	2.08	0.58	0.74	0.40	0.40	-0.13
2.60	0.50	0.26	2.57	0.55	0.69	0.40	0.33	-0.19
			2.99	0.51	0.69	0.36	0.38	-0.03

Table 10. Li-7 Chemical Shifts of $LiClO_4$ (0.010 M) in the Presence of C222D in CH_3NO_2 at Various Temperatures.

Mole Ratio	Temperature, °C					Mole Ratio	Temperature, °C		
	-29°	0°	27°	80°	102°		-20°	-13°	-7°
0.00	1.71	0.70	0.62	-0.22	-1.04	0.00	1.47	1.25	1.11
0.30	1.50	0.61	0.41	-0.64	-1.30	0.25	1.20	0.95	0.83
0.52	1.40	0.40	0.25	-0.85	-1.51	0.49	0.94	0.66	0.62
0.67	1.29	0.35	0.09	-1.06	-1.68	0.69	0.78	0.48	0.44
0.80	1.18	0.24	-0.01	-1.17	-1.78	0.86	0.63	0.32	0.29
0.90	1.03	0.17	-0.16	-1.32	-1.88	0.96	0.55	---	0.23
0.96	0.98	0.17	-0.19	-1.38	-1.98	1.11	0.46	0.19	---
1.10	0.92	0.03	-0.27	-1.42	-2.04	1.26	---	---	0.08
1.25	0.87	-0.02	-0.27	-1.42	-1.99	1.36	0.36	0.16	0.07
1.35	0.82	-0.02	-0.30	-1.42	-1.99	1.58	0.31	0.09	0.04
1.58	0.77	-0.02	-0.27	-1.42	-1.94	2.03	0.28	0.06	0.02
1.98	0.72	-0.02	-0.27	-1.47	-2.04	2.72	0.25	0.04	0.00
2.52	0.67	-0.02	-0.32	-1.42	-2.09				

Table 11. Li-7 Chemical Shifts of $LiClO_4$ (0.020 M) in the Presence of C222D in Pyridine

Table 11. Li-7 Chemical Shifts of $LiClO_4$ (0.020 M) in the Presence of C222D in Pyridine at Various Temperatures.

Mole Ratio	Temperature, °C				
	-33°	0°	25°	61°	90°
0.00	-1.33	-1.85	-2.06	-3.22	-3.85
0.27	-1.02	-1.54	-1.70	-2.88	-3.48
0.49	-0.76	-1.27	-1.44	-2.60	-3.17
0.83	-0.29	-0.86	-1.02	-2.15	-2.81
0.96	-0.18	-0.70	-0.86	-2.02	-2.70
1.26	-0.03	-0.61	-0.70	-1.97	-2.65
1.52	0.03	-0.61	-0.70	-1.97	-2.65
1.76	0.08	-0.61	-0.70	-1.97	-2.65
2.08	0.13	-0.61	-0.70	-1.97	-2.65
2.25	0.13	-0.61	-0.70	-1.97	-2.65
2.62	0.13	-0.61	-0.70	-1.97	-2.65
3.00	0.13	-0.61	-0.70	-1.97	-2.65

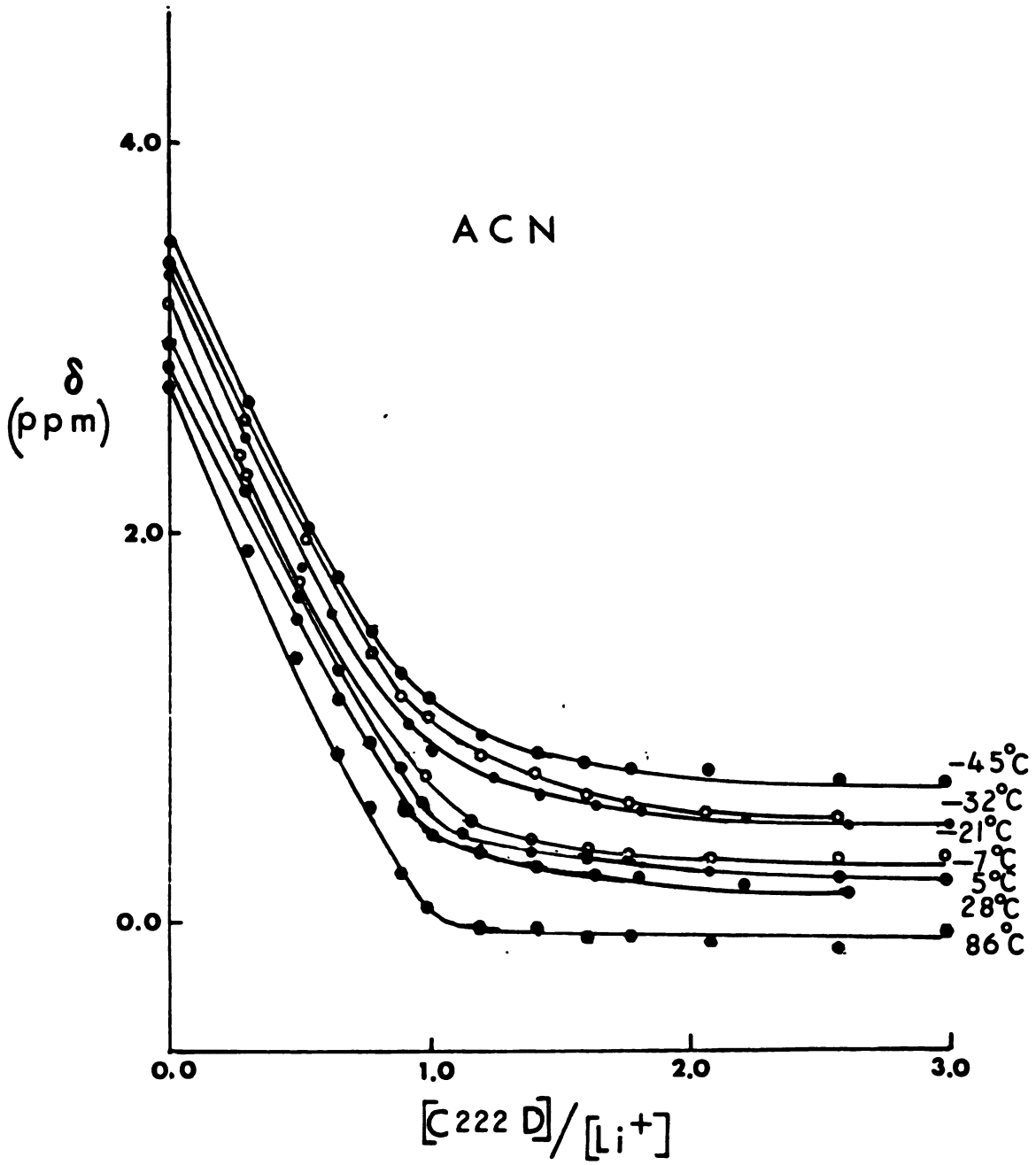

Figure 17. Lithium-7 chemical shifts as a function of C222D/Li^+ mole ratio in acetonitrile at various temperatures.

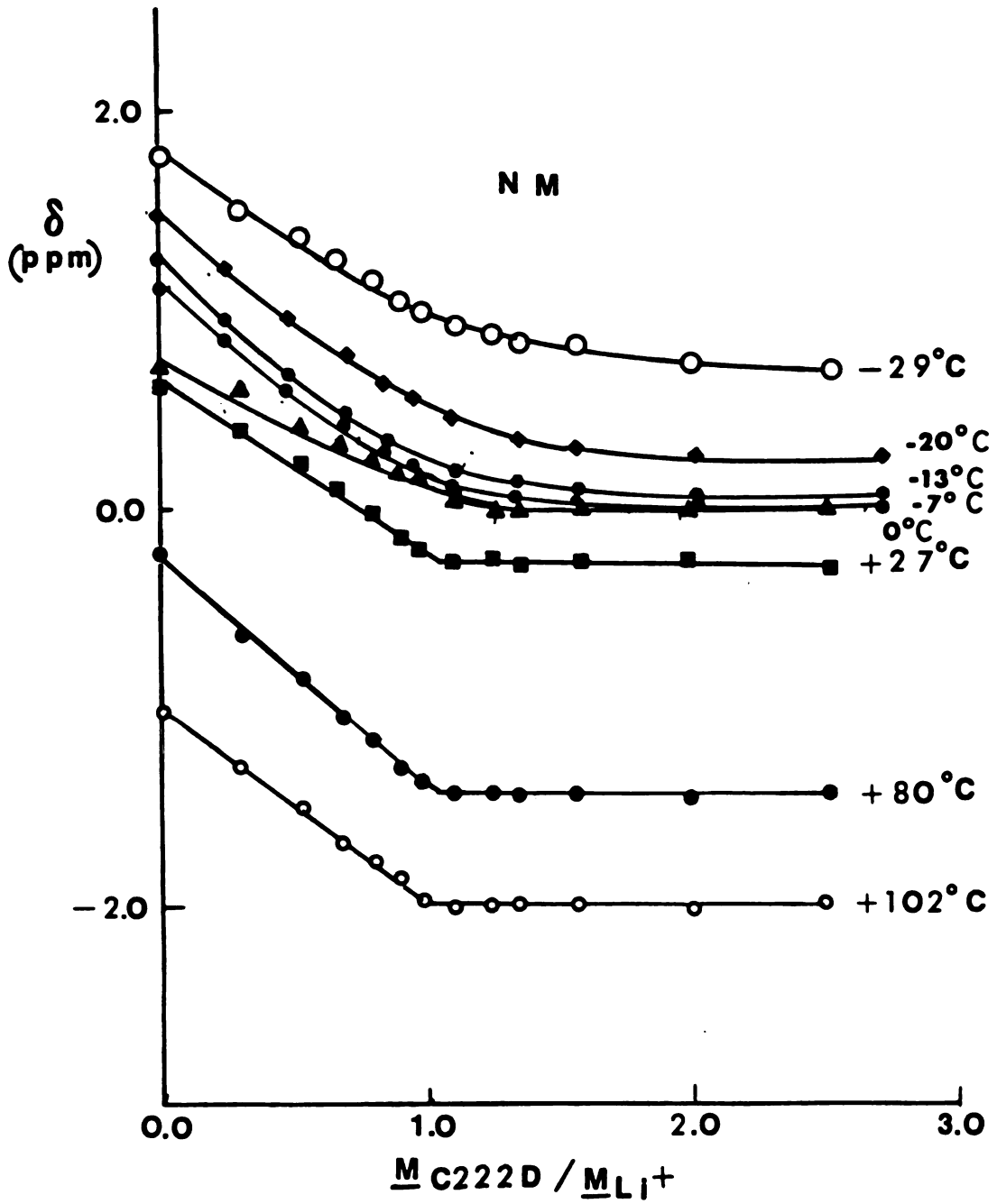

Figure 18. Lithium-7 chemical shifts as a function of $C222D/Li^+$ mole ratio in nitromethane at various temperatures.

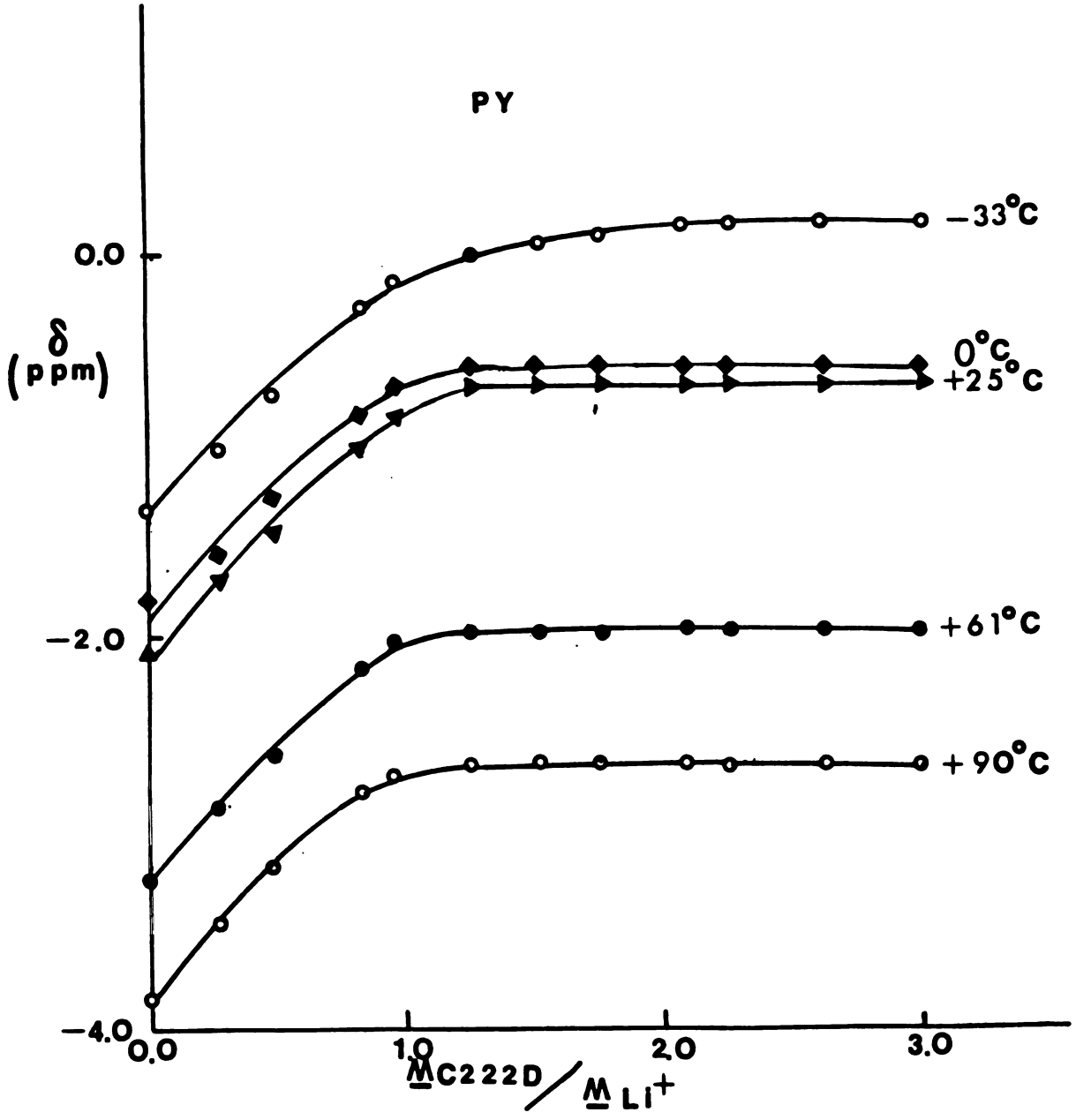

Figure 19. Lithium-7 chemical shifts as a function of $C222D/Li^+$ mole ratio in pyridine at various temperatures.

it can only be concluded that log $K_f \geq 4$. In the case of pyridine the same endothermic behavior is observed.

Unfortunately, no values for the formation constants were obtained in this case because the two unknowns in our equation seemed strongly coupled and it was not possible to calculate the formation constants at different temperatures. From the curvature of the mole ratio plots we can only conclude that formation constants become larger as the temperature increases.

The relevant thermodynamic parameters are calculated by the following relationships:

$$\Delta G = -RT \ln K \tag{14}$$

$$\Delta G = \Delta H - T\Delta S \tag{15}$$

$$\ln K = \frac{\Delta S}{R} - \frac{\Delta H}{RT} \tag{16}$$

By plotting lnK vs 1/T a straight line is obtained with a slope of $-\frac{\Delta H}{R}$ and an intercept of $+\frac{\Delta S}{R}$ provided ΔH is independent of temperature. Such a plot is shown in Figure 20 for the Li^+-C222D complex in acetonitrile and nitromethane. The lines obtained are straight. By linear least squares fitting of the data the slope and intercept of the lines are calculated and the corresponding thermodynamic quantities are listed in Table 17. In acetonitrile $\Delta H = 1.58 \pm 0.22$ kcal/mole while $\Delta S = 21.7 \pm 0.87$ while in nitromethane $\Delta H = 6.10 \pm 0.16$ and $\Delta S = 38.4 \pm 0.62$ cal/mole·^oK. In both cases the complex is enthalpy destabilized but entropy stabilized. A possible explanation is that Li^+ is a small

Table 12. Formation Constants for the Complexation of $LiClO_4$ by C222D in CH_3NO_2 and CH_3CN at Various Temperatures.

T°C	T°K	$10^3/T$	log K	ln K
	System: $LiClO_4$ + C222D in CH_3NO_2			
-29	244	4.10	2.93 ± 0.06	6.74
-20	253	3.95	3.14 ± 0.07	7.23
-13	260	3.85	3.27 ± 0.09	7.53
- 7	266	3.76	3.38 ± 0.06	7.78
0	273	3.66	3.85 ± 0.33	8.86
27	300	3.33	>4	---
80	353	2.83	>4	---
102	375	2.67	>4	---
	System: $LiClO_4$ + C222D in CH_3CN			
-45	228	4.39	3.19 ± 0.07	7.35
-32	241	4.15	3.26 ± 0.10	7.51
-21	252	3.97	3.42 ± 0.10	7.87
- 7	266	3.76	3.45 ± 0.14	7.95
5	278	3.60	3.50 ± 0.16	8.07
28	301	3.32	3.54 ± 0.25	8.16
55	328	3.05	---	---
86	359	2.78	---	---

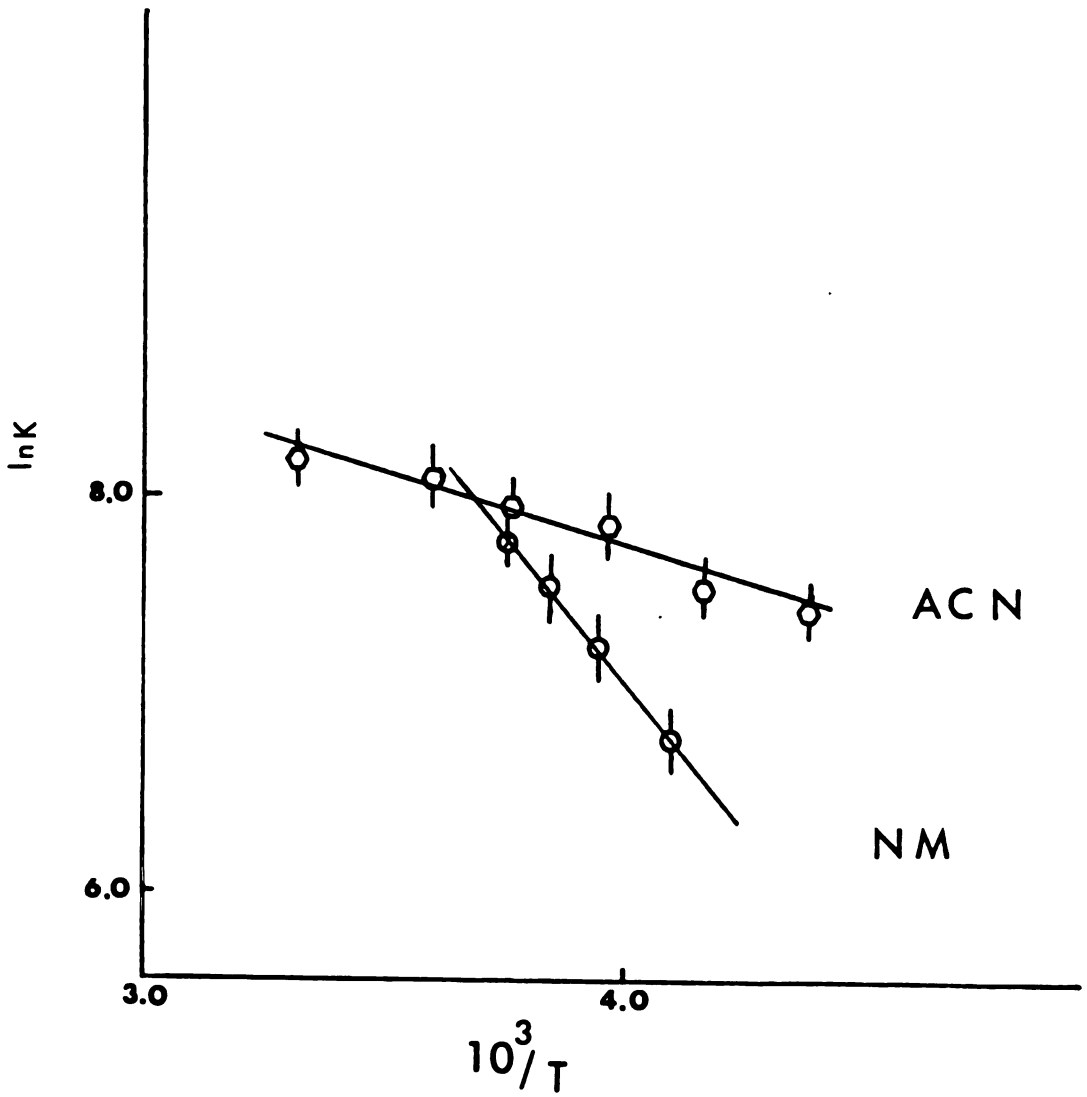

Figure 20. A plot of ln K vs 1/T for the complexation reactions of Li^+ with C222D in acetonitrile and nitromethane.

ion and is so strongly solvated that considerably more energy must be expended in the desolvation step than for larger ions like Cs^+. In this case this desolvation energy is not replaced in the complexation step. Unfortunately, there are not many data available in the literature for lithium-macrocycle complexes to which our data can be compared. Kauffmann *et al.* (65) studied Li^+-C211 and Li^+-C221 complexes in water and report ΔH = -5.1 kcal/mole and ΔS = 8 cal/mole·°K for the former and ΔH = 0.0 kcal/mole and ΔS = 11.4 cal/mole·°K for the latter. In both cases $\Delta S > 0$ and ΔH becomes more positive for larger ligands.

All the Cs-133 chemical shifts measured at various temperatures are listed in Tables 13-15 and shown in Figures 21-23. The formation constants calculated by the KINFIT program are listed in Table 16. All the formation constants listed in Table 16 have been calculated by using the model,

$$\delta_{obs} = X_M\delta_M + X_{ML}\delta_{ML} + X_{MA}\delta_{MA} \qquad (6)$$

which takes into account ion pair formation as described in Chapter III and Appendix II. In the three systems studied, $CsB\phi_4$ and C222D in pyridine, CsSCN and C222D in CH_3NO_2 and CsSCN and C222D in acetonitrile, the curvature in the mole ratio plots is more pronounced as the temperature decreases. This trend implies that the complex formed is stronger at lower temperature.

From the calculated formation constants we can see that this is indeed the case. In pyridine the log K = 3.29 ± 0.06 at -39°C and it decreases as the temperature increases and at 85°C it has a value of log K = 2.55 ± 0.02. In the case of nitromethane the complex formed is weaker and the variation of log K with temperature smaller. At -30°C log K = 1.85 ± 0.06 and at 100°C is log K = 1.64 ± 0.06. The Cs^+-C222D complex in acetonitrile is also rather weak. At -37°C log K = 2.03 ± 0.07 while at 72°C log K = 1.46 ± 0.13. In all three systems studied the complexation reaction is exothermic. Plots of lnK vs 1/T for the above data are shown in Figure 24 and the thermodynamic quantities obtained by linear least squares fitting of these plots are listed in Table 17. In all cases $\Delta H < 0$ and $\Delta S > 0$, which indicates that the Cs^+-C222D complex is both enthalpy and entropy stabilized in all three solvents.

Temperature dependence study of the Na^+-C222D complexation in pyridine and nitromethane was also attempted. But the line widths are extremely broad since sodium has a large quadrupole moment and C222D provides an unsymmetrical environment around the nucleus. In the case of nitromethane at 5°C the line widths are of the order of 1000 Hz therefore there is a large experimental error involved in the chemical shift measurements and formation constant of the complexes cannot be measured very accurately.

Table 13. Cs-133 Chemical Shifts of $CsBPh_4$ (0.015 M) in the Presence of C222D in Pyridine at Various Temperatures.

Mole Ratio	Temperature, °C							
	-39°	-25°	-12°	3°	25°	44°	66°	85°
0.00	24.71	29.01	31.51	33.91	39.41	43.81	48.71	52.61
0.53	4.41	---	13.51	16.11	22.91	28.91	35.21	40.91
0.80	- 3.49	---	6.51	9.21	16.41	22.71	19.31	35.51
1.20	-13.09	- 7.89	- 3.09	0.11	8.21	14.61	---	28.41
1.81	-22.59	-16.89	-12.39	- 9.19	- 1.39	5.01	12.61	19.71
2.07	-24.79	---	-15.19	-12.09	- 3.89	2.41	9.91	17.51
2.33	-26.09	-21.19	-17.59	-13.79	- 6.19	- 0.09	7.31	15.01
2.80	-28.49	-22.99	-19.99	-17.19	- 9.54	- 3.69	4.31	11.01
3.66	-30.59	-25.79	-22.49	-19.89	-12.69	- 7.29	0.61	7.31
4.37	-32.59	-27.79	-24.69	-21.69	-14.89	- 9.59	- 2.19	4.31
4.98	-33.79	-28.99	-26.59	-22.69	-16.49	-11.09	- 3.99	2.01
10.00	-35.49	-31.79	-30.09	-27.59	-21.59	-16.99	-10.99	- 5.39

Table 14. Cs^{+}-133 Chemical Shifts of CsSCN (0.010 M) in the Presence of C222D in CH_3NO_2

Table 14. Cs-133 Chemical Shifts of CsSCN (0.010 M) in the Presence of C222D in CH_3NO_2 at Various Temperatures.

Mole Ratio	Temperature, °C	Mole Ratio	Temperature, °C			
	25°		-1°	-30°	77°	100°
0.00	54.62	0.00	52.07	47.48	61.53	63.40
0.27	50.59	0.40	44.94	40.17	57.65	59.83
0.59	46.33	0.69	41.38	36.13	54.86	57.81
0.99	42.69	1.38	34.09	28.22	49.90	53.01
1.30	39.82	1.83	30.06	24.34	47.10	50.21
1.60	36.87	2.25	27.73	22.01	44.78	48.35
2.13	33.47	2.55	25.86	20.31	43.38	46.65
2.70	30.12	3.00	23.85	18.76	41.52	45.40
3.20	28.57	3.60	21.52	16.43	39.81	43.39
5.20	22.21	4.20	19.82	13.95	37.48	41.37
		5.04	16.82	11.47	35.85	---

Table 15. Mole-Ratio-Temperature Data for the Chemical Shift of CsSCN (0.01 M) in the Presence of C222D in CH_3CN.

Mole Ratio	Temperature, °C			
	72°	26°	-5°	-37°
0.00	-26.88	-34.64	-39.91	-43.16
0.37	-26.11	-33.71	-38.98	-42.39
0.74	-25.65	-33.24	-38.36	-41.61
1.28	-25.18	-32.31	-37.58	-40.84
1.71	-24.41	-31.54	-36.80	-39.91
2.50	-23.48	-30.92	-36.19	-39.29
2.84	-23.17	-30.61	-35.88	-39.13
3.58	-22.54	-30.30	-35.41	-38.82
4.03	-22.07	-29.98	-35.26	-38.59
5.02	-21.61	-29.52	-34.64	-38.37

Table 16. Formation Constants for the Complexation of Cs^+ by C222D in Py, CH_3NO_2 and CH_3CN at Various Temperatures.

T°C	T°K	$10^3/T$	log K	ln K
	System = $CsBPh_4$ + C222D in Py			
-39	234	4.27	3.29 ± 0.06	7.59
-25	248	4.03	3.14 ± 0.03	7.24
-12	261	3.83	3.07 ± 0.04	7.07
3	270	3.70	2.96 ± 0.02	6.82
25	298	3.35	2.86 ± 0.01	6.59
44	317	3.15	2.79 ± 0.01	6.41
66	339	2.95	2.64 ± 0.01	6.08
85	358	2.79	2.55 ± 0.02	5.87
	System = CsSCN + C222D in CH_3NO_2			
-30	243	4.11	1.85 ± 0.06	4.25
- 1	272	3.68	1.82 ± 0.05	4.20
25	298	3.35	1.79 ± 0.03	4.11
77	350	2.86	1.69 ± 0.04	3.90
100	373	2.68	1.64 ± 0.06	3.77
	System = CsSCN + C222D in CH_3CN			
-37	236	4.24	2.03 ± 0.07	4.68
- 5	268	3.73	1.75 ± 0.10	4.03
26	299	3.34	1.70 ± 0.08	3.92
72	345	2.90	1.46 ± 0.13	3.36

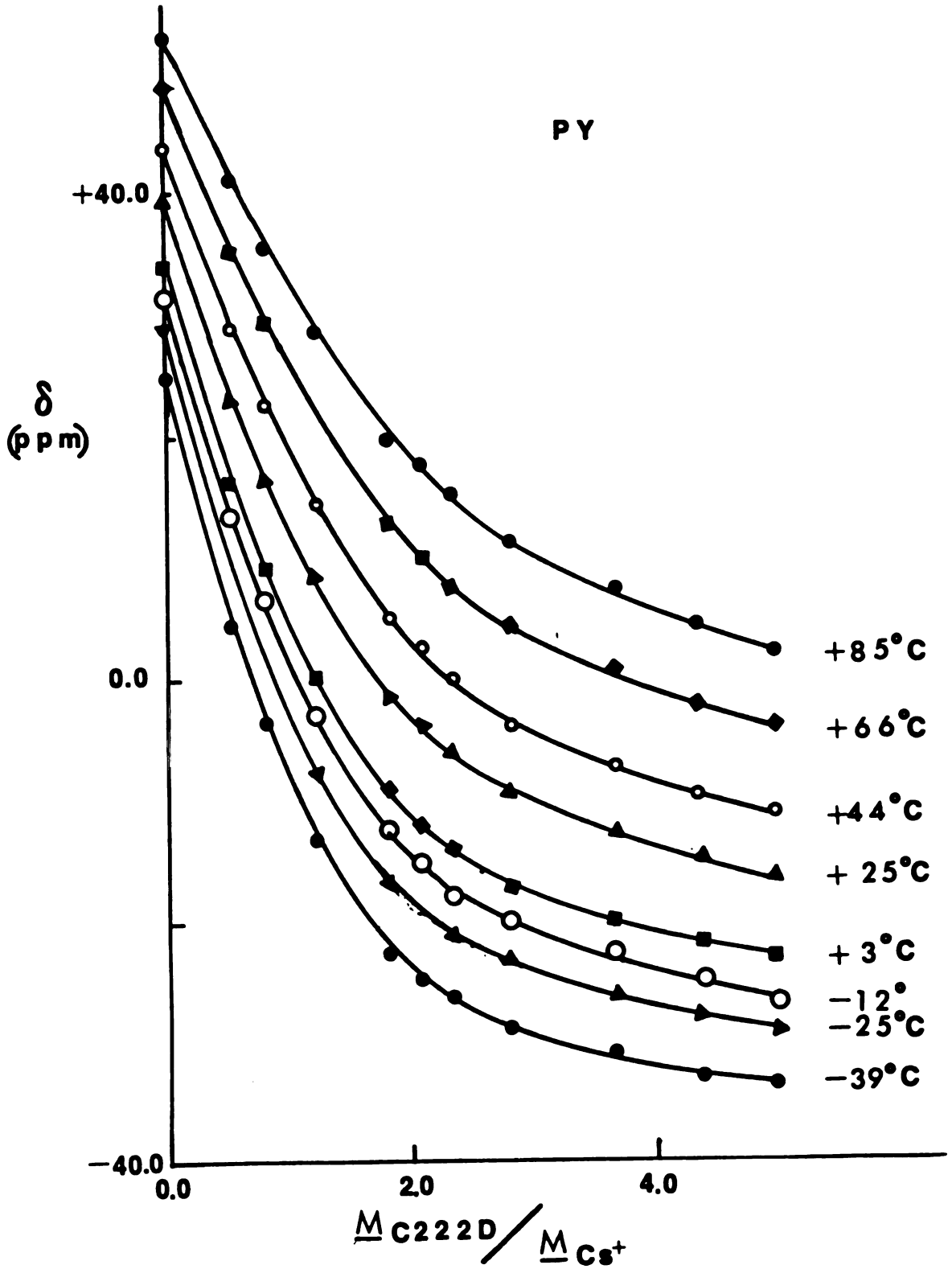

Figure 21. Cesium-133 chemical shifts as a function of C222D/Cs^+ mole ratio in pyridine at various temperatures.

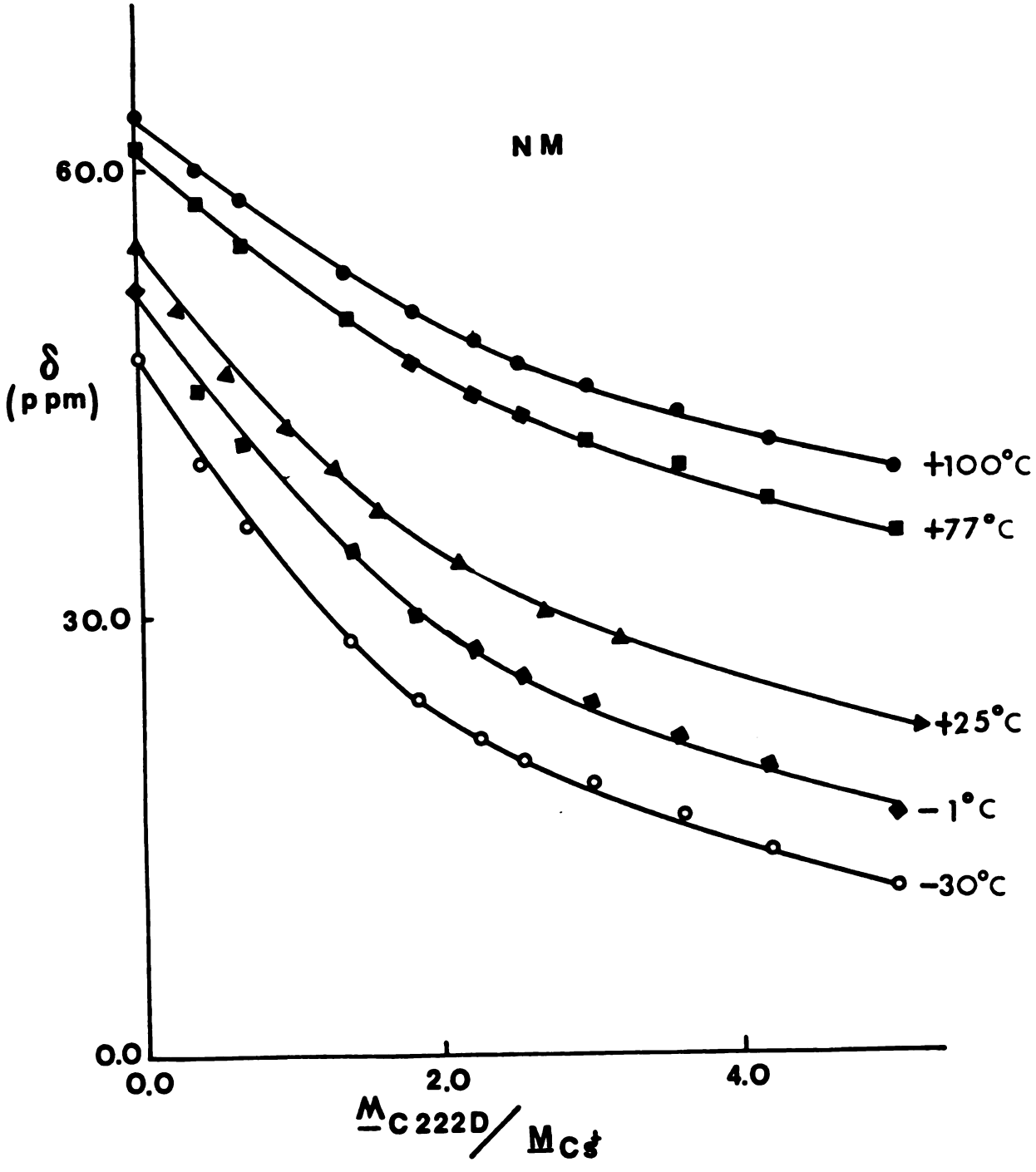

Figure 22. Cesium-133 chemical shifts as a function of C222D/Cs^+ mole ratio in nitromethane at various temperatures.

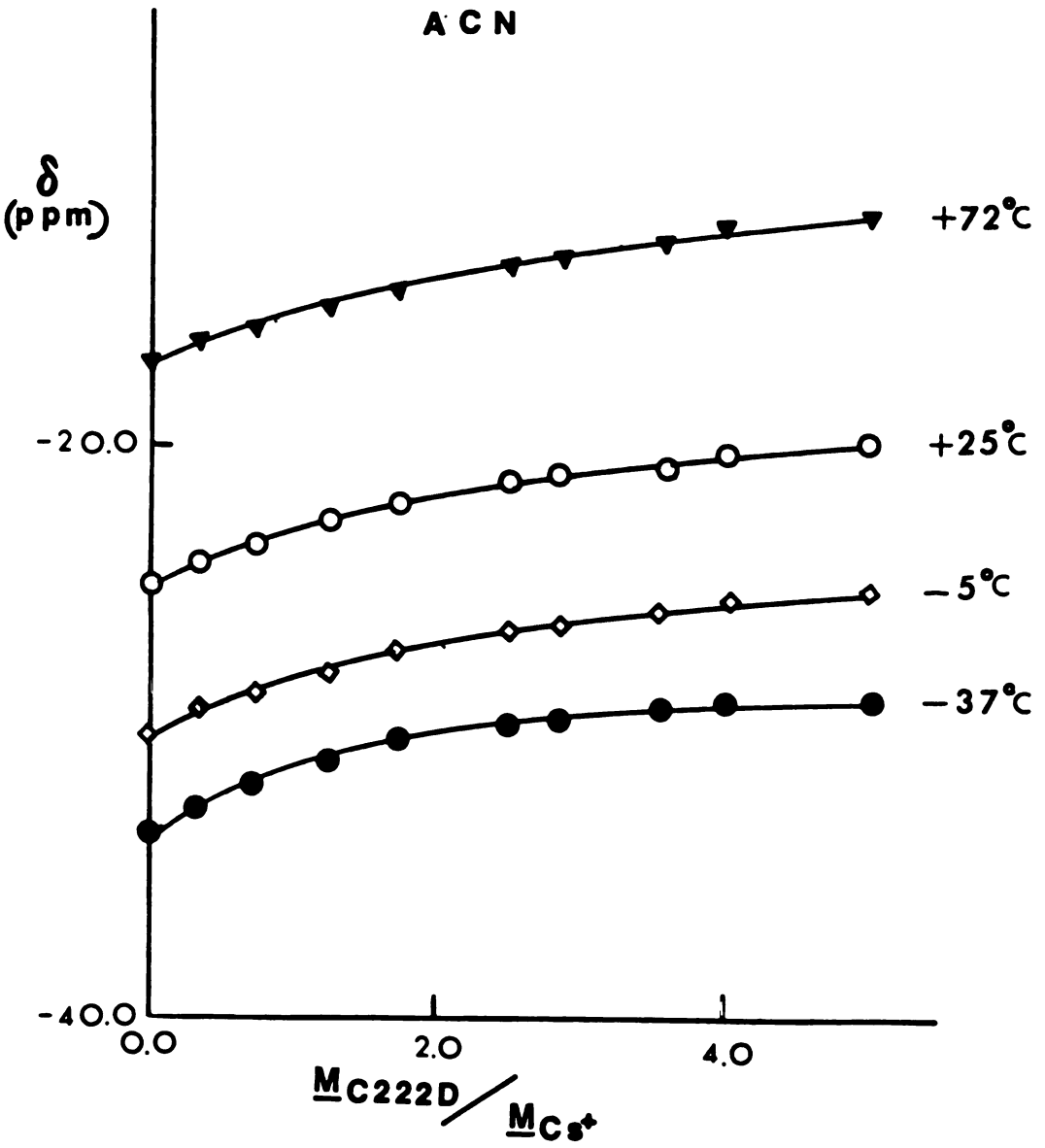

Figure 23. Cesium-133 chemical shifts as a function of C222D/Cs^+ mole ratio in acetonitrile at various temperatures.

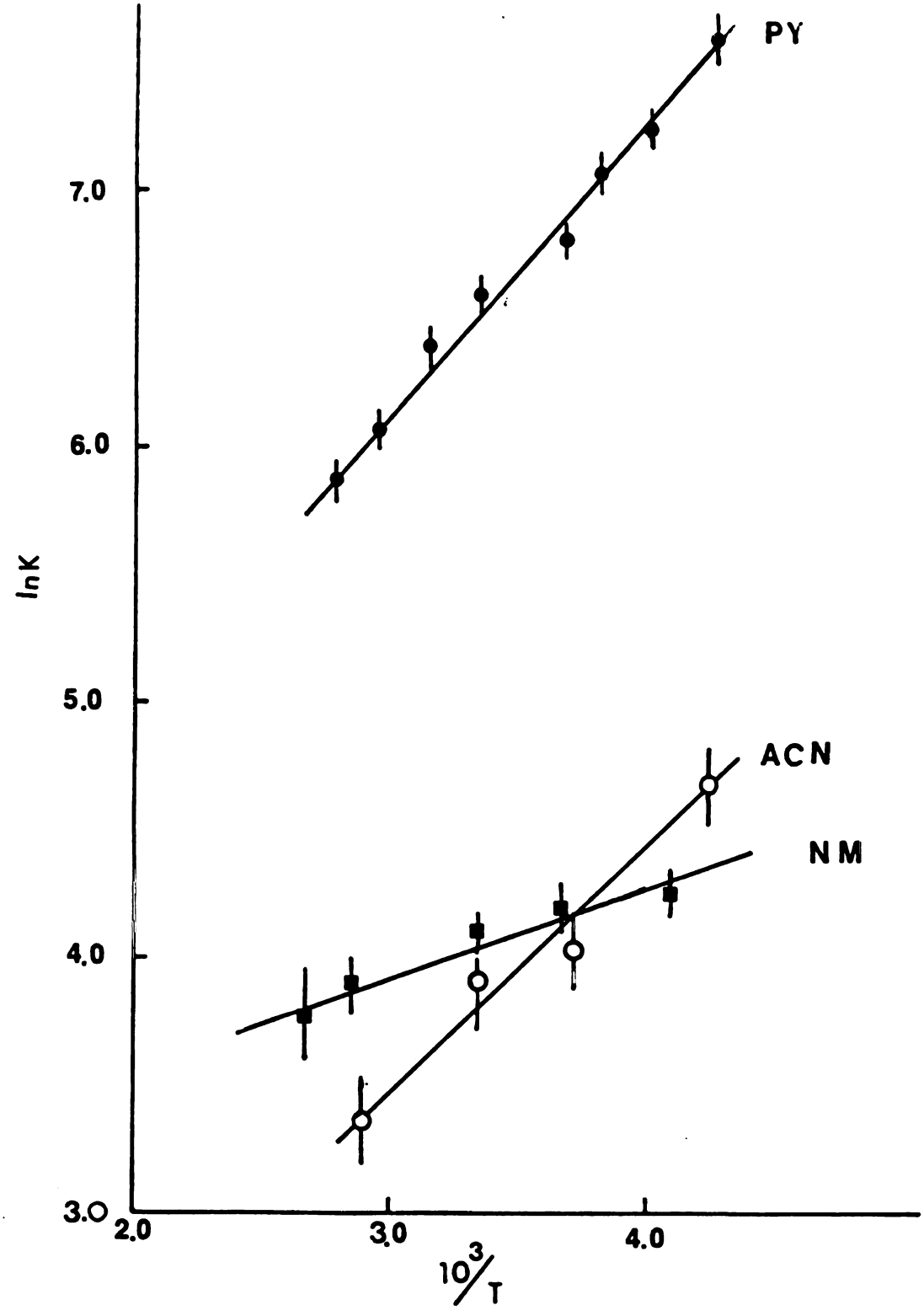

Figure 24. A plot of ln K vs 1/T for the complexation reactions of Cs^+ with C222D in pyridine, acetonitrile and nitromethane.

Table 17. Thermodynamic Quantities for the Complexation of Li^+ and Cs^+ by C222D in Various Solvents.

System	ΔS cal/mole·°K	ΔH kcal/mole	ΔG_{298} kcal/mole
$CsBPh_4$ + C222D in Py	5.69 ± 0.33	-2.18 ± 0.09	-3.91
CsSCN + C222D in CH_3NO_2	5.81 ± 0.33	-0.67 ± 0.10	-2.44
CsSCN + C222D in CH_3CN	1.37 ± 0.93	-1.85 ± 0.26	-2.32
$LiClO_4$ + C222D in CH_3NO_2	38.4 ± 0.62	6.10 ± 0.16	<0
$LiClO_4$ + C222D in CH_3CN	21.7 ± 0.87	1.58 ± 0.22	-4.84
$LiClO_4$ + C222D in Py	>0	>0	<0

CHAPTER V

SPECTROSCOPIC STUDIES OF COMPLEXATION OF ALKALI METAL IONS, WITH 2,2' BIPYRIDINE IN NONAQUEOUS SOLVENTS

INTRODUCTION

Studies of the crystal structure of 2,2'-bipyridine have shown that the two pyridine rings are coplanar with the N atoms and that the molecule has the transconfiguration (112-114) shown below.

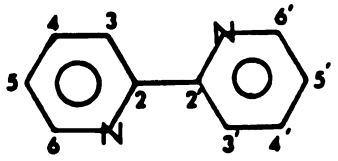

Dipole moment measurements of the above compound in solution indicate that the molecule is approximately planar, with the two nitrogen atoms in trans positions about the 2:2' bond (115-117). 2,2'-bipyridine forms strong complexes with many metal ions. The complexes have a metal to ligand stoichiometry of 1:1, 1:2 or 1:3. In the complexation with a metal or with the hydrogen ions there is chelate ring formation and it is undoubtedly accepted that the ligand has the cis conformation. Most probably the 5-membered chelate ring is coplanar with the rest of the bipyridine molecule.

The alkali metals are not expected to form complexes as stable as those of other metals. The predicted trend within the group of the alkali metals is for stability to increase with decreasing atomic number. Quantitative data are not available, but it has been reported that lithium, sodium and potassium complexes of 1:10 phenanthroline, which is quite similar to 2,2'-bipyridine, have been obtained from a methanolic solution but not complexes of rubidium or

cesium. The complexes $Li(Phen)\ ClO_4$ and $Na(Phen)_2\ ClO_4$ are the ones obtained (117). Schilt et al. (118) tried to prepare the above lithium complex but they obtained a product that appeared to be a mixture of both mono and bis complexes. Grillone et al. (119) report recently the preparation and isolation of a 1:1 adduct of $KBPh_4$ with 2,2'-bipyridine (2,2'BP). The $K(2,2'\ BP)BPh_4$ complex was isolated from acetone solutions which contained 2,2'BP/salt ratios of 6:1-7:1. The IR spectrum of the above compound in Nujol was also obtained. Attempts to isolate 2,2'BP adducts of $KClO_4$, even by the use of 2,2'BP/salt ratios up to 10:1 were unsuccessful.

In general the complexation of 2,2'-bipyridine with alkali metal ions has not been studied in detail. Quite often alkali metal salts are used to achieve high and constant ionic strength in solutions, when complexation of 2,2'-bipyridine with other metal complexes is studied, with the assumption that there is no interaction of the ligand with the alkali metal ions (120). Today we know that alkali metal ions do form stable complexes with many ligands and, therefore, it was of interest to study if there is interaction between 2,2'-bipyridine and alkali metal ions in nonaqueous solvents. For this purpose the reaction of Li^+, Na^+ and Cs^+ ion with 2,2'-bipyridine in different solvents and of Na^+ with 2,2'-biquinoline and 4,4'-dimethyl,2,2'-bipyridine was investigated by using alkali metal NMR and ^{13}C NMR.

RESULTS AND DISCUSSION

Sodium-23, lithium-7 and cesium-133 chemical shifts were determined as a function of ligand/metal ion mole ratios. In all cases only one population average resonance of the metal ion was observed. It is accepted that the first step in the formation of the metal chelate complex is the formation of the unidentate complex and then it is followed by a rapid chelate ring closure (121). In this reaction the solvent plays an important role. The donicity of the solvent, reflected by its ability to solvate the metal ion, usually expressed by Gutmann's donor number, its dielectric constant and its structure, are quite important factors in determining whether the ligand can successfully compete with the solvent for position in the primary solvation shell. In this study an investigation of the influence of the solvent and of the size of the metal ion as well as the substituent groups on the ligand in the reaction of 2,2'-bipyridine with Li^+, Na^+ and Cs^+ was attempted.

The reaction of 2,2'-bipyridine with $LiBPh_4$ was studied in tetrahydrofuran, methanol, dimethylformamide and propylene carbonate solutions and with $LiClO_4$ in nitromethane. All the lithium-7 chemical shifts measured are listed in Table 18. The frequency of the lithium-7 resonance in tetrahydrofuran, methanol and formamide was found to be essentially independent of the ligand/Li^+ mole ratio (Figure 25). In these solvents the immediate environment of the lithium ion is not changed upon addition

Table 18. Mole Ratio Study of 2,2'-Bipyridine Complexes with Lithium in Various Solvents by Li-7 NMR at 25°C.

Solvent	Salt	$[Li^+]M$	$[2,2'BP]/[Li^+]$	$\Delta\delta$(ppm)
THF	$LiBPh_4$	0.05	0.00	0.93
			1.02	1.04
			2.00	1.04
			3.02	1.04
			4.06	0.83
DMF	$LiBPh_4$	0.05	0.00	-0.45
			0.97	-0.23
			2.19	-0.14
			2.98	-0.14
			4.00	-0.29
PC	$LiBPh_4$	0.05	0.00	0.55
			1.05	0.34
			2.04	-0.13
			3.14	-0.65
			4.00	-0.97
CH_3OH	$LiBPh_4$	0.05	0.00	0.43
			1.00	0.72
			2.04	0.72
			3.15	0.67
			4.03	0.83

Table 18. Continued

Solvent	Salt	$[Li^+]$ M	[2,2'BP]/$[Li^+]$	Δδ(ppm)
CH_3NO_2	$LiClO_4$	0.05	0.00	0.20
			0.33	-0.53
			0.50	-0.95
			0.70	-1.42
			1.00	-2.10
			1.22	-2.68
			1.39	-2.94
			1.61	-3.31
			1.85	-3.62
			2.00	-3.84
			2.22	-3.99
			2.43	-3.99
			2.72	-3.99
			3.06	-3.93
			3.44	-3.93
			3.81	-3.99
			4.58	-3.93
			5.02	-3.93

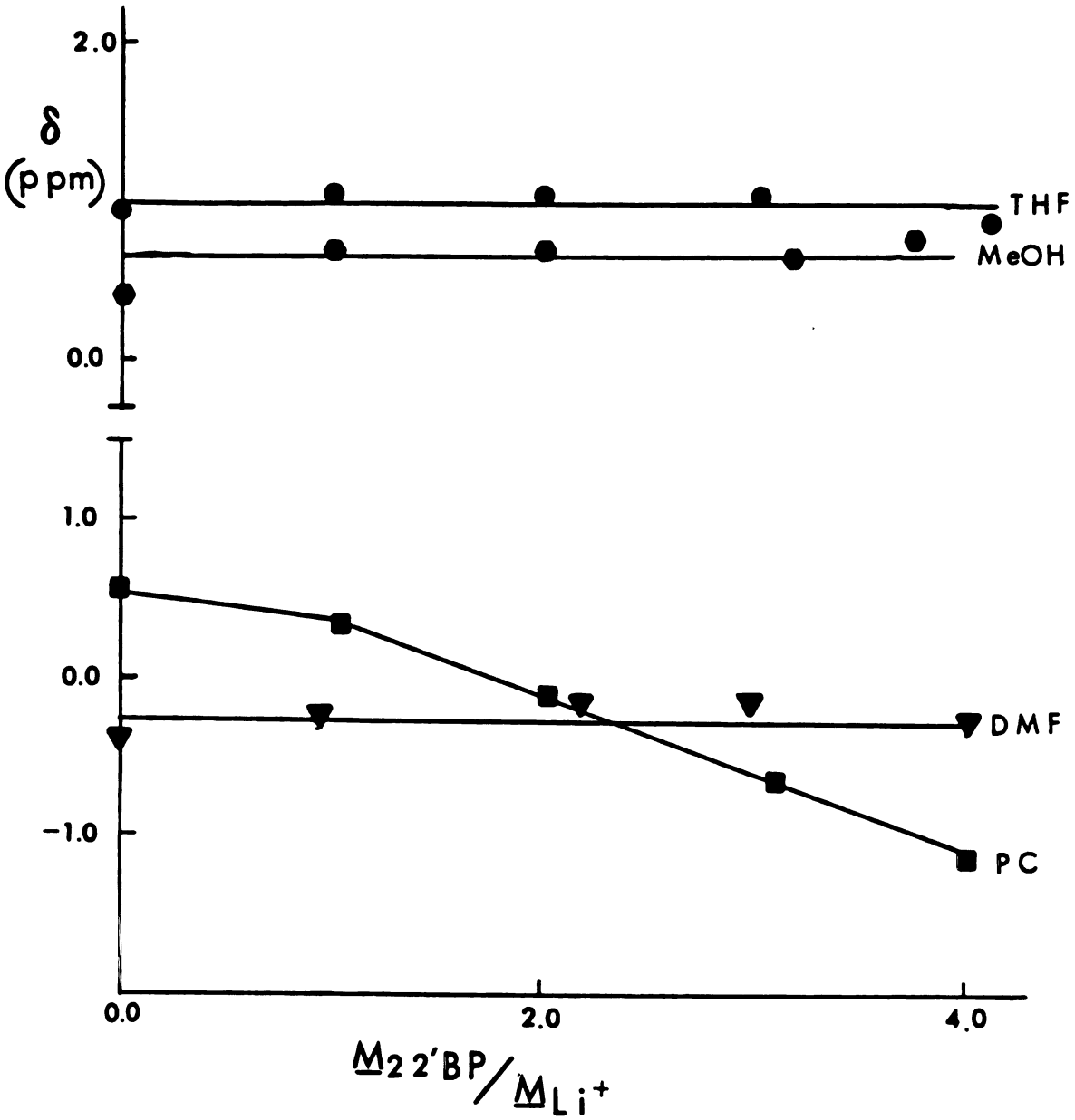

Figure 25. Lithium-7 chemical shift as a function of 2,2'BP/Li^+ mole ratio in THF, MeOH, DMF, and PC solutions.

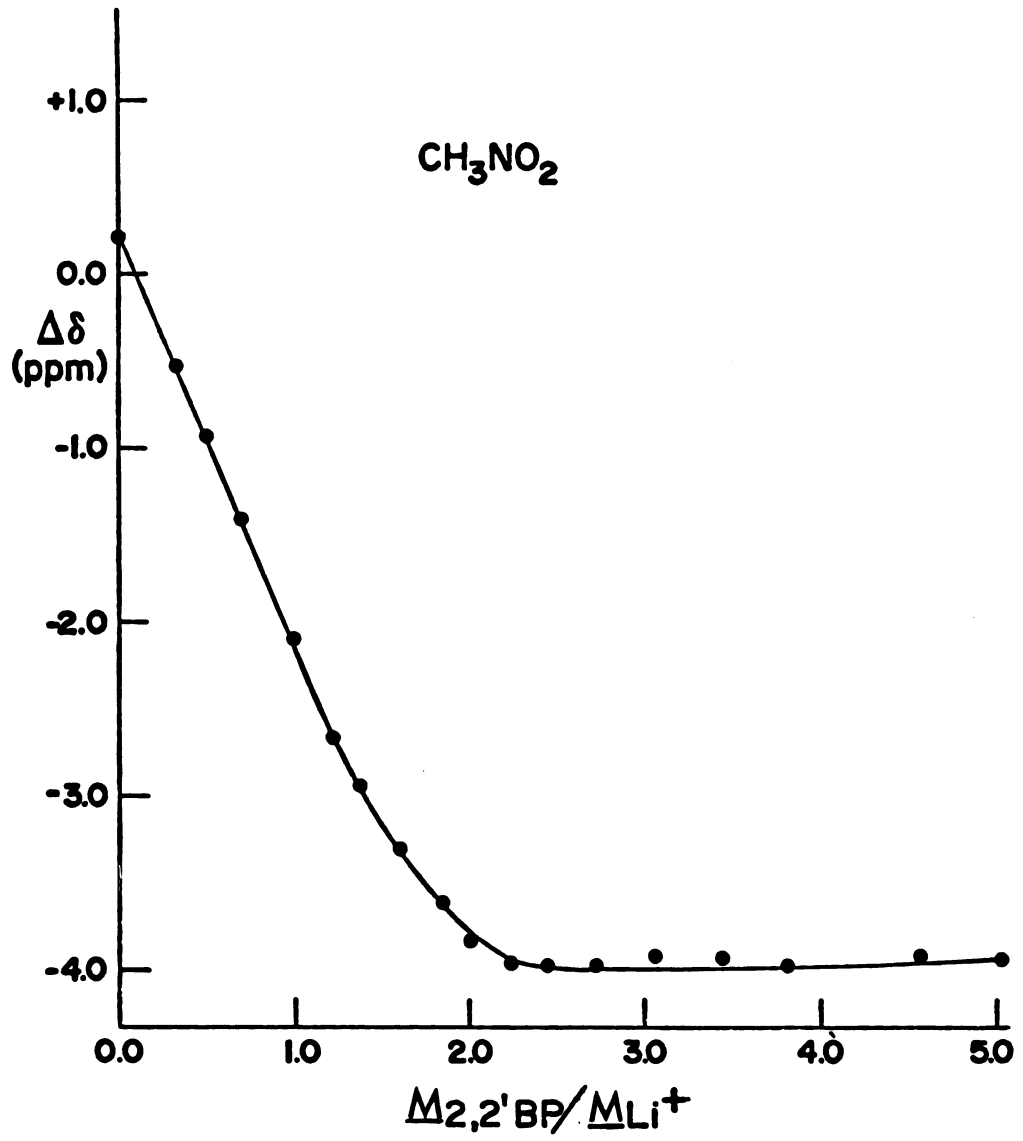

Figure 26. Lithium-7 chemical shift as a function of 2,2'BP/Li^+ mole ratio in nitromethane solutions.

of ligand and, therefore, there is no evidence for the formation of a complex. The above solvents have a strong solvating ability (Gutmann donor numbers of 20.0, 25.7 and 26.6 respectively) and can compete quite successfully with the ligand for a position in the primary solvation shell.

In the case of propylene carbonate (Figure 25), a solvent of intermediate solvating ability (Gutmann donor number 15.1), there is a downfield chemical shift change from the position characteristic of the solvated lithium ion upon addition of the ligand. This shift indicates that there is interaction between Li^+ and 2,2'-bipyridine but the complex formed seems rather weak since until a mole ratio of 4.0 there is no indication of approaching the limiting chemical shift.

In nitromethane, on the other hand, which is a solvent of weak solvating ability (Gutmann donor number of 2.7) there is a large change of the lithium-7 chemical shift (about 4 ppm) (Figure 26) which indicates a drastic change in the immediate environment of the Li^+, from that of the solvated lithium by nitromethane to that of the complexed lithium by 2,2'-bipyridine. From the mole ratio plot of Figure 26 we can conclude that the complex formed is a rather strong one and that it has a stoichiometry of 2:1 since the limiting chemical shift reaches a constant value at a mole ratio of about 2.0.

In order to obtain more supporting evidence for the above conclusion, the carbon-13 nmr spectra of

2,2'-bipyridine with $LiClO_4$ in the nitromethane at various mole ratios were obtained with the results listed in Table 19 and shown in Figure 27. The spectrum of 2,2'-bipyridine in nitromethane consists of 4 peaks. The most downfield one was assigned to the 2,2' carbon atoms and the most upfield one to the 5,3,5',3' carbon atoms, with the peaks for the 6,6' and 4,4' carbon atoms in between. Upon addition of $LiClO_4$ to the bipyridine solution all the peaks shift downfield and the chemical shift tends to level off after a mole ratio of $[Li^+]/[2,2'BP]$ of about 0.5. The magnitude of the chemical shift change is different for the different carbon atoms, the largest one, being for C6,6' and the smallest one for C2,2', while the chemical shift change for the C5,3,5',3' passes through a maximum at a mole ratio of 0.5. The carbon-13 data strongly support the lithium-7 nmr data that there is indeed a strong $Li(2,2'BP)_2$ complex formed.

In order to study further the complexation ability of 2,2'-bipyridine, its reaction with $NaBPh_4$ was studied in dimethyl sulfoxide, methanol, dimethylformamide, nitromethane, tetrahydrofuran, propylene carbonate and acetonitrile. All the sodium-23 chemical shifts and line widths measured in the different solvents are listed in Table 20 and shown in Figures 28-30. In dimethyl sulfoxide, dimethylformamide and methanol, solvents of strong solvating ability, the sodium-23 chemical shift is independent of the $[2,2'BP]/[Na^+]$ mole ratio (Figure 28) indicating that at best there is only a very weak interaction between sodium ion and ligand. In

Table 19. ^{13}C Chemical Shifts (ppm)[a,b] for 2,2'-Bipyridine (0.20 M) with $LiClO_4$ in Nitromethane.

$[Li^+]/[2,2'BP]$	$\delta_{C2,2'}$	$\delta_{C6,6'}$	$\delta_{C4,4'}$	$\delta_{C5,3,5',3'}$
0.00	150.47	138.21	125.13	121.91
0.30	150.73	139.51	125.88	122.41
	(0.26)	(1.30)	(0.75)	(0.50)
0.40	150.83	139.89	126.12	122.55
	(0.36)	(1.68)	(0.99)	(0.64)
0.50	150.93	140.28	126.33	122.67
	(0.46)	(2.07)	(1.20)	(0.76)
0.61	150.94	140.39	126.39	122.67
	(0.47)	(2.18)	(1.26)	(0.76)
0.75	150.91	140.50	126.43	122.63
	(0.44)	(2.29)	(1.30)	(0.72)
1.00	150.93	140.46	126.39	122.53
	(0.46)	(2.25)	(1.26)	(0.62)
1.20	150.93	140.53	126.42	122.51
	(0.46)	(2.32)	(1.29)	(0.60)
2.00	150.86	140.50	126.39	122.44
	(0.39)	(2.29)	(1.26)	(0.53)

[a]All chemical shifts reported are referenced to TMS.

[b]Numbers in parentheses represent the differences $\delta - \delta^{free}_{bipy}$.

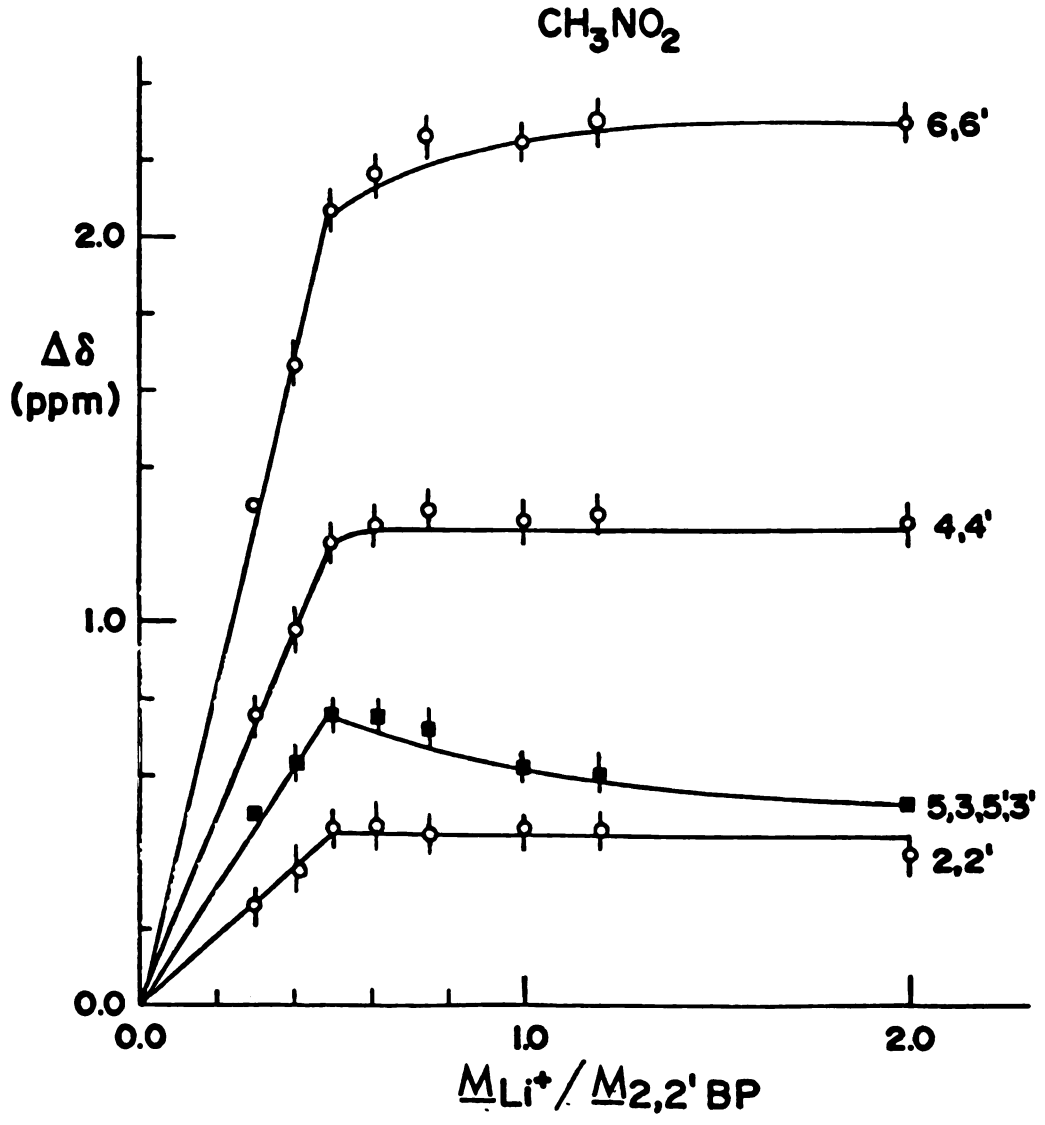

Figure 27. Carbon-13 chemical shifts as a function of Li^+/2,2'BP mole ratio in nitromethane solutions.

Table 20. Mole Ratio Study of 2,2'-Bipyridine Complexes with $NaBPh_4$ in Various Solvents by Na-23 NMR at 25°C.

Solvent	$[Na^+]M$	$[2,2'BP]/[Na^+]$	δ(ppm)	$\Delta\nu_{\frac{1}{2}}$(Hz)
DMSO	0.075	0.00	1.3	52
		0.47	1.0	52
		1.00	1.0	55
		2.00	1.2	58
		3.08	1.0	59
		3.95	0.9	64
CH_3OH	0.075	0.00	4.1	31
		0.47	3.9	30
		1.00	3.9	30
		2.04	3.8	30
		2.80	3.6	28
		4.00	3.6	30
DMF	0.075	0.00	5.4	37
		1.00	5.2	38
		2.00	5.2	40
		2.90	5.2	40
		4.05	5.2	40
CH_3NO_2	0.150	0.00	14.7	12
		0.09	13.9	27
		0.19	13.1	46
		0.27	12.4	61

Table 20. Continued

Solvent	$[Na^+]$M	[2,2'BP]/$[Na^+]$	δ(ppm)	$\Delta\nu_{\frac{1}{2}}$(Hz)
		0.36	11.1	83
		0.40	10.6	74
		0.47	10.1	100
		0.63	9.0	124
		0.70	8.2	149
		0.77	7.8	154
		0.83	6.8	181
		0.90	6.7	198
		1.00	6.8	227
		1.13	5.0	
		1.33	3.6	268
		1.44	3.8	325
		1.60	1.6	347
		2.01	1.1	354
		2.30	-0.7	441
		2.60	-2.2	432
		3.04	-1.8	495
		3.30	-3.8	574
		3.60	-3.8	605
		4.00	-2.8	625
		4.70	-4.3	586
		5.00	-4.3	600
THF	0.075	0.00	8.1	26
		1.01	6.9	56

Table 20. Continued

Solvent	$[Na^+]$M	$[2,2'\ BP]/[Na^+]$	δ(ppm)	$\Delta\nu_{\frac{1}{2}}$(Hz)
THF	0.075	2.03	5.0	94
		3.03	3.7	104
		4.05	3.5	128
PC	0.075	0.00	9.7	64
		0.98	8.1	200
		2.00	6.4	260
		3.04	5.3	352
		4.04	4.2	362
CH_3CN	0.075	0.00	7.7	11
		1.05	5.9	28
		2.04	4.8	42
		3.03	3.9	52
		4.02	3.1	67

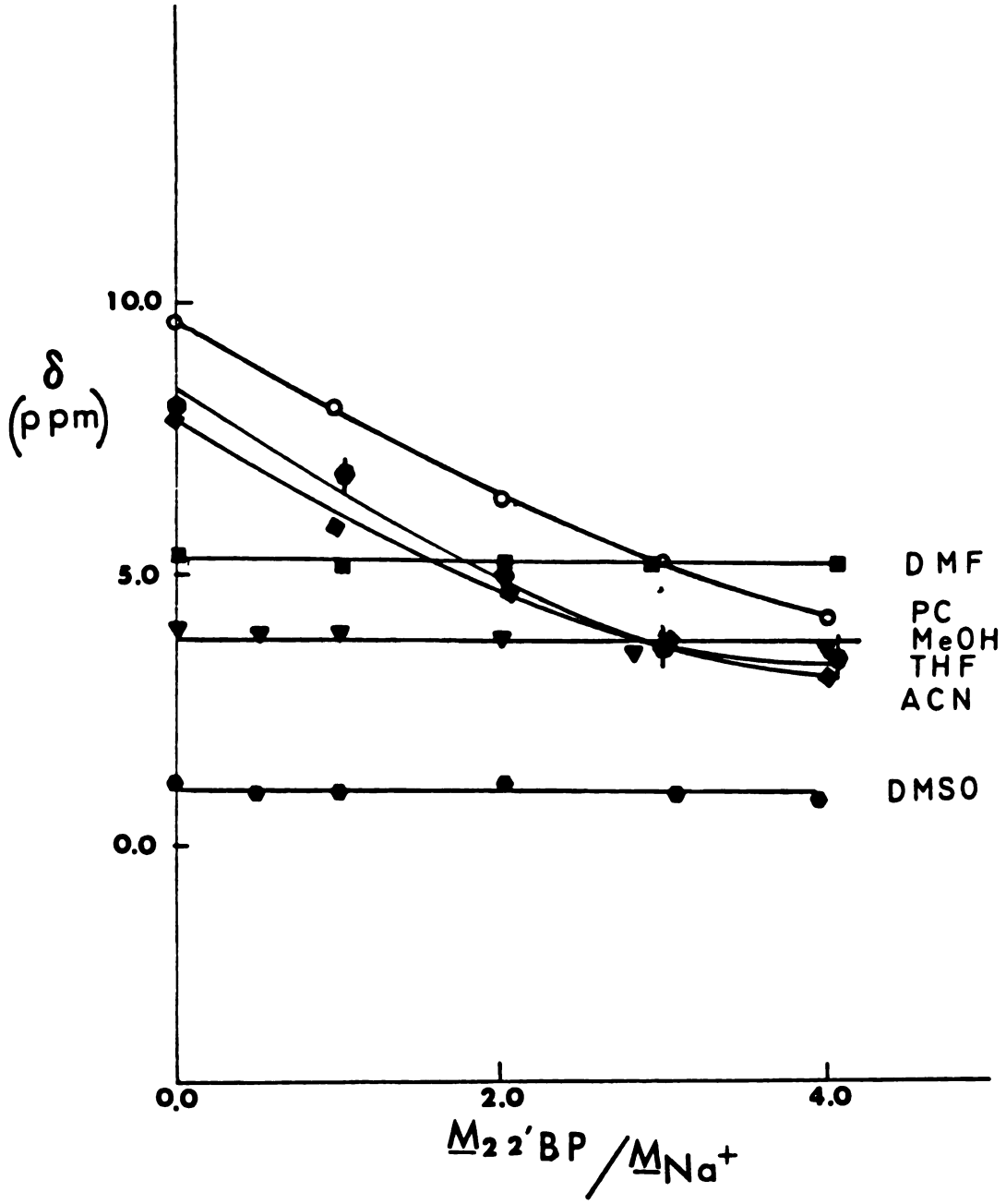

Figure 28. Sodium-23 chemical shift as a function of 2,2'BP/Na^+ mole ratio in DMF, CH_3OH, THF, PC, CH_3CN, and DMSO solutions.

the case of tetrahydrofuran, propylene carbonate and acetonitrile, solvents of medium solvating ability (respective Gutmann donor numbers of 20.0, 15.1 and 14.1) there is a downfield chemical shift change and considerable line-broadening of the sodium-23 resonance line upon addition of the ligand. This indicates that there is interaction of the metal ion with the ligand because the immediate environment of the sodium ion changes and from the symmetric environment of the solvated metal ion it goes to a more unsymmetric one as the increase of the linewidth indicates. The interaction of 2,2'-bipyridine with $NaBPh_4$ in the above solvents should be rather weak because until a mole ratio of 4.0 the limiting chemical shift has not been reached. The change in the linewidths also follows the same trend. In the case of nitromethane a large change in the chemical shift is observed (about 20 ppm), which indicates a drastic change in the environment of Na^+, from an oxygen donor like nitromethane, to a nitrogen donor like the 2,2'-bipyridine. Although the chemical shift change is very large, the complex formed should be rather weak because the mole ratio plot starts leveling off at a mole ratio close to 5.0. The linewidths of the sodium-23 resonance lines follow the same trend (Figure 30). We observe a tremendous change of the linewidth from 12 Hz for the solvated sodium to about 600 Hz for the complexed sodium indicating that 2,2'-bipyridine forms an unsymmetric environment for the sodium ion. From our data we can

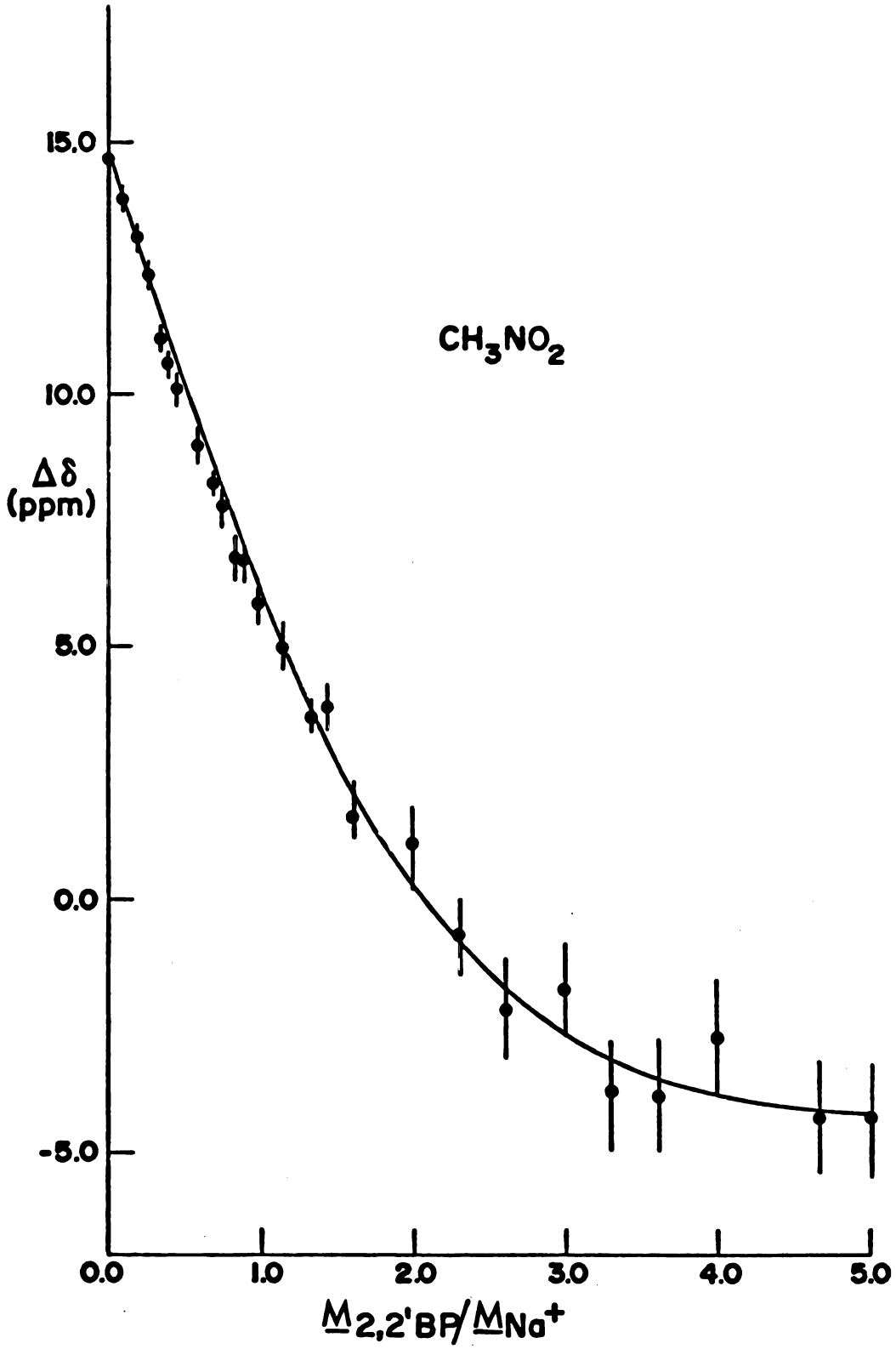

Figure 29. Sodium-23 chemical shift as a function of 2,2'BP/Na^+ mole ratio in nitromethane solutions.

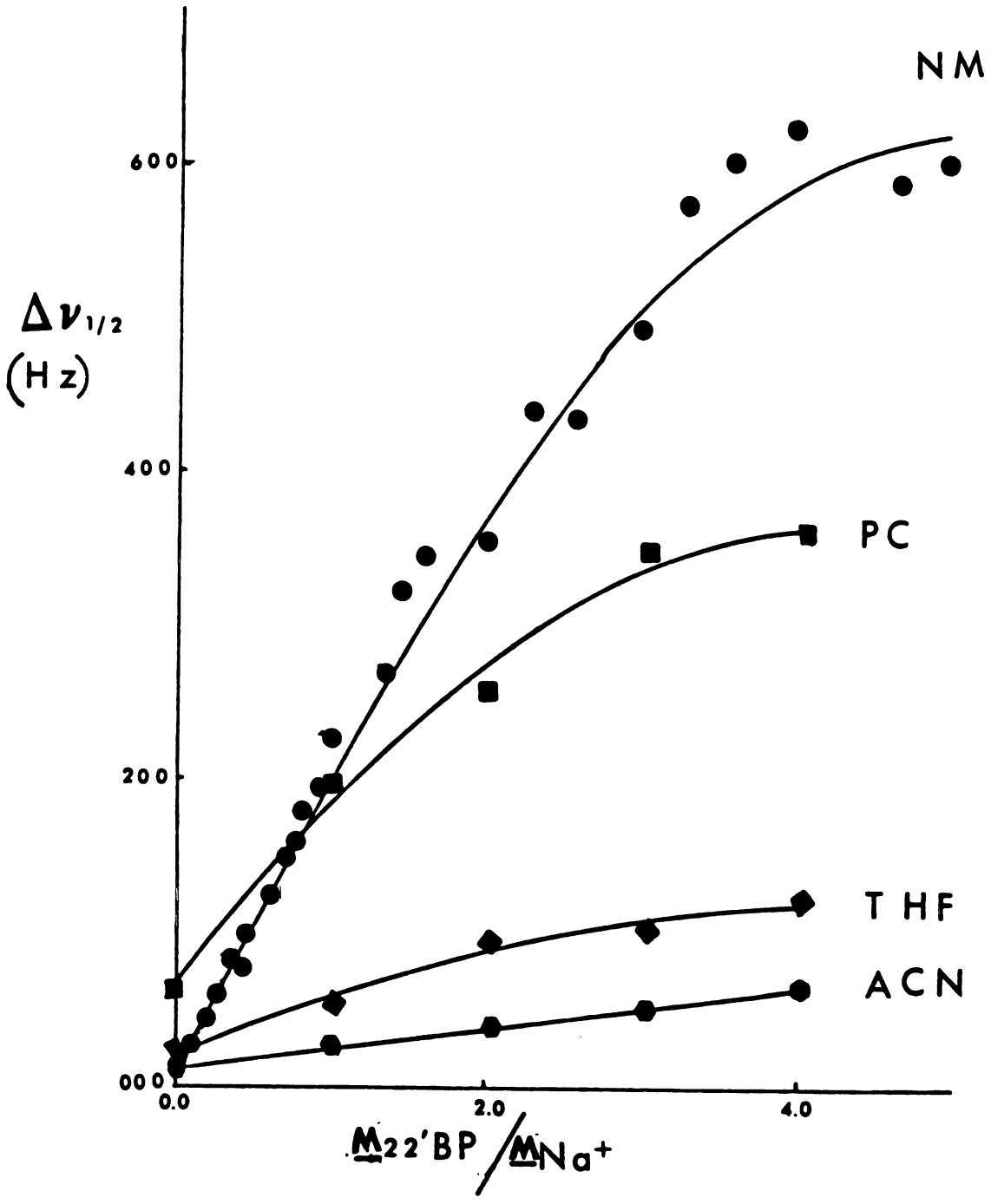

Figure 30. Linewidth change of the sodium-23 resonance as a function of mole ratio in CH_3NO_2, PC, THF and CH_3CN solutions.

unambiguously conclude that there is a complex formed between Na^+ and 2,2'bipyridine since we have such a large change of the sodium-23 chemical shift upon addition of the ligand into the salt solution, and that also the complex formed is a rather weak one. What we cannot unambiguously conclude is the stoichiometry of the complex formed. It is not clear from our data if the complex is 1:1 or a 2:1 as it is the case for the lithium-bipyridine complex. When the above data were analyzed by using the equation for a 1:1 complex, a formation constant of the order of 10 was obtained. Supporting evidence to our assumption that the complex might be a 2:1 is the large change of the chemical shift which seems to indicate that the Na^+ is in a completely different environment than that of the Na^+ solvated by nitromethane and that the ligand insulates it from the solvent. In order to see if we can get any clearer picture of the whole situation, the ^{13}C spectra of different mole ratios of $[NaBPh_4]/[2,2'\text{-bipyridine}]$ in nitromethane were taken with the results listed in Table 21. The chemical shift changes for each of the four carbon signals from the ones of the free ligand as a function of the $[Na^+]/[2,2'\text{Bipy}]$ mole ratio are shown in Figure 31. The carbon-13 nmr data agree with the sodium-23 nmr ones. There is considerable change in the chemical shift but not clear-cut evidence about the stoichiometry of the complex. The largest change is for the 6,6' carbons and the smallest one for the 4,4' carbons. UV-visible double

Table 21. ^{13}C Chemical Shifts (ppm)[a] for 2,2'-Bipyridine (0.20 M) with $NaBPh_4$ in Nitromethane.

$[Na^+]/[2,2'\ BP]$	$\delta_{C2,2'}$	$\delta_{C6,6'}$	$\delta_{C4,4'}$	$\delta_{C5,3,5',3'}$
0.00	150.47	138.21	125.13	121.91
0.20	150.73	138.68	125.31	122.35
	(0.26)[b]	(0.47)	(0.18)	(0.44)
0.30	150.85	138.85	125.41	122.56
	(0.38)	(0.64)	(0.28)	(0.65)
0.50	151.03	139.18	125.56	122.86
	(0.56)	(0.97)	(0.43)	(0.95)
0.70	151.14	139.43	125.66	123.03
	(0.67)	(1.22)	(0.53)	(1.12)
0.90	151.21	139.53	125.71	123.12
	(0.74)	(1.32)	(0.58)	(1.21)
1.00	151.20	139.58	125.71	123.14
	(0.73)	(1.37)	(0.58)	(1.23)
1.10	151.23	139.62	125.74	123.13
	(0.76)	(1.41)	(0.61)	(1.22)
1.25	151.23	139.66	125.75	123.19
	(0.76)	(1.45)	(0.62)	(1.28)
1.70	151.21	139.72	125.77	123.23
	(0.74)	(1.51)	(0.64)	(1.32)

Table 21. Continued

$[Na^+]/[2,2'\ BP]$	$\delta_{C2,2'}$	$\delta_{C6,6'}$	$\delta_{C4,4'}$	$\delta_{C5,4,5',3'}$
2.00	151.23	139.74	125.79	123.28
	(0.76)	(1.53)	(0.66)	(1.37)

[a]All chemical shifts are referenced to TMS.

[b]Numbers in parentheses represent the differences $\delta - \delta^{free}_{bipy}$

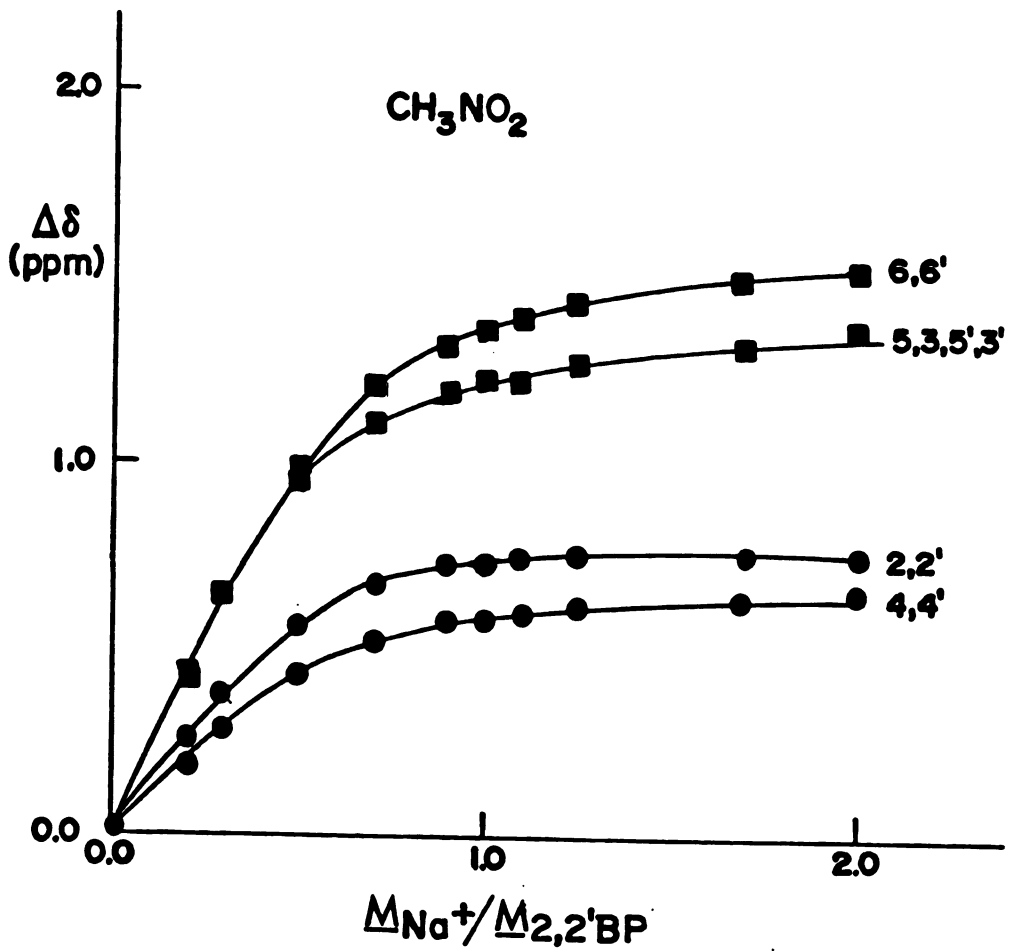

Figure 31. Carbon-13 chemical shifts as a function of Na^+/2,2'BP mole ratio in nitromethane solutions.

beam spectroscopy was also tried but nitromethane strongly absorbs in the whole UV region. The only peak that was obtained was a weak broad one at about 625 nm. This technique does not seem suitable for our study.

The complexation of 2,2'-bipyridine with Cs^+ was investigated in nitromethane, dimethylformamide, pyridine, propylene carbonate, acetonitrile and methanol by using cesium-133 nmr with all the results listed in Table 22 and shown in Figure 32. There is no evidence of complexation in any of the above solvents. As it is shown in Figure 32, the cesium-133 resonance line is independent of the 2,2'BP / Cs^+ mole ratio in all solvents studied.

Two substituted bipyridines, the 4,4'-dimethyl,2,2'-bipyridine (4,4' dm, 2,2' BP) and 2,2'-biquinoline (2,2 BQ) shown below

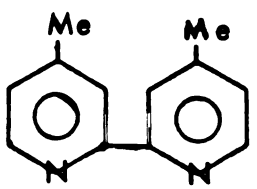

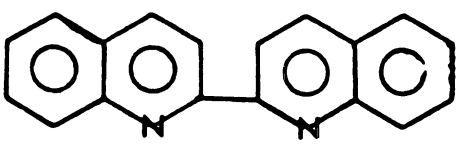

4,4'-dimethyl,2,2'-bipyridine 2,2'-biquinoline

were used as ligands to study the effect of the substituent groups on the complexation with Na^+. The method used for the study was sodium-23 nmr. The results are listed in Tables 23-24. In the case of the 4,4'-dimethyl,2,2'-bipyridine the only solvent that could be used was

Table 22. Mole Ratio Study of 2,2'-Bipyridine Complexes with Cesium in Various Solvents by Cs-133 NMR at 25°C.

Solvent	Salt	$[Cs^+]$	[2,2' BP]/$[Cs^+]$	Δν(ppm)
CH_3NO_2	CsSCN	0.05	0.00	61.81
			2.06	61.35
			2.88	61.19
			3.89	60.88
DMF	CsSCN	0.05	0.00	7.51
			1.10	7.51
			1.97	7.51
			2.97	7.51
			3.97	7.51
Py	$CsBPh_4$	0.015	0.00	49.0
			1.73	49.9
			3.47	49.9
PC	CsSCN	0.05	0.00	41.07
			0.92	40.76
			2.06	40.45
			3.20	40.45
			4.16	40.14
CH_3CN	CsSCN	0.05	0.00	-27.37
			0.97	-27.37
			2.05	-27.37
			3.09	-27.68
			4.10	-27.37

Table 22. Continued

Solvent	Salt	$[Cs^+]$	[2,2' BP]/$[Cs^+]$	$\Delta\nu$(ppm)
CH_3OH	CsSCN	0.05	0.00	51.99
			1.12	51.68
			2.01	51.68
			2.96	51.37
			3.78	51.06

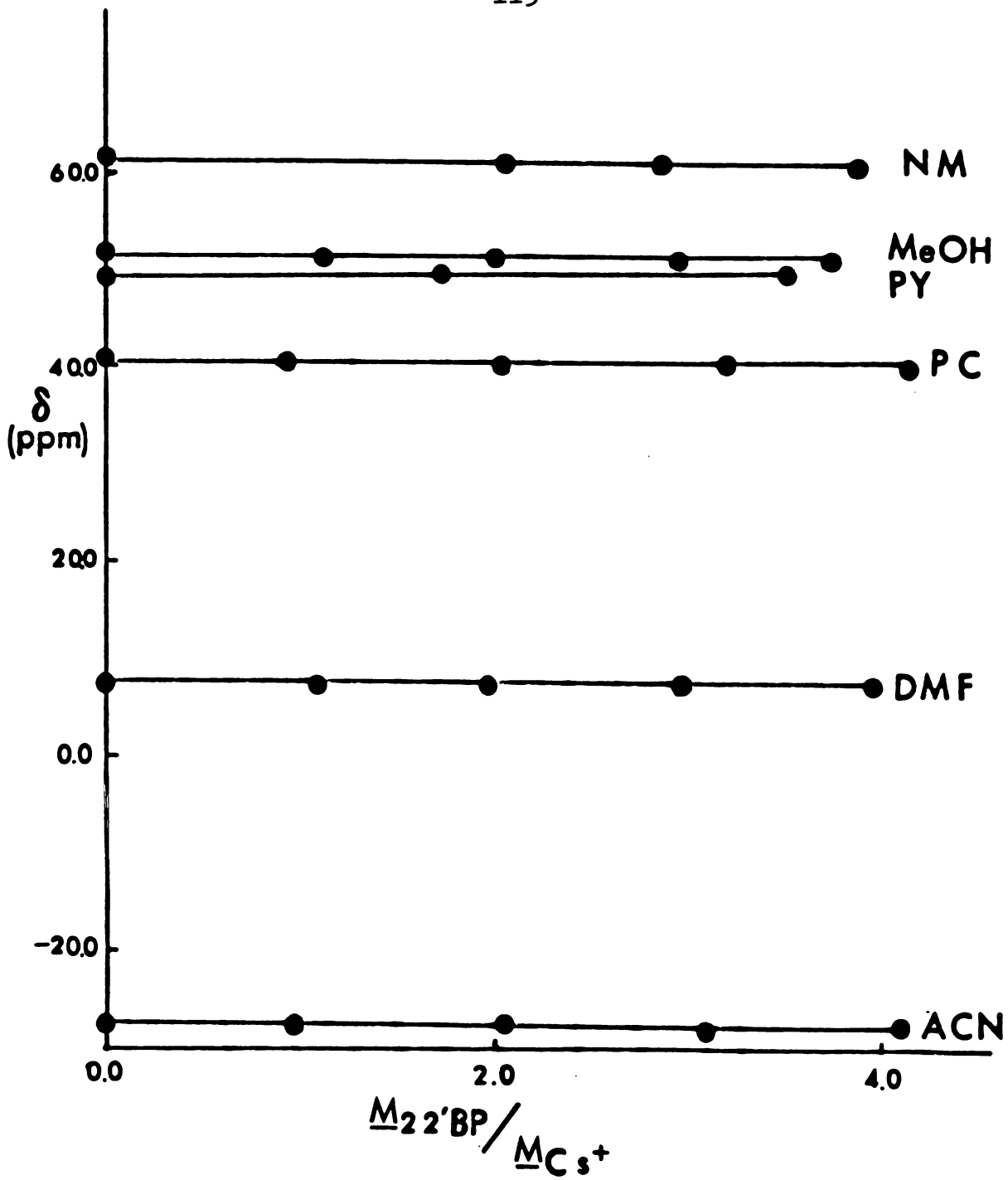

Figure 32. Cesium-133 chemical shift as a function of 2,2' BP/Cs^+ mole ratio in CH_3NO_2, CH_3OH, Py, PC, DMF and CH_3CN solutions.

nitromethane. The ligand was not soluble enough in any of the other solvents used in this study. In nitromethane the highest mole ratio we could get was 2.01 for a concentration of $NaBPh_4$ of 0.15 M, above that the ligand was insoluble. From Figure 33 we can see that the mole ratio plot up to mole ratio 2.01 that was studied, looks identical to the one obtained with 2,2'-bipyridine and Na^+ in nitromethane. These results indicate that the two methyl groups do not change the electronic cloud around the nitrogen atoms very much. They do provide though a more unsymmetrical environment for the Na^+ than the unsubstituted ligand as the linewidths indicate. Biquinoline was only soluble in CH_3NO_2 up to a mole ratio of ligand/salt of 1.34 and in DMSO up to a mole ratio of about 3.0 for a salt concentration of 0.075 M. There is no indication of complexation in DMSO (Figure 34) while in nitromethane the solubility limits any conclusions. Chemical shift changes are observed for the solutions studied and all that can be said is that the slope of the mole ratio plot appears to be different than that for the 2,2'-bipyridine itself which seems to indicate that there is some influence of the added benzene rings on the complexing ability of the ligand.

Table 23. Mole Ratio Study of 4,4'Dimethyl, 2,2'-Bipyridine Complexes with 0.150 M $NaBPh_4$ in CH_3NO_2 by Na-23 NMR at 25°C.

[4,4' dm,2,2' BP]/ $[Na^+]$	$\Delta\delta$(ppm)	$\Delta\nu_{\frac{1}{2}}$(Hz)
0.00	14.5	13
0.09	13.6	41
0.19	12.5	76
0.26	11.8	83
0.33	11.3	100
0.39	10.7	132
0.43	10.4	130
0.51	10.0	151
0.57	9.5	173
0.63	8.5	198
0.70	8.4	198
0.84	7.0	251
0.94	6.5	298
1.00	6.0	389
1.04	6.2	415
1.14	4.7	466
1.36	3.6	493
1.43	2.4	517

Table 23. Continued

[4,4' dm,2,2' BP]/ [Na^+]	$\Delta\delta$(ppm)	$\Delta\nu_{\frac{1}{2}}$(Hz)
2.01	-0.1	830
2.46*	---	---

*Insoluble

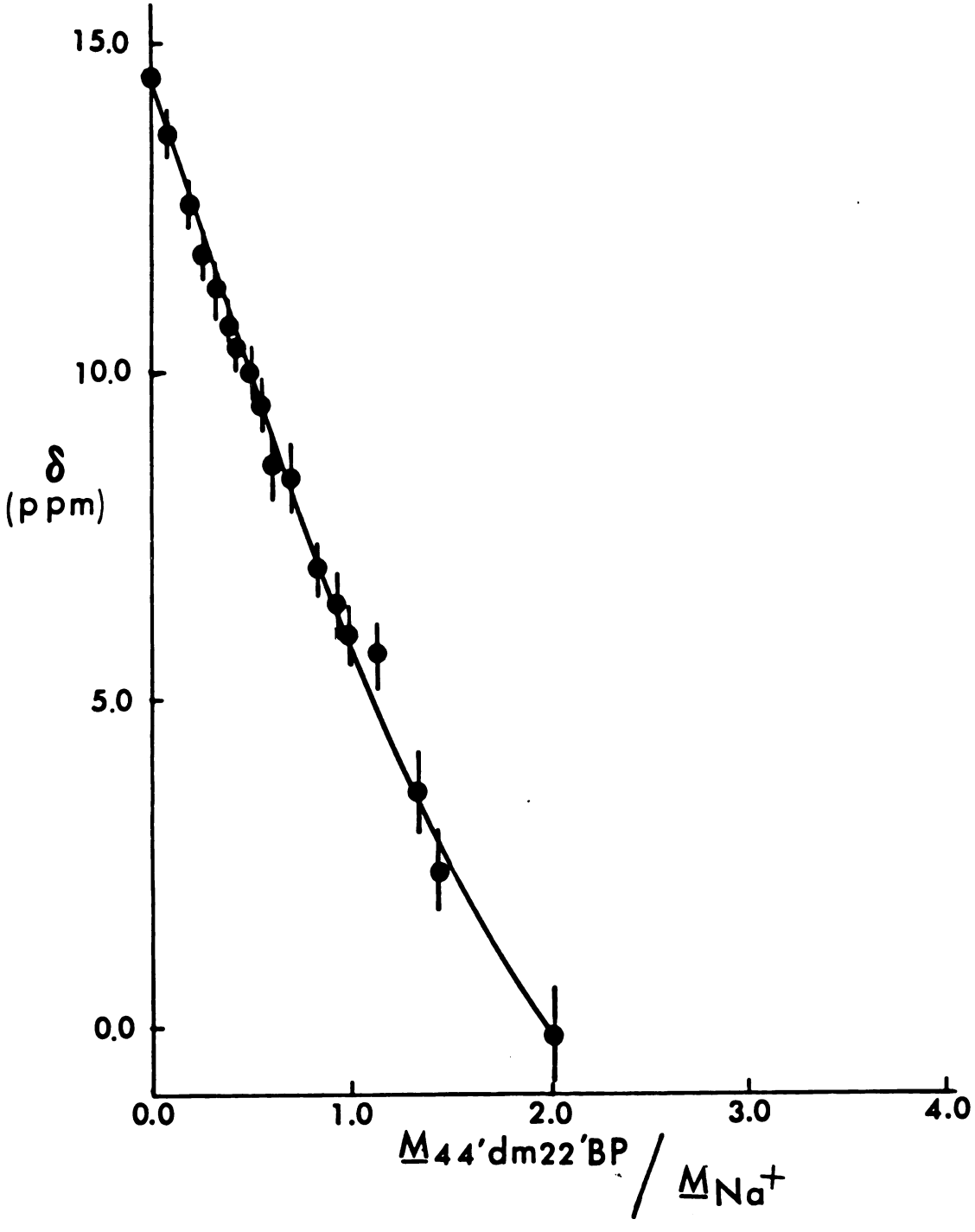

Figure 33. Sodium-23 chemical shift as a function of 4,4' dm,2,2' BP/Na^+ mole ratio in nitromethane solutions.

Table 24. Mole Ratio Study of 2,2'-Biquinoline Complexes with 0.075 M $NaBPh_4$ in CH_3NO_2 and DMSO by Na-23 NMR at 25°C.

Solvent	[2,2'-Biquinoline]/[Na^+]	$\Delta\delta$(ppm)	$\Delta\nu_{\frac{1}{2}}$(Hz)
CH_3NO_2	0.00	13.9	19
	0.60	12.5	
	1.01	11.1	178
	1.34	9.9	244
DMSO	0.00	1.3	52
	1.03	1.2	64
	1.97	1.0	61
	2.96	1.0	64
	4.06*	---	---

*Insoluble

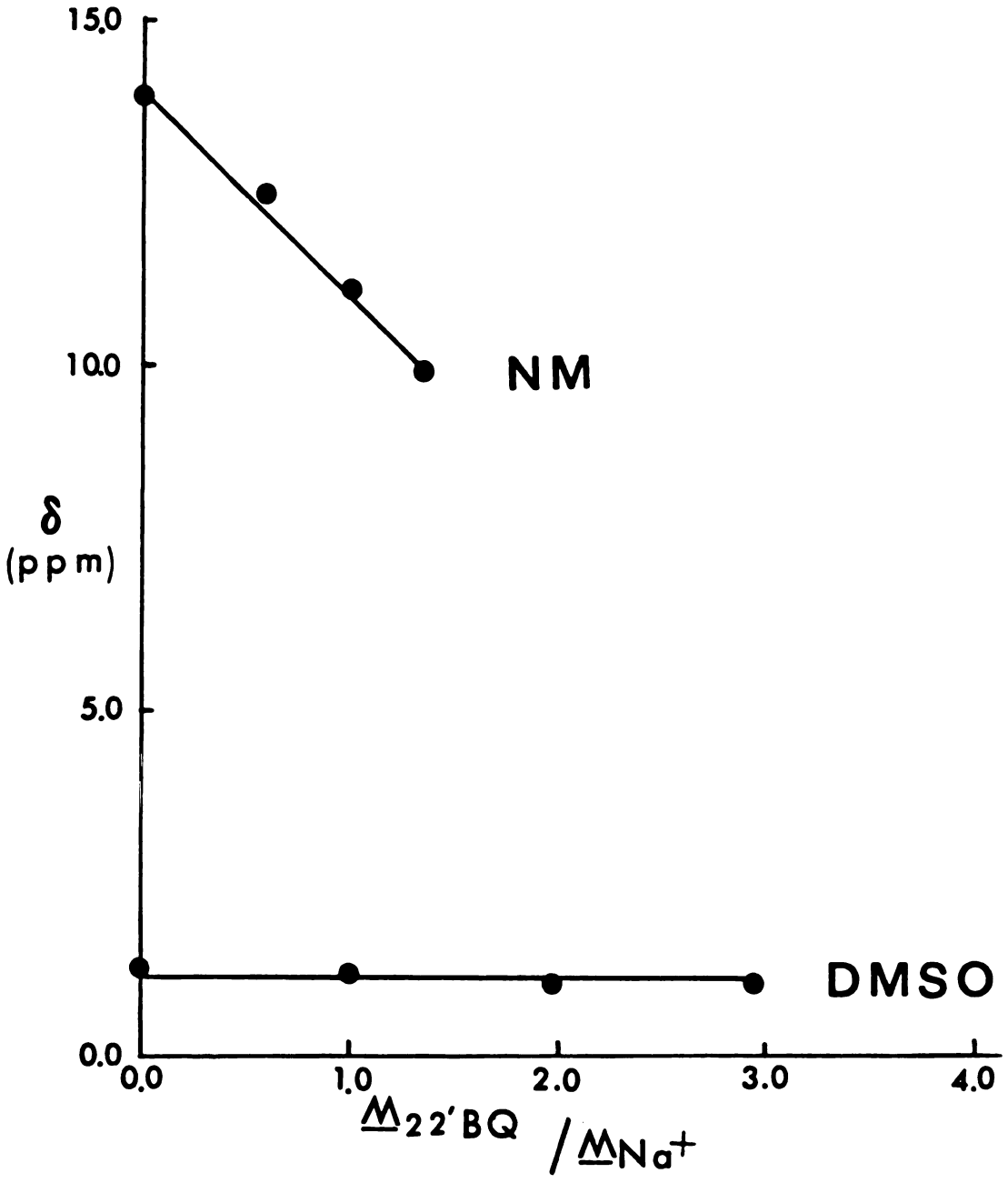

Figure 34. Sodium-23 chemical shift as a function of 2,2' BQ/Na^+ mole ratio in nitromethane solutions.

LITERATURE CITED

LITERATURE CITED

1. W. E. Morf and W. Simon, Helv. Chim. Acta, 54, 2683 (1971).
2. C. J. Pedersen, J. Amer. Chem. Soc., 89, 7017 (1967).
3. C. J. Pedersen, J. Amer. Chem. Soc., 92, 386 (1967).
4. C. J. Pedersen and H. K. Frensdorff, Angew. Chem., 84, 16 (1972); Angew Chem. Intern. Ed., 14, 46 (1972).
5. J. J. Christensen, D. J. Eatough and R. M. Izatt, Chem. Rev., 74, 351 (1974).
6. B. Dietrich, J.-M. Lehn and J. P. Sauvage, Tetrahedron Letters, 1969, 2889.
7. B. Dietrich, J.-M. Lehn and J. P. Sauvage, Tetrahedron Letters, 1969, 2885.
8. B. Dietrich, J.-M. Lehn and J.P. Sauvage, Tetrahedron, 29, 1647 (1973).
9. B. Dietrich, J.-M. Lehn, J. P. Sauvage and J. Blanzat, Tetrahedron, 29, 1629 (1973).
10. J. M. Lehn and F. Montavon, Tetrahedron Letters, 1972, 4557.
11. B. Metz, D. Moras and R. Weiss, Chem. Comm., 217 (1970).
12. D. Moras, B. Metz and R. Weiss, Acta Crystallogr., B29, 388 (1973).
13. D. Moras, B. Metz and R. Weiss, Acta Crystallogr., B29, 383 (1973).
14. D. Moras and R. Weiss, Acta Crystallogr., B29, 396 (1973).
15. D. Moras and R. Weiss, Acta Crystallogr., B29, 400 (1973).
16. J.-M. Lehn and J. P. Sauvage, Chem. Commun., 440 (1971).
17. J.-M. Lehn, Structure and Bonding, 16, 1 (1973).

18. J.-M. Lehn and J. P. Sauvage, J. Amer. Chem. Soc., 97, 6700 (1975).

19. B. Dietrich, J.-M. Lehn and J. P. Sauvage, J. Chem. Soc. Chem. Commun., 15 (1973).

20. B. Dietrich, J.-M. Lehn and J. P. Sauvage, Chem. Comm., 1055 (1970).

21. J.-M. Lehn and F. Mohtavon, Helv. Chim. Acta, 59, 1566 (1976).

22. J.-M. Lehn, J. P. Sauvage, B. Dietrich, J. Amer. Chem. Soc., 92, 2916 (1970).

23. J. M. Ceraso, J. L. Dye, J. Amer. Chem. Soc., 95, 4432 (1973).

24. J. P. Kintzinger, J.-M. Lehn, J. Amer. Chem. Soc., 96, 3313 (1974).

25. Y. M. Cahen, J. L. Dye and A. I. Popov, J. Phys. Chem., 79, 1289 (1975).

26. Y. M. Cahen, J. L. Dye and A. I. Popov, J. Phys. Chem., 79, 1292 (1975).

27. V. M. Loyola, R. Pizer, and R. G. Wilkins, JACS, 99, 7185 (1977).

28. J. L. Dye, "Metal Solutions in Amines and Ethers," Electrons in Fluids, p. 77-95, Springer-Verlag, Berlin, Heidelberg, New York (1973).

29. J. L. Dye, Mei Tak Lok, F. J. Tehan, R. B. Cooley, N. Papadakis, J. M. Ceraso and M. G. Debacker, Verlag Chemie Gmbh, Weinheim/Bergstr. Band., 75, Heft 7 (1971).

30. Mei Tak Lok, F. J. Tehan and J. L. Dye, J. Phys. Chem., 76, 2975 (1972).

31. J. L. Dye, J. M. Ceraso, Mei Tak Lok, B. L. Barnett, F. J. Tehan, J. Amer. Chem. Soc., 96, 608 (1974).

32. F. J. Tehan, B. L. Barnett, J. L. Dye, J. Amer. Chem. Soc., 96, 7203 (1974).

33. J. M. Ceraso and J. L. Dye, J. Chem. Phys., 61, 1585 (1974).

34. J. L. Dye, C. N. Andrews, and J. M. Ceraso, J. Phys. Chem., 79, 3076 (1975).

35. J. Cheney, J.-M. Lehn, J. P. Sauvage, and M. E. Stubbs, J. Chem. Soc. Chem. Commun., 1100 (1972).

36. J.-M. Lehn, J. Simon and J. Wagner, Angew. Chem. Internat. Ed., 12, 578 (1973).

37. J.-M. Lehn, J. Simon, and J. Wagner, Angew. Chem. Internat. Ed., 12, 579 (1973).

38. J.-M. Lehn, and J. Simon, Helv. Chim. Acta, 60, 141 (1977).

39. J.-M. Lehn, M. E. Stubbs, J. Amer. Chem. Soc., 96, 4011 (1974).

40. E. Graf, J.-M. Lehn, J. Amer. Chem. Soc., 97, 5022 (1975).

41. E. Graf, J.-M. Lehn, J. Amer. Chem. Soc., 98, 6403 (1976).

42. B. Metz, J. M. Rosalky, and R. Weiss, J. Chem. Soc. Chem. Commun., 533 (1976).

43. P. U. Fruh, J. T. Clerc, and W. Simcn, Helv. Chim. Acta, 54, 1445 (1971).

44. W. K. Lutz, P. U. Fruh and W. Simon, Helv. Chim. Acta, 54, 2767 (1971).

45. Ch. U. Zust, P. U. Fruh and W. Simon, Helv. Chim. Acta, 56, 495 (1973).

46. H. J. Moschler, H. G. Weder, and R. Schwyzer, Helv. Chim. Acta, 54, 1437 (1971).

47. R. Winkler, Structure and Bonding, 10, 1 (1972).

48. H. K. Frensdorff, J. Amer. Chem. Soc., 93, 600 (1971).

49. D. K. Cabbiness, D. N. Margerum, J. Amer. Chem. Soc., 91, 6540 (1969).

50. F. P. Hinz and D. W. Margerum, Inorganic Chem., 13, 2941 (1974).

51. A. Dei and R. Gori, Inorg. Chim. Acta, 14, 157 (1975).

52. p. Paoletti, L. Fabbrizzi, R. Barbucci, Inorg. Chem., 12, 1961 (1973).

53. M. Kodawa, E. Kimura, J. Chem. Soc. Chem. Commun., 326 (1975).

54. R. M. Izatt, J. H. Rytting, D. P. Nelson, B. L. Haymore and J. J. Christensen, Science, 164, 443 (1969).

55. J. J. Christensen, J. O. Hill, R. M. Izatt, Science, 174, 459 (1971).

56. R. M. Izatt, D. P. Nelson, J. H. Rytting, B. L. Haymore, and J. J. Christensen, J. Amer. Chem. Soc., 93, 1619 (1971).

57. R. M. Izatt, D. J. Eatough and J. J. Christensen, Structure and Bonding, 16, 161 (1973).

58. R. M. Izatt, R. E. Terry, B. L. Haymore, L. D. Hansen, N. K. Dalley, A. G. Avondet, and J. J. Christensen, J. Amer. Chem. Soc., 98, 7620 (1976).

59. R. M. Izatt, R. E. Terry, D. P. Nelson, Y. Chang, D. J. Eatough, J. S. Bradshaw, L. D. Hansen, and J. J. Christensen, J. Amer. Chem. Soc., 98, 7626 (1976).

60. R. M. Izatt, J. D. Lamb, G. E. Maas, R. E. Asay, J. S. Bradshaw, J. J. Christensen, J. Amer. Chem. Soc., 99, 2365 (1977).

61. R. M. Izatt, J. D. Lamb, R. E. Asay, G. E. Maas, J. S. Bradshaw, and J. J. Christensen, J. Amer. Chem. Soc., 99, 6134 (1977).

62. E. Shchori and J. Jagur-Grodzinski, Israel J. Chem., 11, 243 (1973).

63. E. Mei, A. I. Popov, and J. L. Dye, J. Amer. Chem. Soc., 99, 5308 (1977).

64. E. Mei, A. I. Popov, and J. L. Dye, J. Phys. Chem., 81, 1677 (1977).

65. E. Kauffmann, J.-M. Lehn and J. P. Sauvage, Helv. Chim. Acta, 59, 1099 (1976).

66. E. Mei, A. I. Popov, and J. L. Dye, J. Amer. Chem. Soc., 99, 6532 (1977).

67. D. H. Haynes, B. C. Pressman, and A. Kowalsky, Biochem., 10, 852 (1971).

68. Paul G. Gertenbach, Ph.D. Thesis, Michigan State University, East Lansing, Michigan (1975).

69. J. L. Wuepper and A. I. Popov, J. Amer. Chem. Soc., 92, 1493 (1970).

70. J. L. Dye, M. T. Lok, F. J. Tehan, J. Ceraso, and K. Voorhees, J. Org. Chem., 38, 1773 (1973).

71. A. Hourdakis, M. S. Thesis, Michigan State University, East Lansing, Michigan (1975).

72. M. S. Greenberg, Ph.D. Thesis, Michigan State University, East Lansing, Michigan (1974).

73. D. D. Traficante, J. A. Simms and M. Mulcay, J. Magn. Reson., 15, 484 (1974).

74. D. A. Wright and M. T. Rogers, Rev. Sci. Instrum., 44, 4489 (1973).

75. J. W. Cooper, "An Introduction to Fourier Transform NMR and the Nicolet 1080 Data System," Nicolet Instrument Corp., Madison, Wisconsin, 1972.

76. D. H. Live and S. I. Chan, Anal. Chem., 42, 791 (1971).

77. G. Foex, G. J. Gorter and L. J. Smits, "Constantes Selectionees, Diamagnetisme et Paramagnetisme, Relaxation Paramagnetique", Massoy and Cie Editeurs, Paris (1957).

78. "CFT-20 NMR Spectrometer System", 87-144-000 Varian Instrument Division.

79. P. R. Handy, Ph.D. Thesis, Michigan State University, East Lansing, Michigan (1972).

80. J. L. Dye and V. A. Nicely, J. Chem. Educ., 48, 443 (1968).

81. R. H. Erlich, E. Roach, and A. I. Popov, J. Amer. Chem. Soc., 92, 4989 (1970).

82. M. Herlem and A. I. Popov, J. Amer. Chem. Soc., 94, 1431 (1972).

83. R. H. Erlich and A. I. Popov, J. Amer. Chem. Soc., 93, 5260 (1971).

84. M. S. Greenberg, R. L. Bodner and A. I. Popov, J. Phys. Chem., 77, 2449 (1973).

85. C. Deverell and R. E. Richards, Mol. Phys., 10, 551 (1966).

86. A. L. Van Geet, J. Amer. Chem. Soc., 94, 5583 (1972).

87. E. G. Bloor and R. G. Kidd, Can. J. Chem., 46, 3425 (1968).

88. E. T. Roach, P. R. Handy and A. I. Popov, Inorg. Nucl. Chem. Lett., 9, 359 (1973).

89. R. L. Bodner, M. S. Greenberg and A. I. Popov, Spectrosc. Lett., 5, 489 (1972).

90. E. Mei, L. Liu, J. L. Dye, and A. I. Popov, J. Solut. Chem., 6, 771 (1977).

91. a) V. Gutmann and E. Wychera, Inorg. Nucl. Chem. Lett., 2, 257 (1966); b) V. Gutmann, "Coordination Chemistry in Nonaqueous Solvents", Springer Verlag, Vienna, 1968.

92. M. S. Greenberg and A. I. Popov, Spectrochim. Acta, 31A, 697 (1975).

93. N. Ahmad, M. C. Day, J. Amer. Chem. Soc., 99, 941 (1977).

94. W. J. DeWitte, L. Liu, E. Mei, J. L. Dye and A. I. Popov, J. Solut. Chem., 6, 337 (1977).

95. L. L. Hsu, M. S. Thesis, Michigan State University, East Lansing, Michigan (1976).

96. Mei-Tak Lok, Ph.D. Thesis, Michigan State University East Lansing, Michigan (1973).

97. J. C. Evans and G. Y. S. Lo, J. Phys. Chem., 69, 3323 (1965).

98. W. F. Edgell, A. T. Watts, J. Lyford and W. M. Risen, Jr., J. Amer. Chem. Soc., 88, 1815 (1966).

99. W. F. Edgell, A. Lyford, IV, R. Wright, W. M. Risen, Jr., and A. Watts, J. Amer. Chem. Soc., 92, 2240 (1970).

100. B. W. Maxey and A. I. Popov, J. Amer. Chem. Soc., 89, 2230 (1967).

101. B. W. Maxey and A. I. Popov, J. Amer. Chem. Soc., 91, 4352 (1969).

102. B. W. Maxey and A. I. Popov, J. Amer. Chem. Soc., 91, 20 (1969).

103. M. K. Wong, W. J. McKinney and A. I. Popov, J. Phys. Chem., 75, 56 (1971).

104. M. K. Wong and A. I. Popov, J. Inorg. Nucl. Chem., 33, 1203 (1971).

105. W. J. McKinney and A. I. Popov, J. Phys. Chem., 74, 535 (1970).

106. P. R. Handy and A. I. Popov, Spectrochim. Acta, 28A, 1545 (1972).

107. M. S. Greenberg, D. M. Wied and A. I. Popov, Spectrochim. Acta, 29A, 1927 (1973).

108. A. T. Tsatsas, R. W. Stearns and W. M. Risen, J. Amer. Chem. Soc., 94, 5247 (1972).

109. Y. M. Cahen and A. I. Popov, J. Solution Chem., 4, 599 (1975).

110. S. Ahrland, Helv. Chim. Acta, 50, 306 (1967).

111. G. Schwarzenbach, Pure Appl. Chem., 24, 307 (1970).

112. F. W. Cagle, Jr., Acta Cryst., 1, 158 (1948).

113. L. L. Merritt, Jr., and E. D. Schroeder, Acta Cryst., 9, 801 (1956).

114. F. Bertinotti, A. M. Liquori, R. Pirisi, Gazz. Chim. Ital., 86, 893 (1956).

115. P. E. Fielding and R. J. W. LeFevre, J. Chem. Soc., 1951, 1811.

116. C. W. N. Cumper, R. F. A. Gimman and A. I. Vogel, J. Chem. Soc., 1962, 1188.

117. P. H. Cureton, C. G. LeFevre and R. J. W. LeFevre, J. Chem. Soc., 1963, 1736.

118. A. A. Schilt and R. C. Taylor, J. Inorg. Nucl. Chem., 9, 211 (1959).

119. M. D. Grillone and M. A. Nocilla, Inorg. Nucl. Chem. Lett., 14, 49 (1978).

120. D. M. W. Buck and P. Moore, J. Chem. Soc. Dalton Trans., 1975, 409.

121. P. Moore and D. M. W. Buck, J. Chem. Soc. Dalton Trans., 1973, 1602.

APPENDICES

APPENDIX I

DETERMINATION OF COMPLEX FORMATION CONSTANTS BY THE NMR TECHNIQUE, DESCRIPTION OF COMPUTER PROGRAM KINFIT AND SUBROUTINE EQUATION.

Let's consider the following equilibrium for a one to one complex,

$$M + L \underset{k_b}{\overset{k_f}{\rightleftharpoons}} ML \qquad (17)$$

with the concentration formation constant K

$$K = C_{ML}/C_M \cdot C_L \qquad (18)$$

C, stands for concentration.

The observed chemical shift of M (δ_{obs}) is a mass average of the characteristic chemical shift of M at each site (M in the bulk solution, and M complexed), assuming that a fast exchange occurs between these two sites with respect to the NMR time scale.

$$\delta_{obs} = X_M \delta_M + X_{ML} \delta_{ML} \qquad (19)$$

where:

δ_M is the characteristic chemical shift for M in the bulk solution, δ_{ML} is the characteristic chemical shift for M complexed (ML), X_M is the fraction of M ($C_M/(C_M + C_{ML})$),

X_{ML} is the fraction of ML ($C_{ML}/(C_M + C_{ML})$), then

$$\delta_{obs} = X_M\delta_M + (1 - X_M)\delta_{ML}$$

$$\delta_{obs} = X_M(\delta_M - \delta_{ML}) + \delta_{ML} \qquad (20)$$

$C_M^t = C_M + C_{ML}$ (the analytical concentration of M) (21)

$$\delta_{obs} = \frac{C_M}{C_M^t}(\delta_M - \delta_{ML}) + \delta_{ML} \qquad (22)$$

$C_L^t = C_{ML} + C_L$ (the analytical concentration of L) (23)

$$C_L = C_L^t - C_{ML}$$

using (21) and (23), $C_L = C_L^t - (C_M^t - C_M)$ and, therefore,

$$K = \frac{C_M^t - C_M}{(C_M)(C_L^t - C_M^t + C_M)} \qquad (24)$$

C_M is solved in (24)

$$C_M(C_L^t - C_M^t + C_M)K = C_M^t - C_M$$

$$KC_M^2 + (KC_L^t - KC_M^t + 1)C_M - C_M^t = 0$$

$$C_M = \frac{-(KC_L^t - KC_M^t + 1) \pm \sqrt{(KC_L^t - KC_M^t + 1)^2 + 4KC_M^t}}{2K}$$

the positive root is

$$C_M = \frac{(KC_M^t - KC_L^t - 1) + \sqrt{K^2C_L^{t\,2} + K^2C_M^{t\,2} - 2K^2C_L^tC_M^t + 2KC_L^t + 2KC_M^t + 1}}{2K} \tag{25}$$

Substitution of C_M from (25) into (22) gives

$$\delta_{obs} = \left[(KC_M^t - KC_L^t - 1) + \sqrt{K^2C_L^{t\,2} + K^2C_M^{t\,2} - 2K^2C_L^tC_M^t + 2KC_L^t + 2KC_M^t + 1}\right]$$

$$(\delta_M - \delta_{ML})/2C_M^tK + \delta_{ML} \tag{26}$$

We assume a constant value for δ_M and that δ_{ML} and K are unknown. In order to fit the calculated shift (the right hand side of Equation (26)) to the observed chemical shift, the program may vary the values of δ_{ML} and K. Hence, the number of unknowns, NOUNK, equals two as does the number of variables, NOVAR.

The first card contains the number of experimental points (columns 1-5 (F.15)), the maximum number of iterations allowed (columns 10-15 (F.15)), the number of constants (columns 36-40 (F.15)) and the maximum value of (Δ parameter/parameter) for convergence to be assumed (0.0001 works well) in columns 41-50 (F10.6). The second data card contains any title the user desires. The third data card contains the value of CONST(1) (C_M^t) columns 1-10 (F10.6) in M, CONST(2) (δ_M) columns 11-20 (F10.6) other constants can be listed on columns 21-30, 31-40, etc. The fourth data card contains the initial estimates of the unknowns U(1) = δ_{ML} and U(2) = K, in columns 1-10 and 11-20 (F10.6), respectively. The

fifth through N data cards contains XX(1) = C_M^t in columns 1-10 (F10.6) variances on XX(1) in columns 11-20, XX(2) = the chemical shift at XX(1) in columns 31-40 (F10.6) followed by the same parameters for the next data point. Each card may contain two data points. If no further data are to be analyzed the next card after the last data point(s) should be a blank card followed by a 6789 card. If more data sets are to be analyzed, the next card after the last data point(s) is the first data card of the next set.

```
      SUBROUTINE EQN
      COMMON KOUNT,ITAPE,JTAPE,IWT,LAP,XINCR,NOPT,NOVAR,NOUNK,X,U,ITMAX, EQN6
     1WTX,TEST,I,AV,RESID,IAR,EPS,ITYP,XX,RXTYP,DXII,FOP,FO,FU,P,ZL,TO,E EQN6
     2IGVAL,XST,Y,DT,L,M,JJJ,Y,DY,VECT,NCST,CONST,NDAT,JDAT,MOPT,LAPT.   EQN6
     3YYY,CONSTS
      COMMON/FREDT/IMETH
      COMMON/POINT/KOPT,JOPT,XXX
      DIMENSION X(4,300),U(20),WTX(4,300),XX(4),FOP(300),FO(300),FU(300) EQ
     1,P(20,21),VECT(20,21),ZL(300),TO(20),EIGVAL(20),XST(300),Y(10),
     2DY(10),CONSTS(50,16),NCST(50),ISMIN(50),RXTYP(50),DXII(50),IRX(50)
     3,MOPT(50),LOPT(50),YYY(50),CONST(16),XXX(15)
      GO TO (2,3,4,5,1,7,8,9,10,11,12)  ITYP
    1 CONTINUE
      ITAPE=A0
      JTAPE=A1
      NOUNK=2
      NOVAR=2
      RETURN
    7 CONTINUE
      RETURN
    8 CONTINUE
      RETURN
    9 CONTINUE
      IF(IMETH.NE.-1) GO TO 35
      RETURN
   35 CONTINUE
      A=(U(2)**2)*(XX(1)**2)
      B=(U(2)**2)*(CONST(1)**2)
      C=2.0*(U(2)**2)*(XX(1))*CONST(1)
      D=2.0*(U(2))*(XX(1))
      E=2.0*(U(2))*(CONST(1))
      AA=(U(2))*(CONST(1))
      BB=-(U(2))*XX(1)
      CC=(CONST(2)-U(1))/(2.*(CONST(1))*(U(2)))
      S=(((AA*BB-1.)*SQRT(ABS(A*B*C*D*E*1.)))*CC)*U(1)
      RESID=S-XX(2)
      RETURN
    3 CONTINUE
      RETURN
    4 CONTINUE
      RETURN
    5 CONTINUE
      IF(IMETH.NE.-1) GO TO 20
      RETURN
   20 CONTINUE
      RETURN
    6 CONTINUE
      RETURN
   10 CONTINUE
      RETURN
   11 CONTINUE
      RETURN
   12 CONTINUE
      RETURN
      END
```

APPENDIX II

DETERMINATION OF COMPLEX FORMATION CONSTANT WITH ION PAIR FORMATION BY THE NMR METHOD

Definition of symbols,

[M] = cation

[A] = anion

[L] = ligand

[MA] = ion pair

[ML] = metal complex

C_M = analytical concentration of metal ion

C_L = analytical concentration of ligand

K_{ip} = ion pair equilibrium constant

K^f = formation constant of complex

Ion pair equilibrium,

$$[M] + [A] \underset{\leftarrow}{\overset{K_{ip}}{\rightarrow}} [MA]$$

$$K_{ip} = \frac{[MA]}{[M][A]} \tag{27}$$

Complexation equilibrium,

$$[M] + [L] \overset{K^f}{\underset{\leftarrow}{\rightarrow}} [ML]$$

$$K^f = \frac{[ML]}{[M][L]} \tag{28}$$

$$C_L = [ML] + [L] \tag{29}$$

$$C_M = [ML] + [M] + [MA] \tag{30}$$

$$C_M = [MA] + [A] \tag{31}$$

From (27),

$$[MA] = K_{ip}[M][A] \tag{32}$$

From (28),

$$[ML] = K^f[M][L] \tag{33}$$

Substitute in (29)

$$C_L = K^f[M][L] + [L] = [L](K^f[M] + 1)$$

$$\therefore [L] = \frac{C_L}{K^f[M] + 1} \tag{34}$$

Substitute in (30),

$$C_M = K^f[M][L] + [M] + K_{ip}[M][A] \tag{35}$$

Substitute in (31),

$$C_M = [A] + K_{ip}[M][A] = [A](1 + K_{ip}[M])$$

$$\therefore [A] = \frac{C_M}{1 + K_{ip}[M]} \tag{36}$$

Substitute (34) and (36) in (35),

$$C_M = \frac{K^f[M]C_L}{K^f[M] + 1} + [M] + \frac{K_{ip}[M]C_M}{1 + K_{ip}[M]} \tag{37}$$

Multiply (37) across by $(1 + K^f[M])(1 + K_{ip}[M])$,

$$C_M(1 + K^f[M])(1 + K_{ip}[M]) = K^fC_L[M](1 + K_{ip}[M])$$

$$+ [M](1 + K^f[M])(1 + K_{ip}[M]) + K_{ip}C_M[M](1 + K^f[M]) \tag{38}$$

$$C_M + K_{ip}C_M[M] + K^fC_M[M] + K^fK_{ip}C_M[M]^2$$

$$= K^fC_L[M] + K^fK_{ip}C_L[M]^2 + [M] + K_{ip}[M]^2$$

$$+ K^f[M]^2 + K^fK_{ip}[M]^3 + K_{ip}C_M[M] + K^fK_{ip}C_M[M]^2 \qquad (39)$$

Collecting terms,

$$K^fK_{ip}[M]^3 + (K^fK_{ip}C_L + K_{ip} + K^f)[M]^2$$

$$+ (K^fC_L + 1 - K^fC_M)[M] - C_M = 0 \qquad (40)$$

$$[M]^3 + \frac{(K^fK_{ip}C_L + K_{ip} + K^f)}{K^fK_{ip}}[M]^2$$

$$+ \frac{(K^fC_L + 1 - K^fC_M)}{K^fK_{ip}}[M] - \frac{C_M}{K^fK_{ip}} = 0 \qquad (41)$$

Solution to cubic equation,

$$y^3 + py^2 + qy + r = 0$$

$$p = \frac{(K^fK_{ip}C_L + K_{ip} + K^f)}{K^fK_{ip}}$$

$$q = \frac{(K^fC_L + 1 - K^fC_M)}{K^fK_{ip}}$$

$$r = \frac{-C_M}{K^fK_{ip}}$$

$$y = x - \frac{p}{3}$$

$$x^3 + ax + b = 0$$

$$a = (3q - p^2)/3$$

$$b = (2p^3 - 9pq + 27r)/27$$

$$A = \sqrt[3]{-\frac{b}{2} + \sqrt{\frac{b^2}{4} + \frac{a^3}{27}}}$$

$$B = \sqrt[3]{-\frac{b}{2} - \sqrt{\frac{b^2}{4} + \frac{a^3}{27}}}$$

Case I $\quad \frac{b^2}{4} + \frac{a^3}{27} > 0 \rightarrow 1$ real root

II $\quad \frac{b^2}{4} + \frac{a^3}{27} = 0 \rightarrow 3$ real roots

III $\quad \frac{b^2}{4} + \frac{a^3}{27} < 0 \rightarrow 3$ real roots

Case I, $x = A + B$

Case II and III, use trigonometric form

$$\text{Cos}\,\phi = -\frac{b}{2} \div \sqrt{(-\frac{a^3}{27})}$$

$$x = 2\sqrt{-\frac{a}{3}}\,\text{Cos}\,\frac{\phi}{3}$$

$$2\sqrt{-\frac{a}{3}}\,\text{Cos}\,(\frac{\phi}{3} + 120^\circ)$$

$$2\sqrt{-\frac{a}{3}}\,\text{Cos}\,(\frac{\phi}{3} + 240^\circ)$$

Now, solve for [M] in (41).

Then substitute in following equations,

$$[ML] = \frac{K^f C_L [M]}{K^f [M] + 1} \qquad (42)$$

$$[MA] = \frac{K_{ip} C_M [M]}{K_{ip} [M] + 1} \qquad (43)$$

$$\delta_{obs} = x_M \delta_M + x_{ML} \delta_{ML} + x_{MA} \delta_{MA} \tag{44}$$

$$\delta_{obs} = \frac{[M]}{C_L} \delta_M + \frac{[ML]}{C_M} \delta_{ML} + \frac{[ML]}{C_M} \delta_{MA} \tag{45}$$

Use final form of δ_{obs} in EQN subroutine.

Coding symbols in EQN,

a = AA	p = PP
b = BB	q = QQ
A = AAA	r = RR
B = BBB	ϕ = FE
y = R	Cos ϕ = CFE
CONST(1) = K_{ip}	
CONST(2) = C_M	
CONST(3) = δ_{ip}	
CONST(4) = δ_M	
U(1) = δ_{ML}	XX(1) = C_L
U(2) = K_c^f	XX(2) = δ_{obs}

```
      SUBROUTINE EQN
      COMMON KOUNT,ITAPE,JTAPE,IWT,LAP,XINCR,NOPT,NOVAR,NOUNK,X,U,ITMAX, EQN4
     1WTX,TEST,T,AV,RESID,IAR,EPS,ITYP,XX,RXTYP,DX11,FOP,FO,FU,P,ZL,TO,E EQN4
     2IGVAL,XST,T,DT,L,M,JJJ,Y,DY,VECT,NCST,CONST,NDAT,JDAT,MOPT,LOPT,   EQN4
     3YYY,CONSTS
      COMMON/FRONT/IMETH
      COMMON/POINT/KOPT,JOPT,XXX
      DIMENSION X(4,300),U(20),WTX(4,300),XX(4),FOP(300),FO(300),FU(300) EQ
     1,P(20,21),VECT(20,21),ZL(300),TO(20),EIGVAL(20),XST(300),Y(10),
     2DY(10),CONSTS(50,16),NCST(50),ISMIN(50),RXTYP(50),DX11(50),IRX(50)
C     DEFINITIONS OF THE TERMS
C          CONST(1)   =  ION PAIR FORMATION CONSTANT
C          CONST(2)   =    TOTAL CONC. OF METAL
C          CONST(3)   =    CHEM. SHIFT OF ION PAIR
C          CONST(4)   =    CHEM. SHIFT OF METAL
C          U(1)   =    CHEM. SHIFT OF COMPLEXED METAL
C          U(2)   =    FORMATION CONSTANT OF COMPLEX
C          XX(1)   =    TOTAL CONC. OF LIGAND
C          XX(2)   =    OBSERVED CHEM. SHIFT
     3,MOPT(50),LOPT(50),YYY(50),CONST(16),XXX(15)
      GO TO (2,3,4,5,1,7,8,9,10,11,12)  ITYP
    1 CONTINUE
      ITAPE=60
      JTAPE=61
      NOUNK=2
      NOVAR=2
      RETURN
    7 CONTINUE
      RETURN
    8 CONTINUE
      RETURN
    9 CONTINUE
      IF(IMETH.NE.-1) GO TO 35
      RETURN
   35 CONTINUE
      CUBD=1./3.
C     SETTING THE COEFFICIENTS OF THE TERMS
      PP=XX(1)+(1./U(2))+(1./CONST(1))
      QQ=(1./(U(2)*CONST(1)))+(XX(1)-CONST(2))/CONST(1)
      RR=-CONST(2)/(U(2)*CONST(1))
      AA=(3.*QQ-PP**2)/3.
      RHS=(2.*(PP**3)-9.*PP*QQ+27.*RR)/27.
C     CHECK POINT FOR WHICH FORM OF THE SOLUTION IS TO BE USED
      TEST=(RR**2)/4.+(AA**3)/27.
      IF (TEST)31,31,32
C     THE ALGEBRIAC FORM IS USED HERE
   32 TA=(-RR/2.+SQRT(TEST))
      AAA=(ABS(TA))**CUBD
      TH=(-RR/2.-SQRT(TEST))
      BHD=(ABS(TB))**CUBD
C     CHECKING THE SIGN OF THE CUBEROOT TERMS
      IF (TA)17,17,18
   17 AAA=-AAA
   18 IF (TH)19,19,25
   19 BHD=-BBB
   25 PR=AAA+BBB
      P=PP/3.
      GO TO 30
C     THE TRIGONOMETRIC FORM OF THE SOLUTION IS USED HERE
   31 FLAG=0.
      PAU=2.*ACOS(-1.)
      ANGLE=PAU/3.
      CFE=(-RR/2.)/(SQRT(ABS((-AA**3)/27.)))
C     CHECK FOR VALIDITY OF COSINE TERM
      IF((CFE.LT.-1.).OR.(CFE.GT.1.)) GO TO 40
      FE=PAU-ACOS(CFE)
   14 PW=2.*(SQRT(ABS(-AA/3.)))*COS(FE/3.+ANGLE*FLAG)
      P=PW-(PP/3.)
C     CHECK FOR VALIDITY OF THE CALCULATED METAL CONC
      IF(P)11,13,30
   40 WRITE(JTAPE,22)
   22 FORMAT(' COSINE OF FEE OUTSIDE OF +1 AND -1')
      STOP
C     GO BACK AND FIND ANOTHER ROOT
   11 FLAG=FLAG+1.
      IF(3.-FLAG)15,15,14
   15 WRITE(JTAPE,21)


   21 FORMAT( ' ALL THREE ROOTS FLUNKED')
      STOP
C     SUBSTITUTE CALCULATED METAL CONC. IN ORIGINAL EQUATION
   30 DELTA=(P*CONST(4)+(U(2)*P*XX(1)*U(1))/(1.+U(2)*P))*(CONST(1)*P*CONS
     1T(2)*CONST(3))/(1.+CONST(1)*P))/CONST(2)
      TEST=DELTA-XX(2)
      RETURN
    3 CONTINUE
      RETURN
    4 CONTINUE
      RETURN
    5 CONTINUE
      IF(IMETH.NE.-1) GO TO 20
      RETURN
   20 CONTINUE
      RETURN
    9 CONTINUE
      RETURN
   10 CONTINUE
      RETURN
   11 CONTINUE
      RETURN
   12 CONTINUE
      RETURN
      END
```